Where we are

From O2 to O3

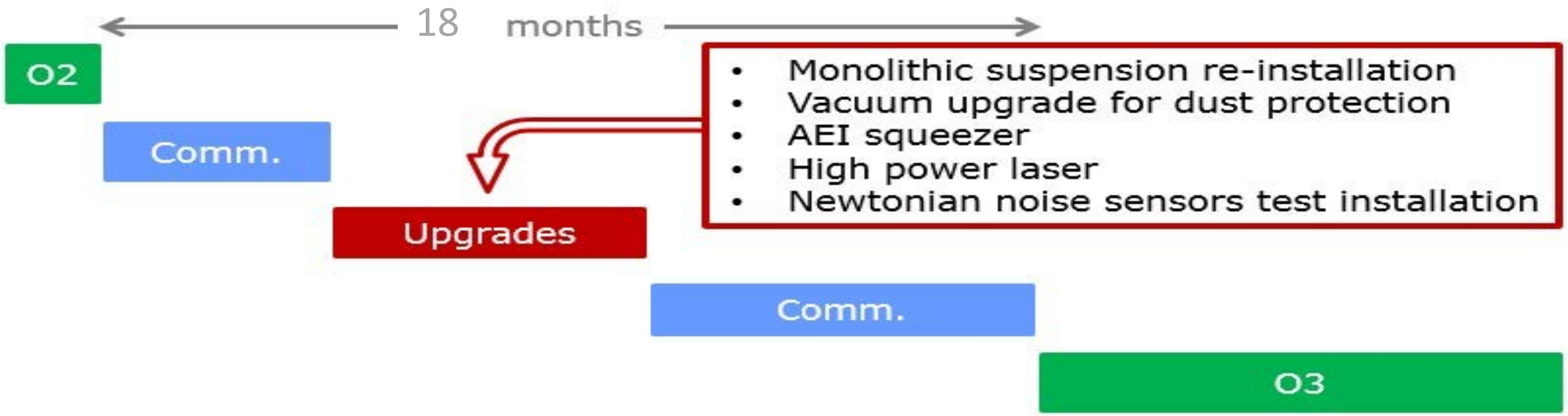

Target sensitivity: *40-60 Mpc* as horizon for a NSNS 1.4 M at SNR=8

Main benefit from putting back the monolithic suspension

Removing the steel wire thermal noise from noise budget gives a 20 Mpc range increase

Theoretical limit of this configuration: 80 Mpc @13W

Main criteria applied to choose the new parts to be installed:
just those new elements that they don't require long commissioning time

Sensitivity prediction: theoretical and experimental one i.e. intrinsic noise of the detector and technical noises

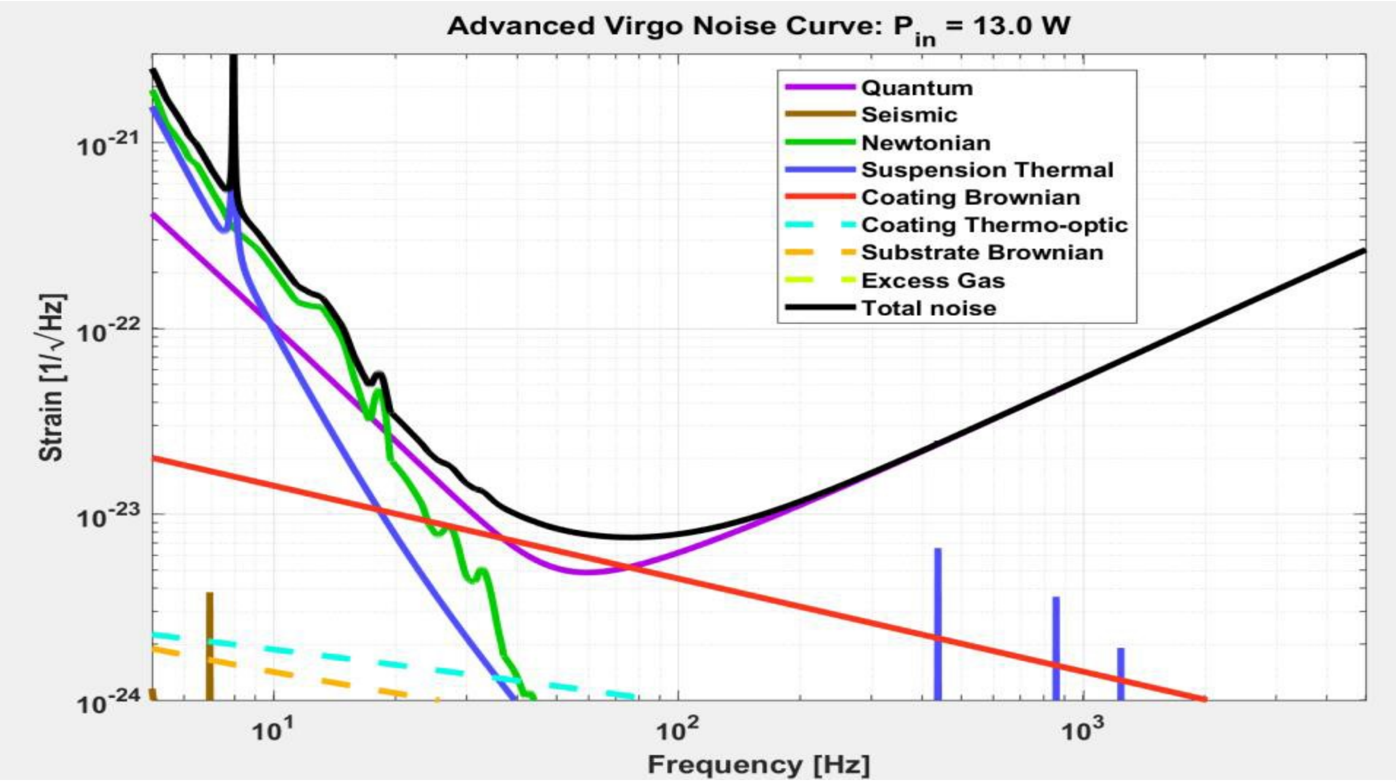

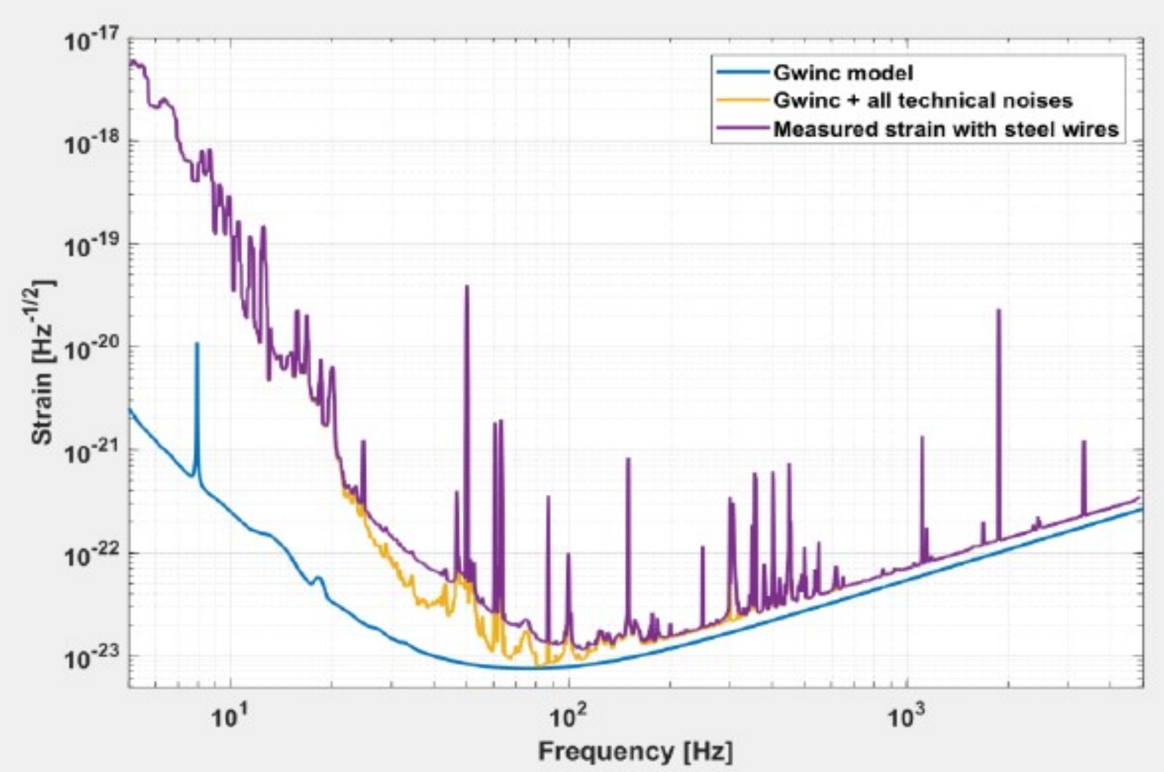

Pre- installation: commissioning to cure glitches

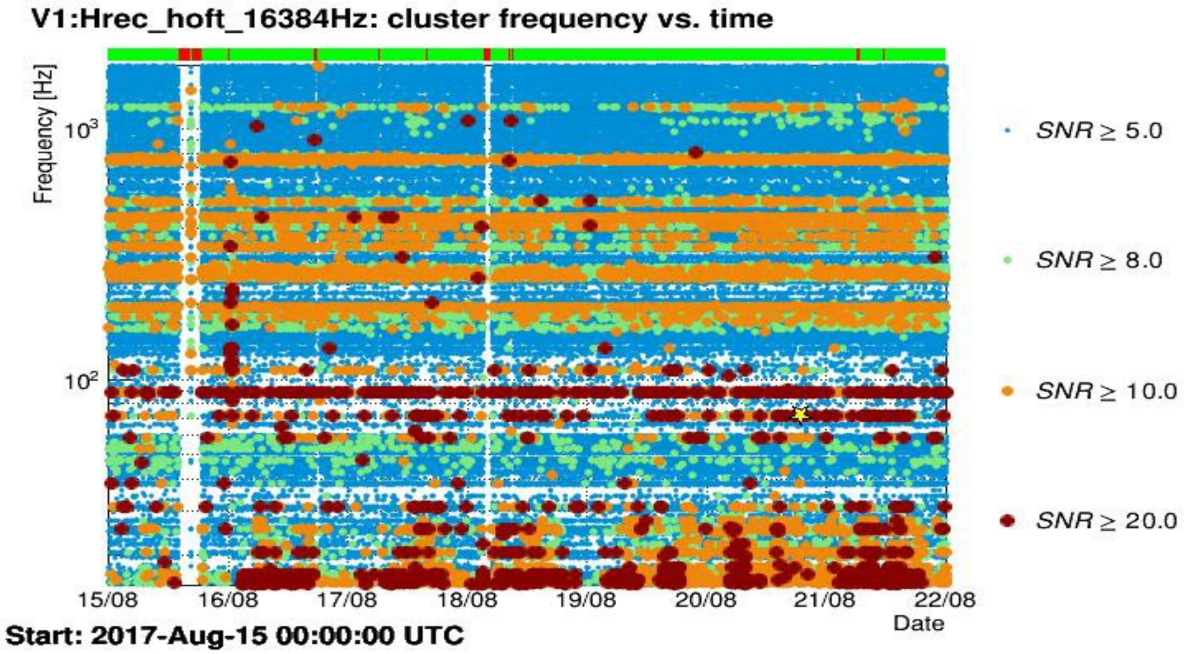

During O2

Post O2

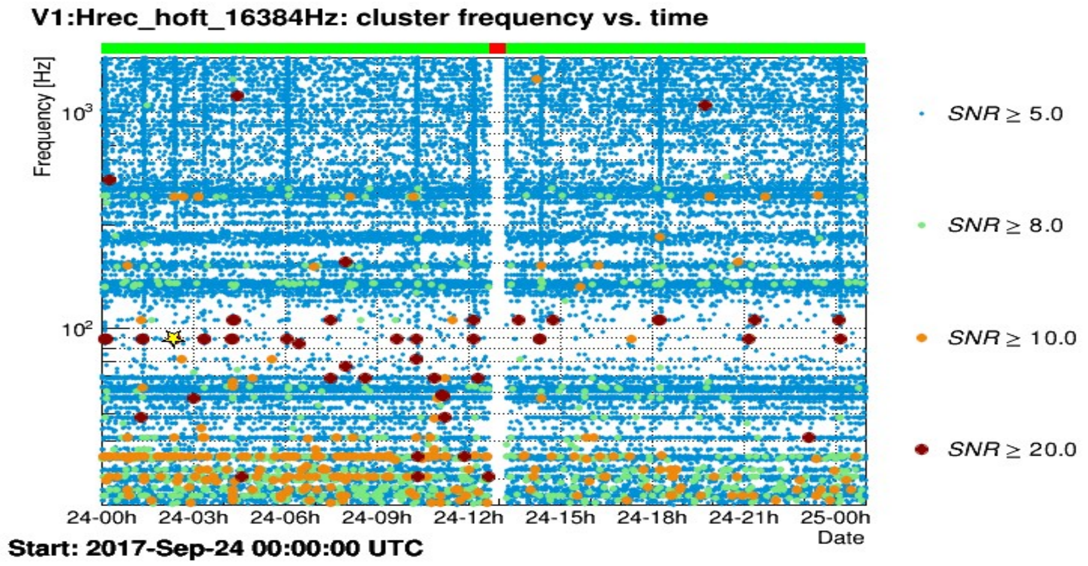

Monolithic suspensions are back

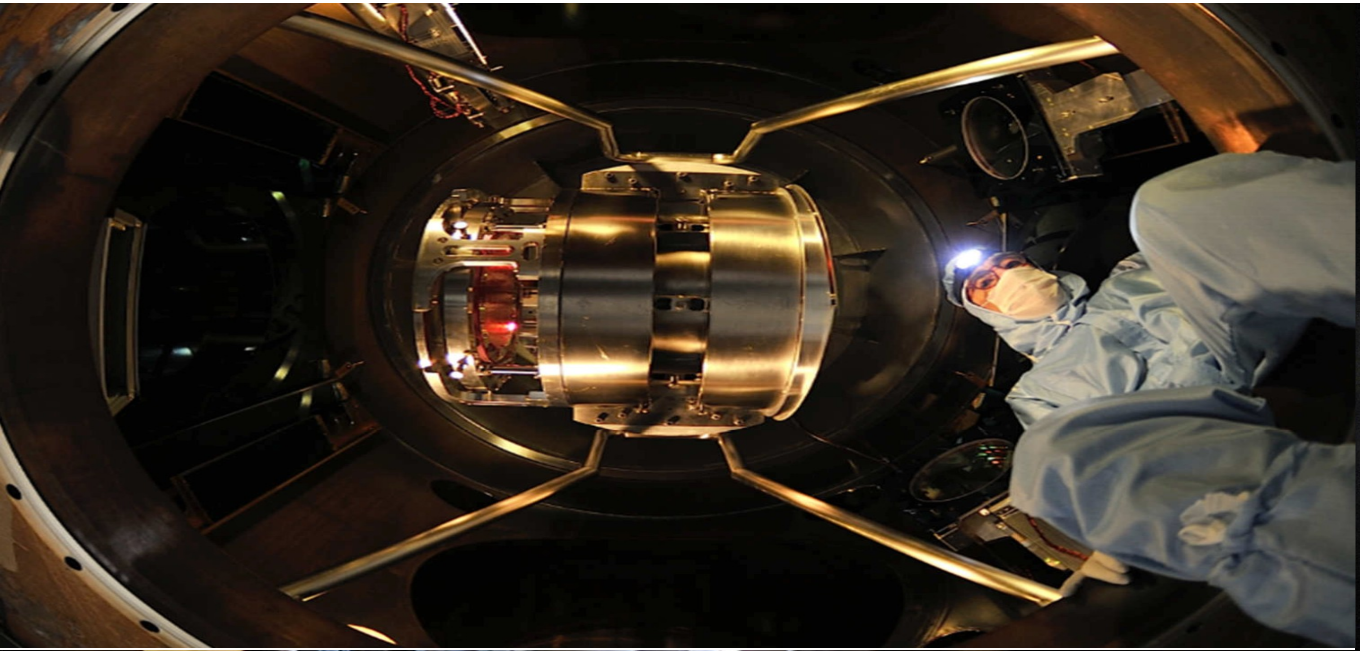

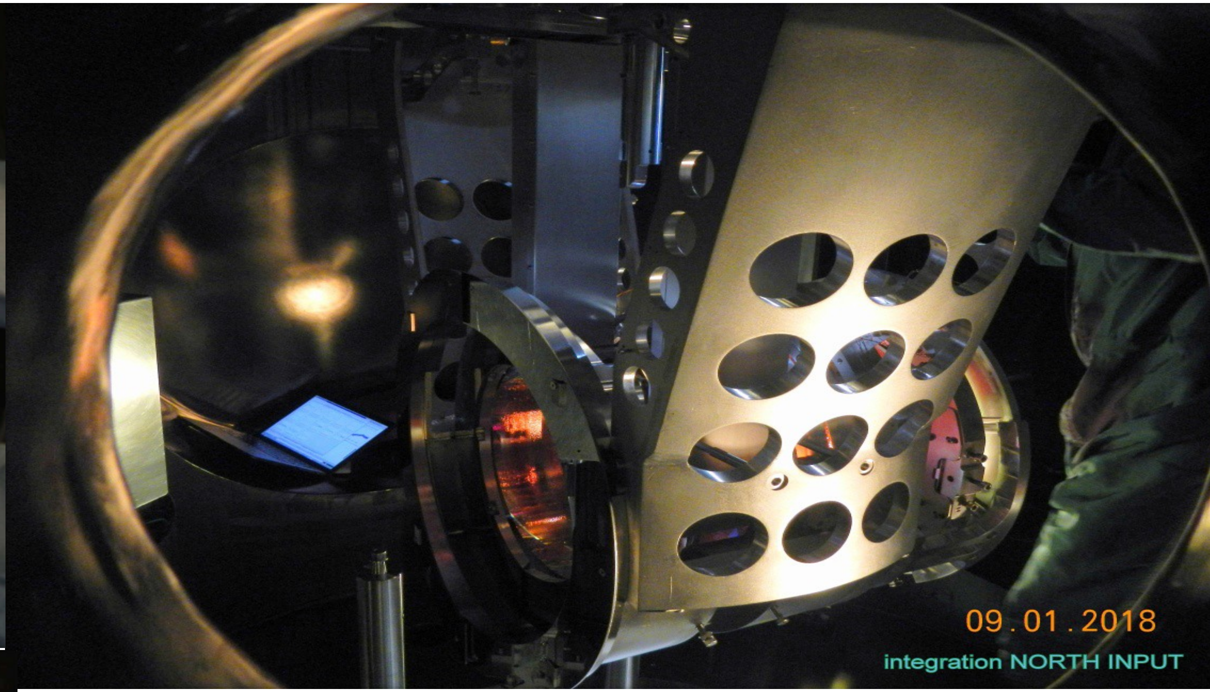

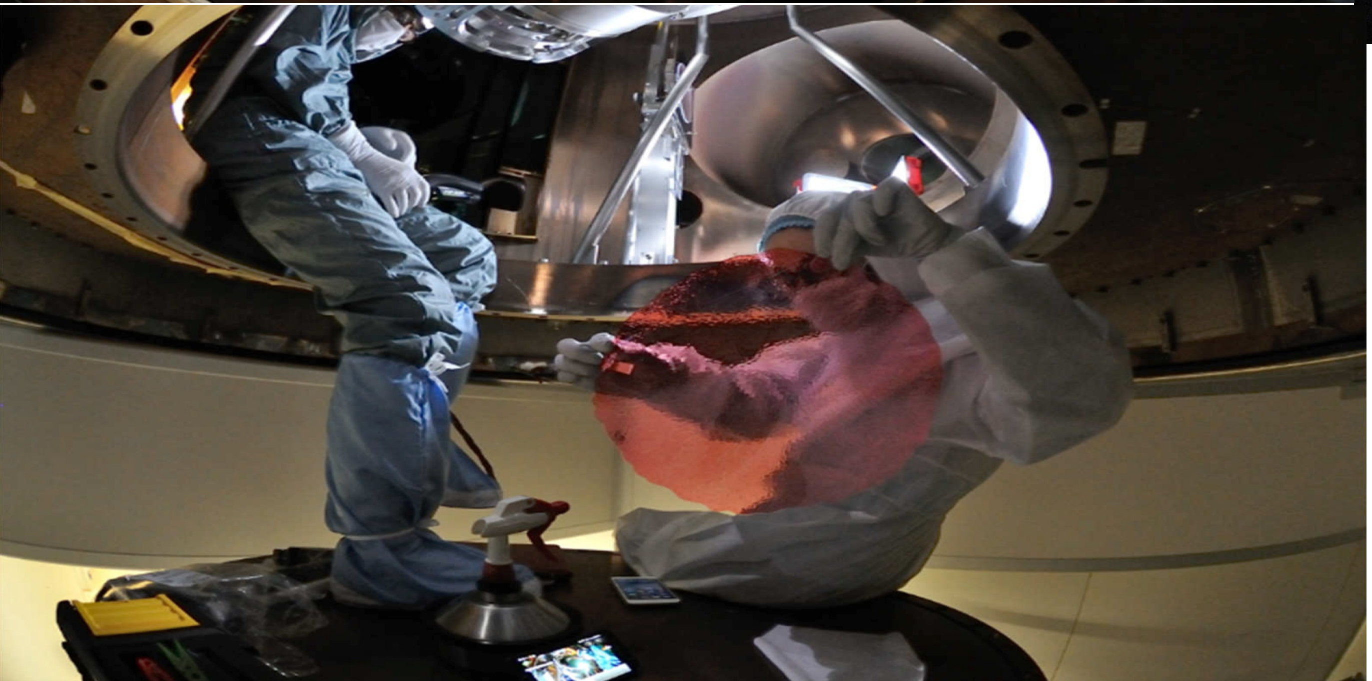

Done in less than four months

- Arm valves closed on Nov 27, reopen March 19
- Include two weeks of commissioning
- Faster than scheduled

Installation: additional highlights

Squeezing bench provided by AEI – MAX Planck
14 – 15 dB squeezed vacuum

(then when we match to the main interferometer significant loss in the gain are added)

Stray light hunting restarted adding extra baffles

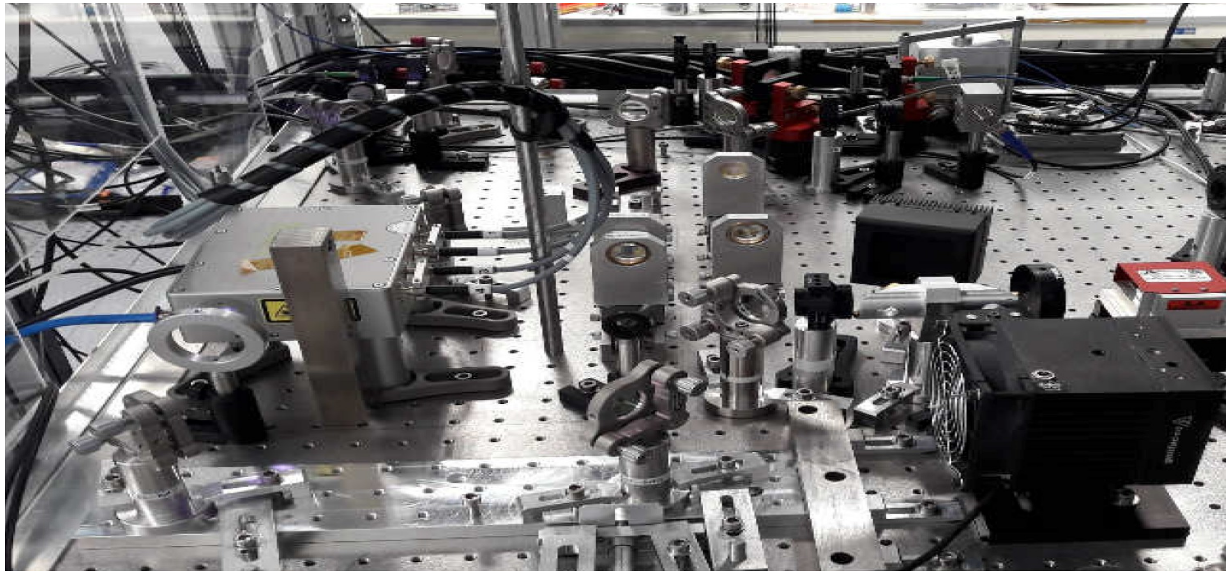

New laser amplifier 70 W ➔ 100 W
New pre-mode cleaner

We can inject in the ITF up to 50 W

Running a Quantum Optics Interferometer

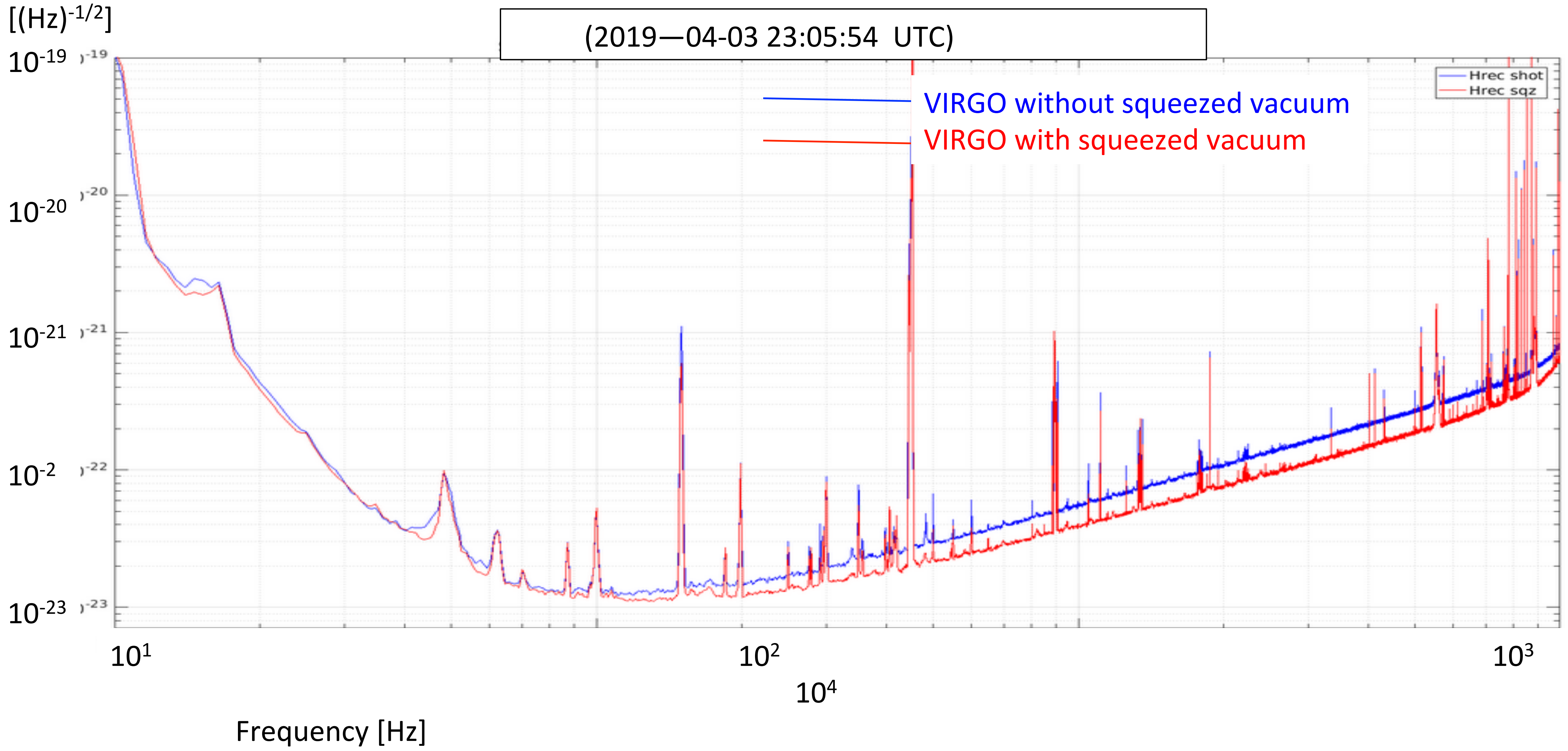

The aLIGO detectors

LIGO status: major hardware upgrade at both LIGO sites

- High power
- Laser noise
- Squeezing
- Signal recycling mirror change

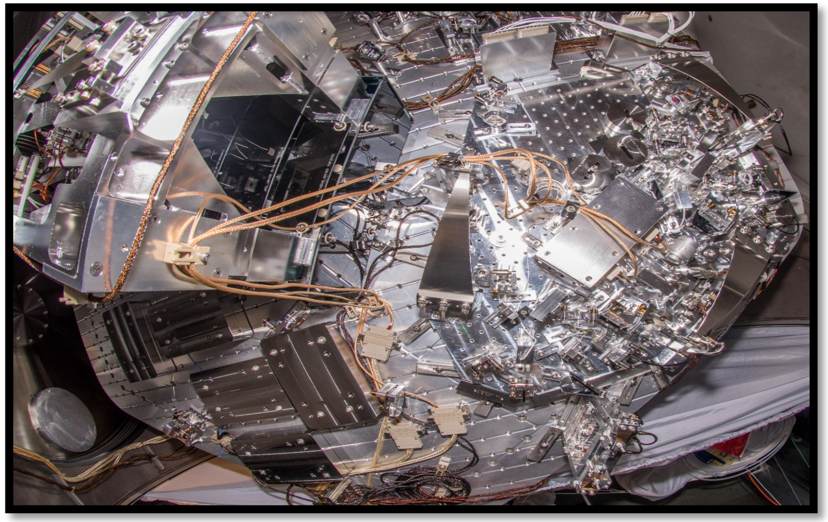

– Stray light control
– Electric field sensors
– Test mass replacements

Pre and post installation of the new baffles

Projection of noise improvements from high power and squeezing: 120 Mpc

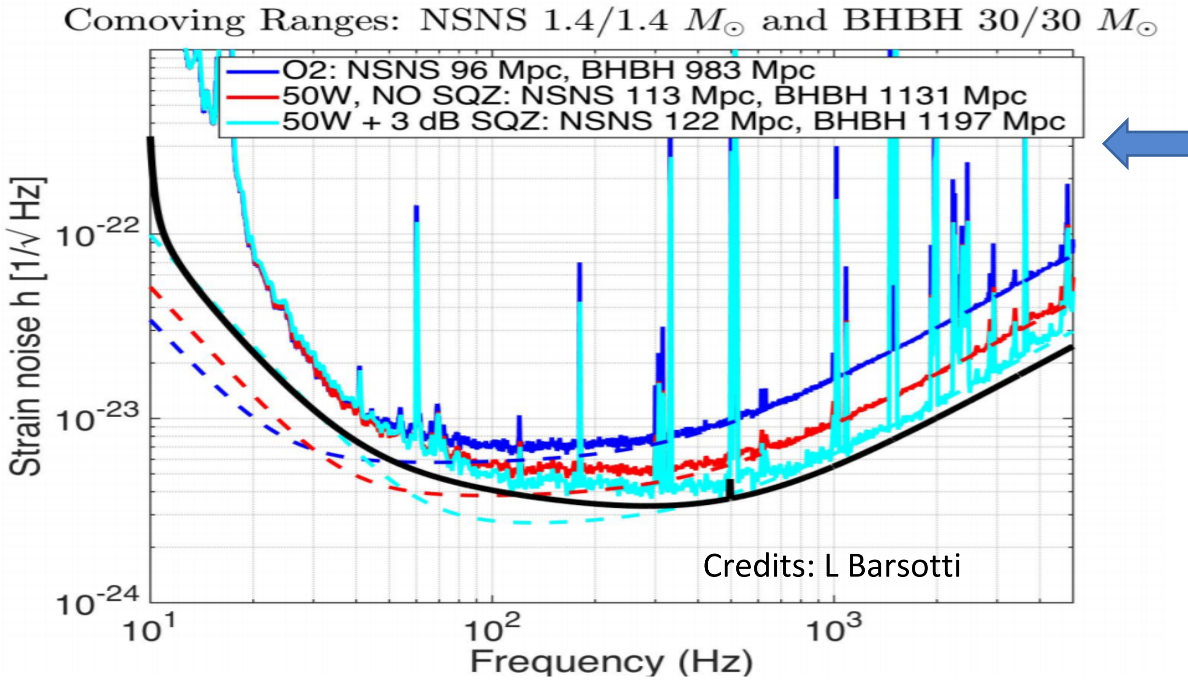

Livingston case

New installations and corresponding sensitivity improvements

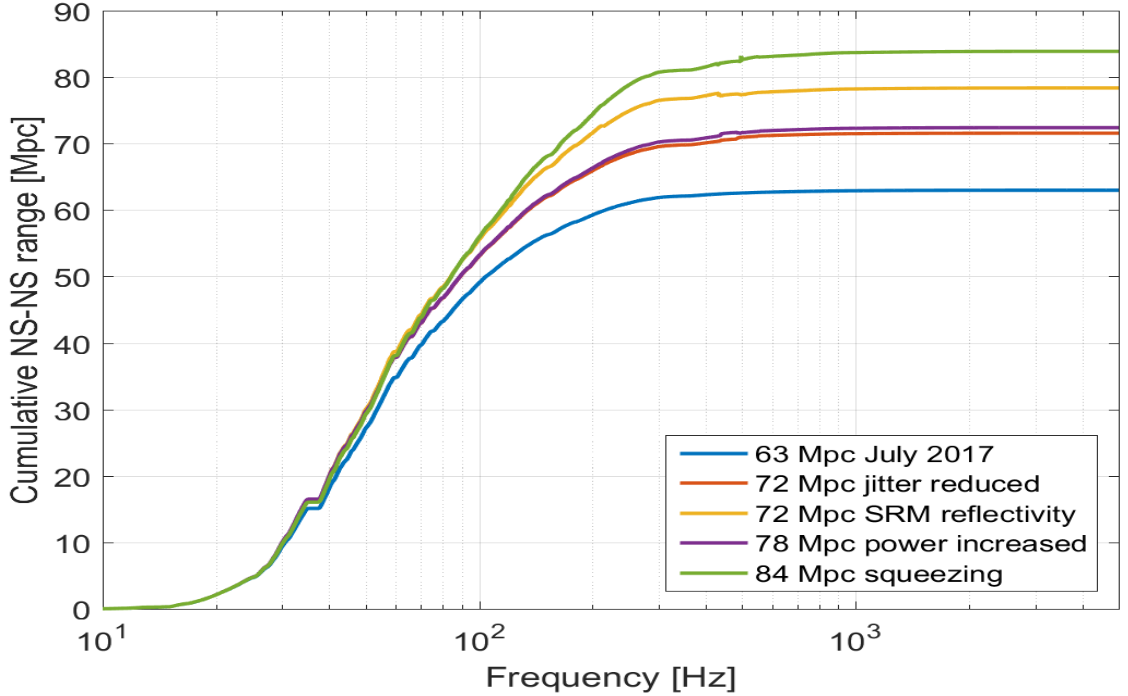

Hanford needs to improve low frequency noise in order to reach sensitivity goal for next observing run

KAGRA: a new partner will join soon the network

KAGRA project

Kamioka mine, Japan

3 km, underground, cryogenic detector (20 K)

KAGRA: from Installation to Commissioning - I

KAGRA: from Installation to Commissioning - II

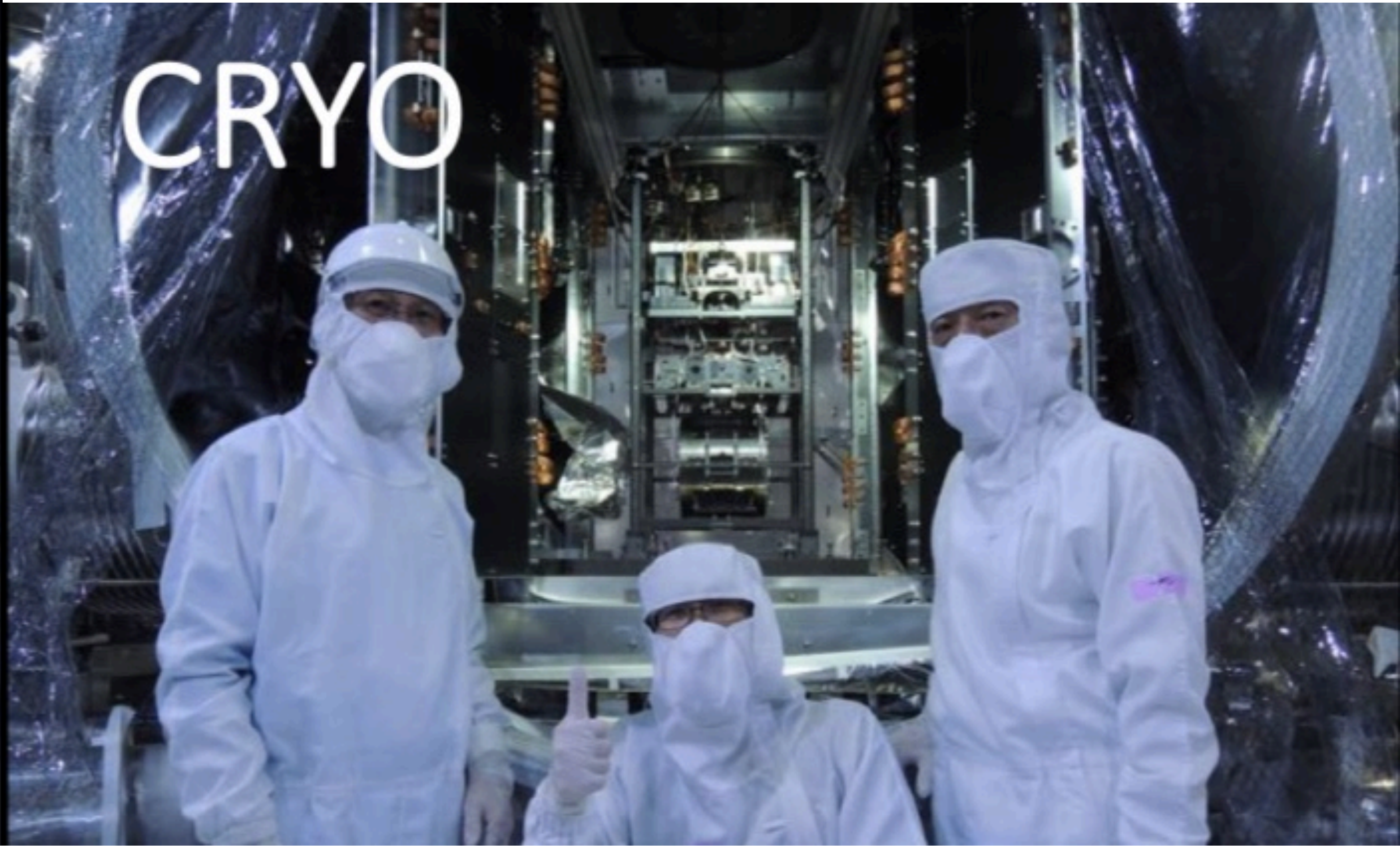

Installation Sequence

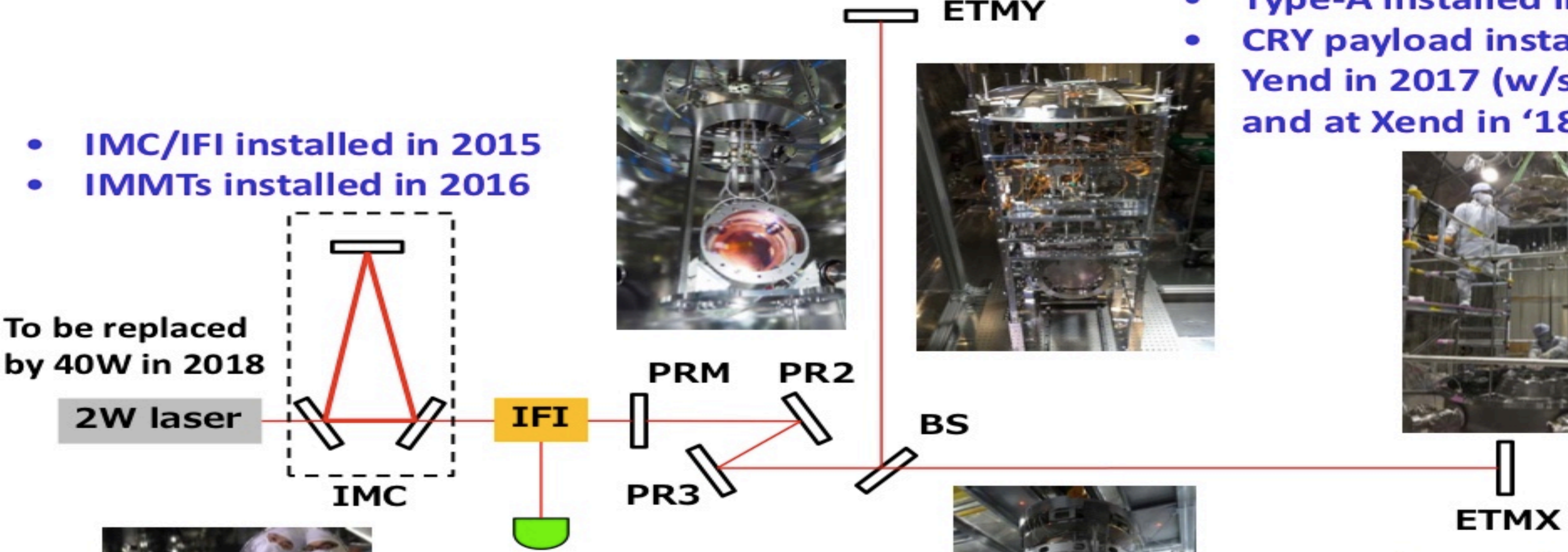

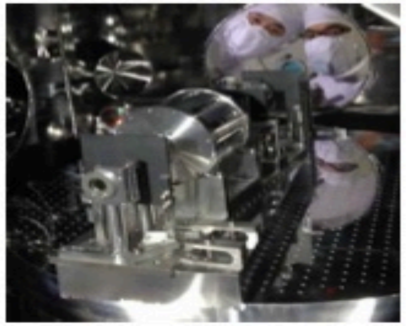

- IMC/IFI installed in 2015
- IMMTs installed in 2016

- Type-A installed in 2017
- CRY payload installed at Yend in 2017 (w/spare TM) and at Xend in '18 Mar.

- PRMs intalled in 2017 (Type-Bp suspension)
- BS installed in 2017 (Type-B suspension)

- Yend in vac '18/Jan
- ETMY cooled '18 Feb (currently T=18K)
- Center in vac '18/Mar
- Xend in vac '18/Apr

Credits : KAGRA coll.

Physics Results

Hunting several categories of GW signals emitted in different processes

TRANSIENT

PERSISTENT

Chirps from
from
Coalescent
Compact
Binaries
CBC

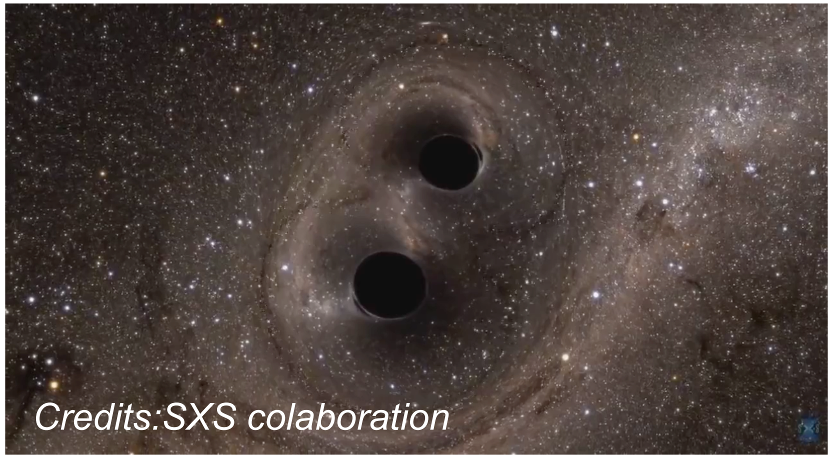

Matched
Filters

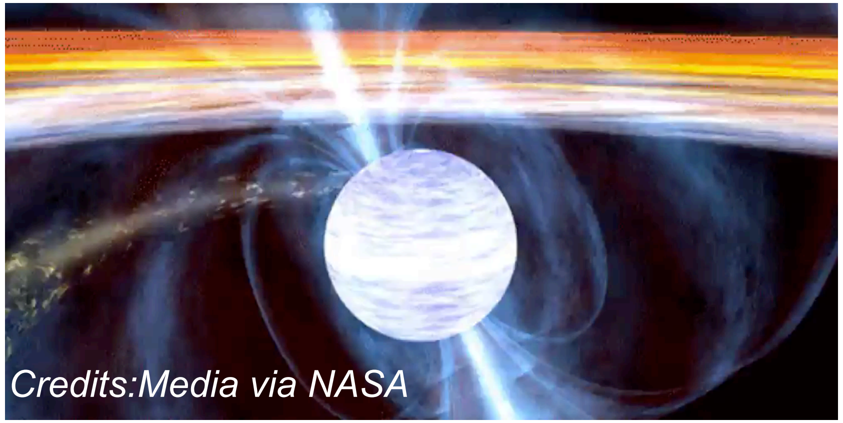

Quasi mono-chromatic signals due o Rotation of Asymmetric Neutron Stars

Burst from
Core
Collapse
Supernovae
CCSN

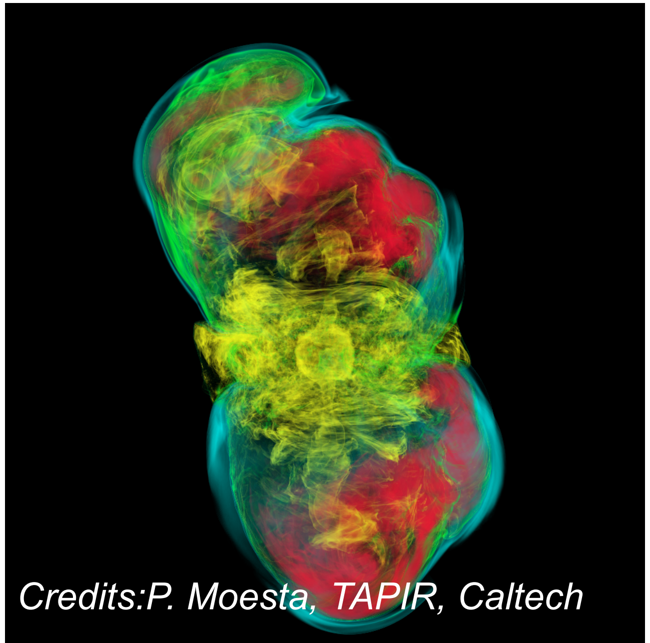

Unmodeled
waveforms

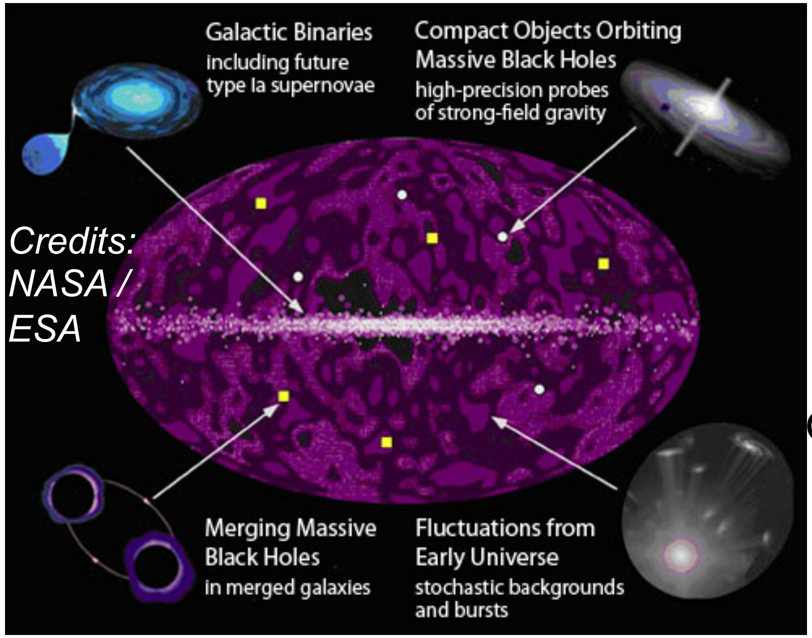

Stochastic signals due to Gravitational Background

A Primer on the GW signal

$$h(t) = F_+(\theta, \phi, \psi)\, h_+(t) + F_\times(\theta, \phi, \psi)\, h_\times(t)$$

(θ, ϕ) are angles describing the location of the source on the sky

ψ polarization angle

$h(t) = F(t)\,(\cos \xi\, h_+ + \sin \xi\, h_\times)$ ➔ spacetime strain seen by the interformeter

$F^2 = F_+^2 + F_\times^2$ (independent of the polarization angle ψ)

$\tan \xi = F_\times / F_+$

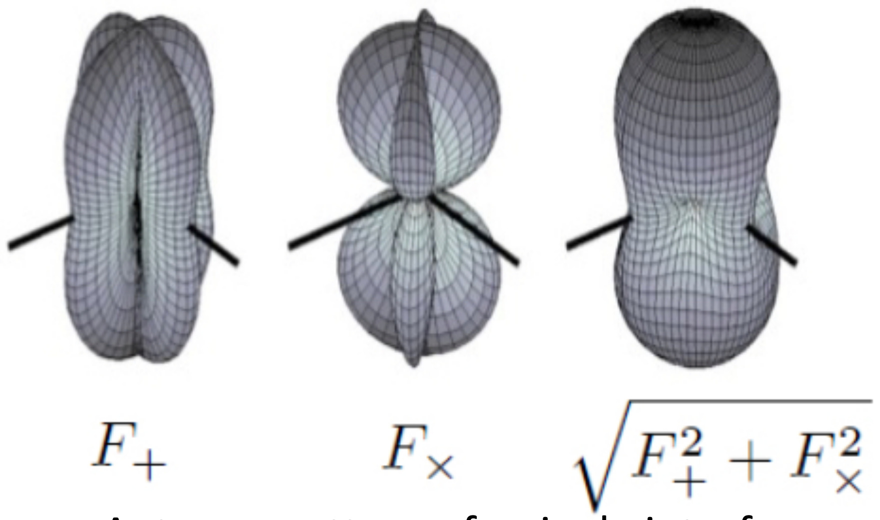

Antenna pattern of a single interferometer

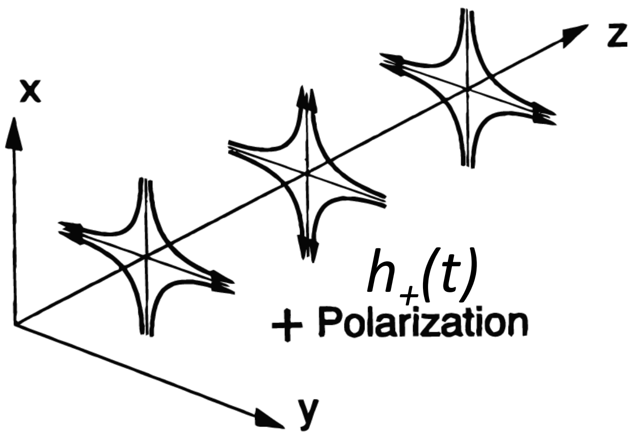

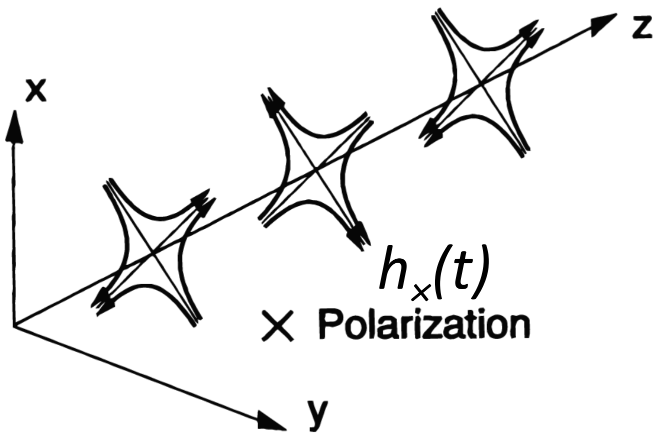

The detected GW signals so far are *Chirps*

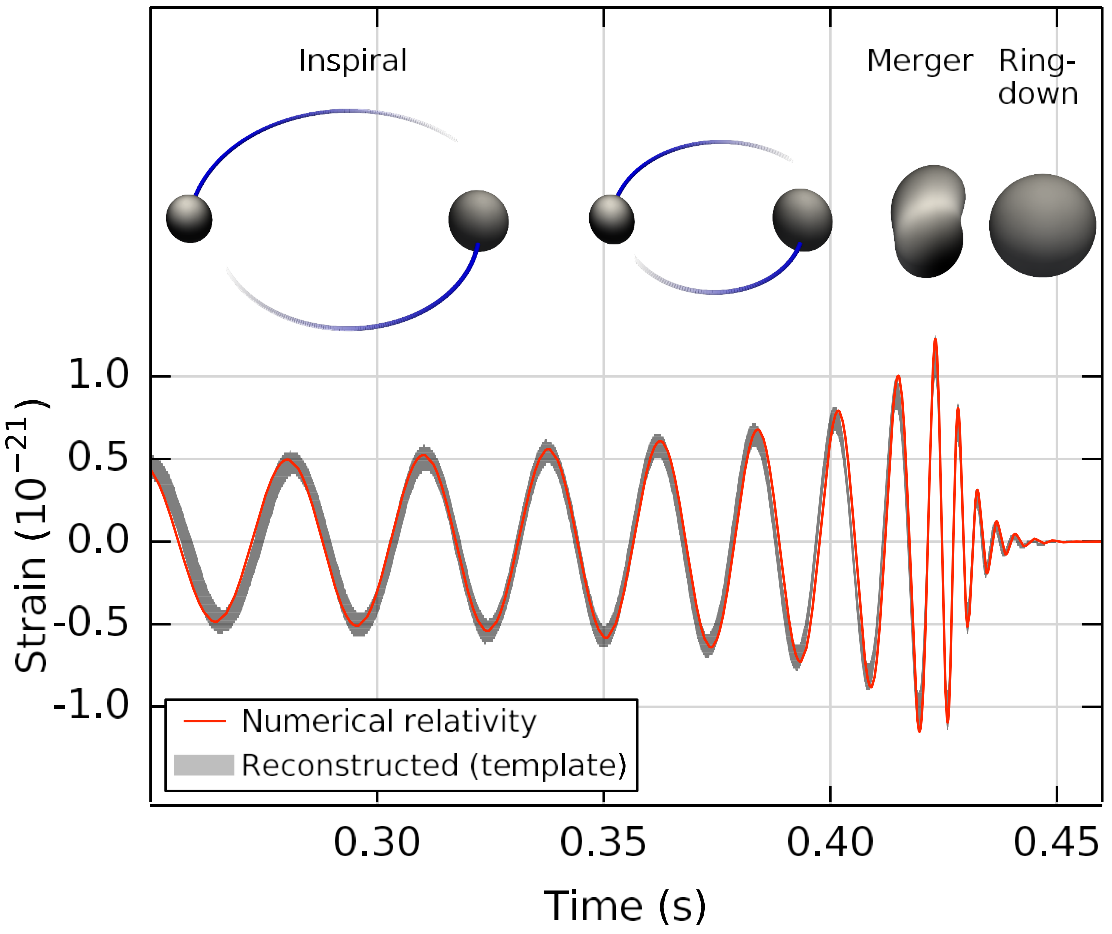

LVC, PRL 116 061102

In the case of with almost equal masses the orbit in the final phase the orbits tend to be circular

The chirp signal depends on 15 parameters

– Masses (2), spins (6), sky position (2), orientation (2), coalescence time and phase (2), distance (1)

- Matter effects add 2 more parameters

- At lowest order the signal phase depends on the chirp mass $\mathscr{M}$ (usually ***the best measured parameter***), then mass ratio, then spins, then matter effects

$$\mathscr{M} = \mu^{3/5} M^{2/5} = \frac{(m_1 m_2)^{3/5}}{(m_1+m_2)^{1/5}} \cong \frac{c^3}{G}\left(\frac{5}{96}\frac{1}{\pi^{8/3}}\nu^{-11}\frac{d\nu}{dt}\right)^{3/5}$$

Emission during the inspiral phase: the quadrupolar contribution

$$h_+ = \frac{2\mathcal{M}_z^{5/3}[\pi f(t)]^{2/3}}{D_L}\left[1+(\hat{L}\cdot\hat{n})^2\right]\cos[\Phi(t)]$$

$$h_\times = \frac{4\mathcal{M}_z^{5/3}[\pi f(t)]^{2/3}(\hat{L}\cdot\hat{n})}{D_L}\sin[\Phi(t)]$$

$$\mathcal{M}_z = (1+z)(m_1 m_2)^{3/5}/(m_1+m_2)^{1/5}$$

$$\mathcal{M} = \frac{(m_1 m_2)^{3/5}}{M^{1/5}} = \frac{c^3}{G}\left[\frac{5}{96}\pi^{-8/3} f^{-11/3}\dot{f}\right]^{3/5}$$

The horizon for NS $M_1 = M_2$ at SNR=8

$$D_L = \frac{1}{8}\left(\frac{5\pi}{24c^3}\right)^{1/2}(G\mathcal{M})^{5/6}\pi^{-7/6}\sqrt{4\int_{f_{low}}^{f_{high}}\frac{f^{-7/3}}{S_n(f)}df}$$

The Catalogue of the GW signals from BBH

BH merger rate density

$R = 53.2(^{+58.5}_{-28.8})\ \mathrm{Gpc^{-3}\,yr^{-1}}$
(90% credibility)
arXiv:1811.12940

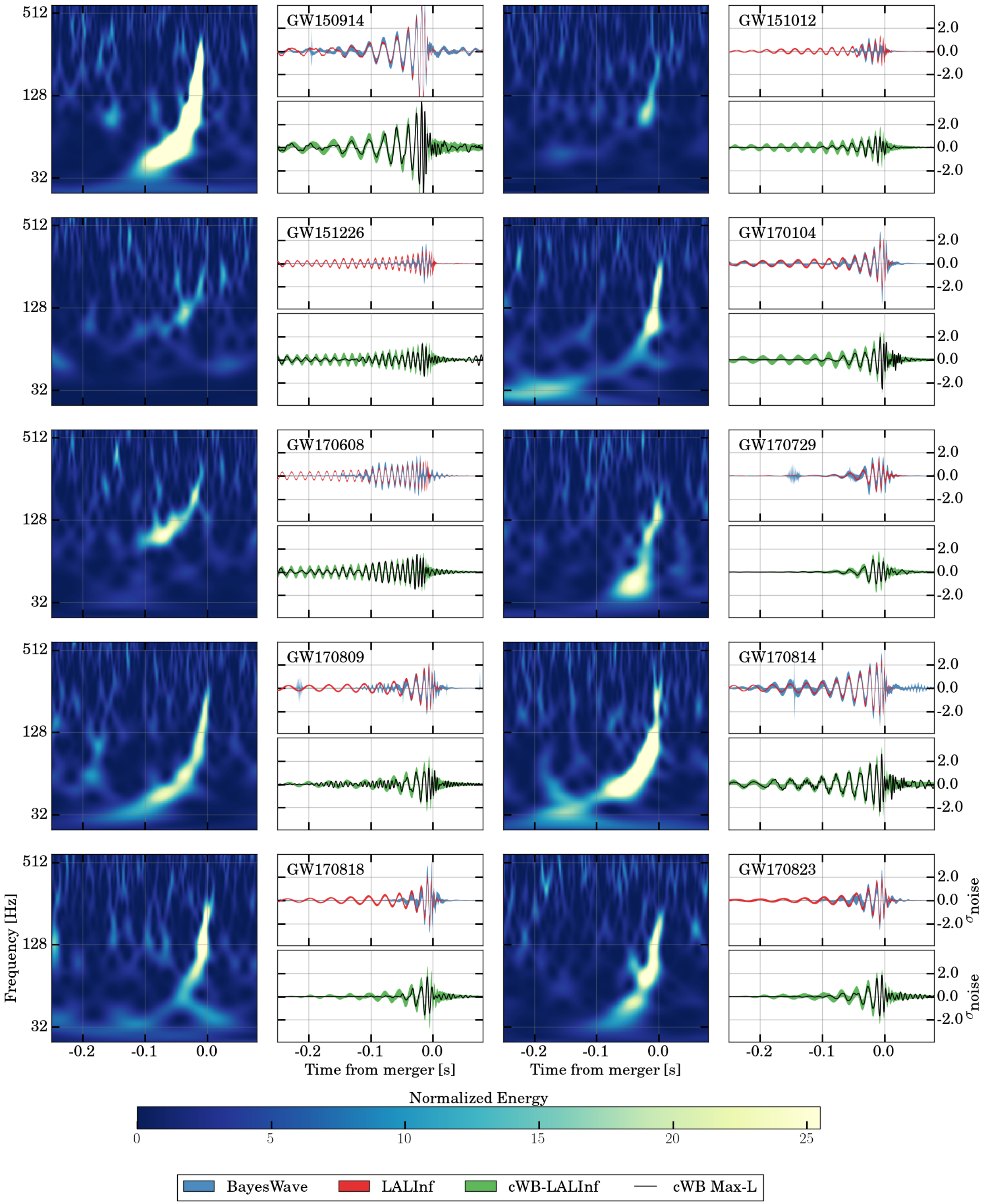

… and from NSNS GW170817

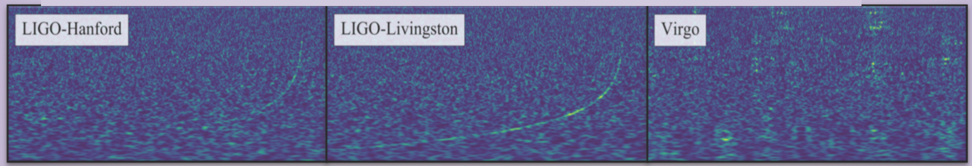

observed by	H, L, V
source type	binary neutron star (NS)
date	17 August 2017
time of merger	12:41:04 UTC
signal-to-noise ratio	32.4
false alarm rate	< 1 in 80 000 years
distance	85 to 160 million light-years
total mass	2.73 to 3.29 $M_\odot$
primary NS mass	1.36 to 2.26 $M_\odot$
secondary NS mass	0.86 to 1.36 $M_\odot$
mass ratio	0.4 to 1.0
radiated GW energy	> 0.025 $M_\odot c^2$
radius of a 1.4 $M_\odot$ NS	likely ≲ 14 km
effective spin parameter	-0.01 to 0.17
effective precession spin parameter	unconstrained
GW speed deviation from speed of light	< few parts in 10^{15}

inferred duration from 30 Hz to 2048 Hz**	~ 60 s
inferred # of GW cycles from 30 Hz to 2048 Hz**	~ 3000
initial astronomer alert latency*	27 min
HLV sky map alert latency*	5 hrs 14 min
HLV sky area†	28 deg^2
# of EM observatories that followed the trigger	~ 70
also observed in	gamma-ray, X-ray, ultraviolet, optical, infrared, radio
host galaxy	NGC 4993
source RA, Dec	$13^h09^m48^s$, -23°22'53"
sky location	in Hydra constellation
viewing angle (without and with host galaxy identification)	≤ 56° and ≤ 28°
Hubble constant inferred from host galaxy identification	62 to 107 km s^{-1} Mpc^{-1}

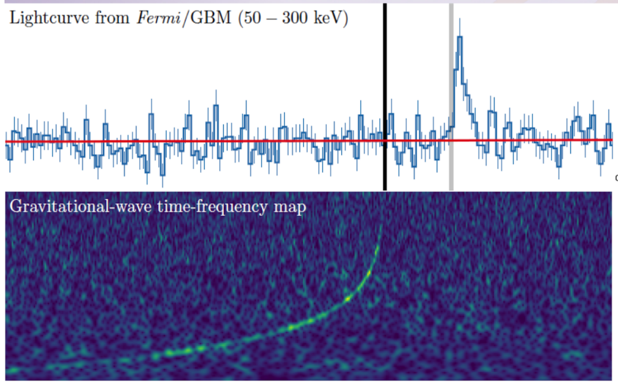

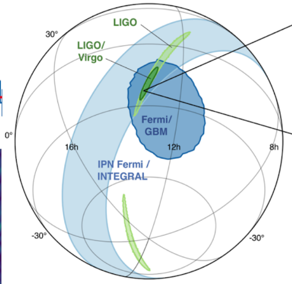

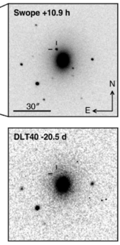

Parameter correlations – I

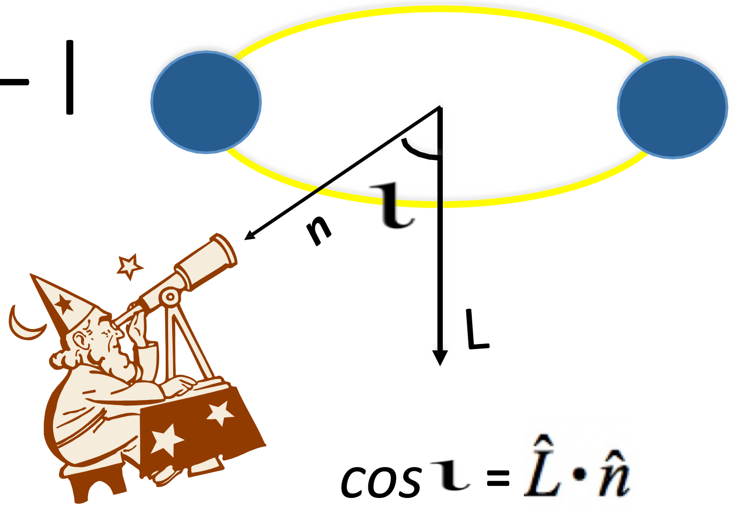

$\cos\iota = \hat{L}\cdot\hat{n}$

- The amplitude of GWs emitted by compact binaries depends on the *luminosity distance D_L*
- The *luminosity distance* enters both polarizations in combination with the *orbital inclination angle* ➔ degeneracies.
- An inclination of θ = 90° means we are looking at the binary (approximately) edge-on.

<u>Polarization</u> can be used to break the degeneracy between distance and inclination
and for this we need

2 LIGOs + Virgo

$$h_+ \propto \frac{(\hat{L}\cdot\hat{n}+1)^2}{2D_L}$$

$$h_\times \propto \frac{\hat{L}\cdot\hat{n}}{D_L}$$

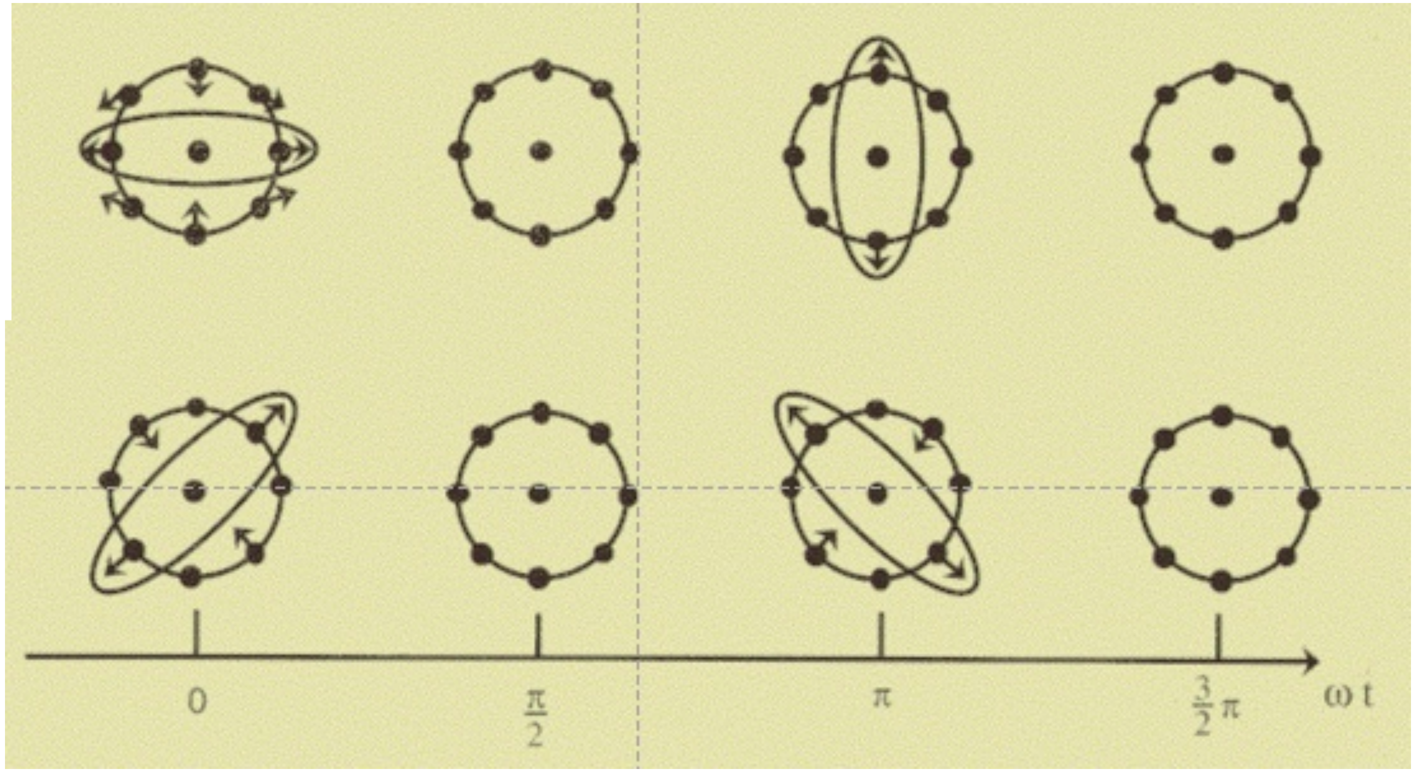

Effect of orientation of binary's orbital plane

Polarization of gravitational waves depends on the orientation of the orbital plan of the binary system.

Face-on we observe a mixture, while edge-on we observe pure h

$q = m_1/m_2$

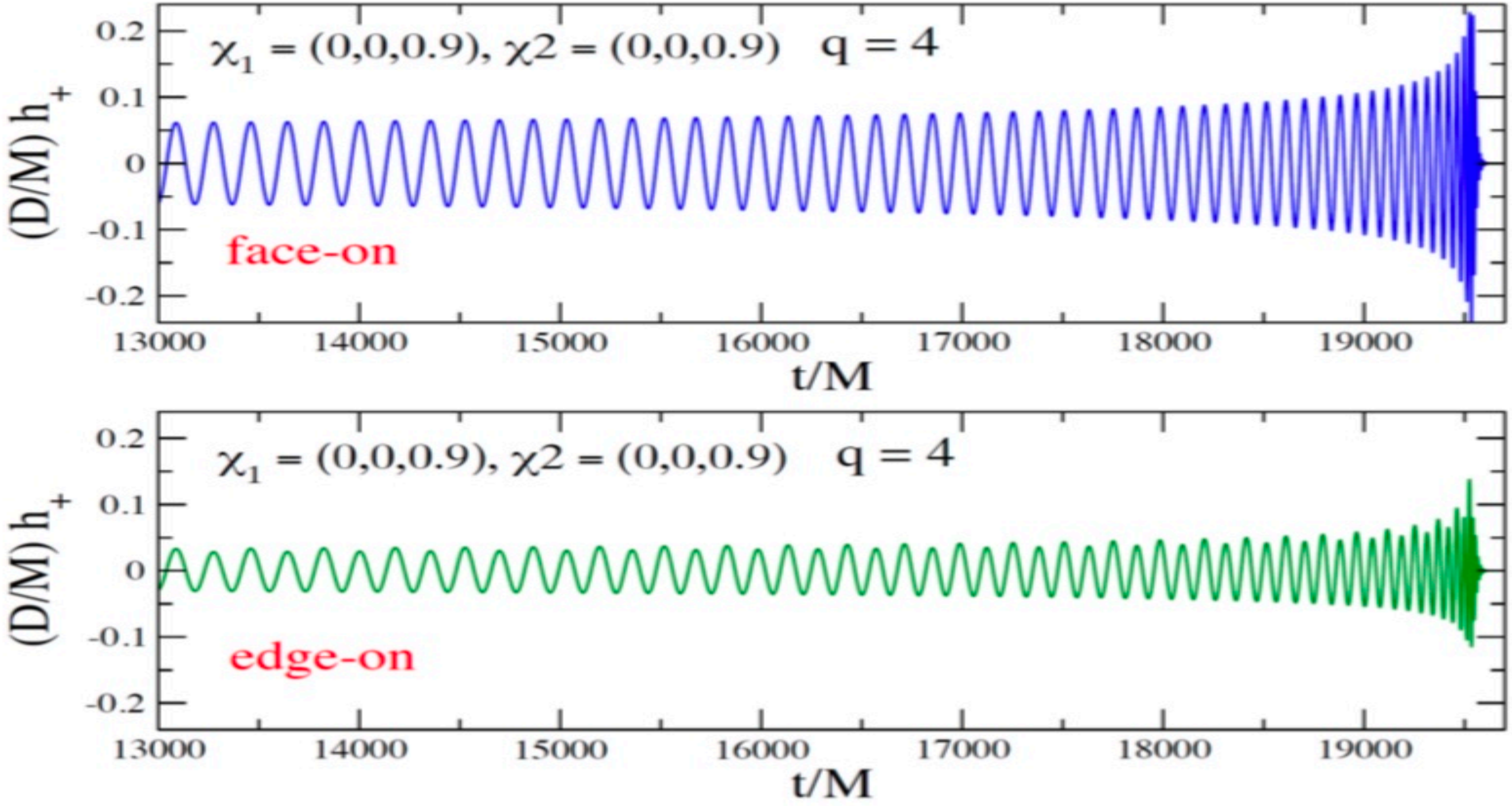

Spinning, but non-precessing binary

SPIN

- We usually work with dimensionless spins $\boldsymbol{a_i = c\ |\vec{S}_i|\ /\ (G\ m_i^2)} \leq 1$ and their components to the respect of the orbital angular momentum:

0 =no spin, ±1=maximally spinning (along the same/opposite direction of the orbital angular momentum)

- Poor accuracy in measuring the individual spins

(Purrer et al. , PRD93,084042; Vitale et al. PRL 112 251101, PRD 95 064053)

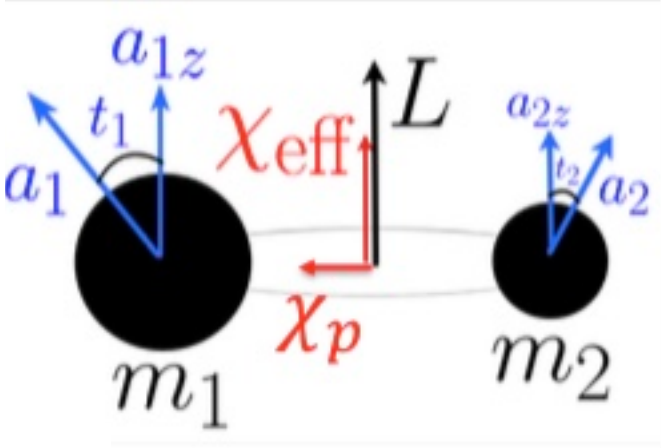

$$\chi_{eff} = \frac{m_1 a_{1z} + m_2 a_{2z}}{m_1 + m_2}$$

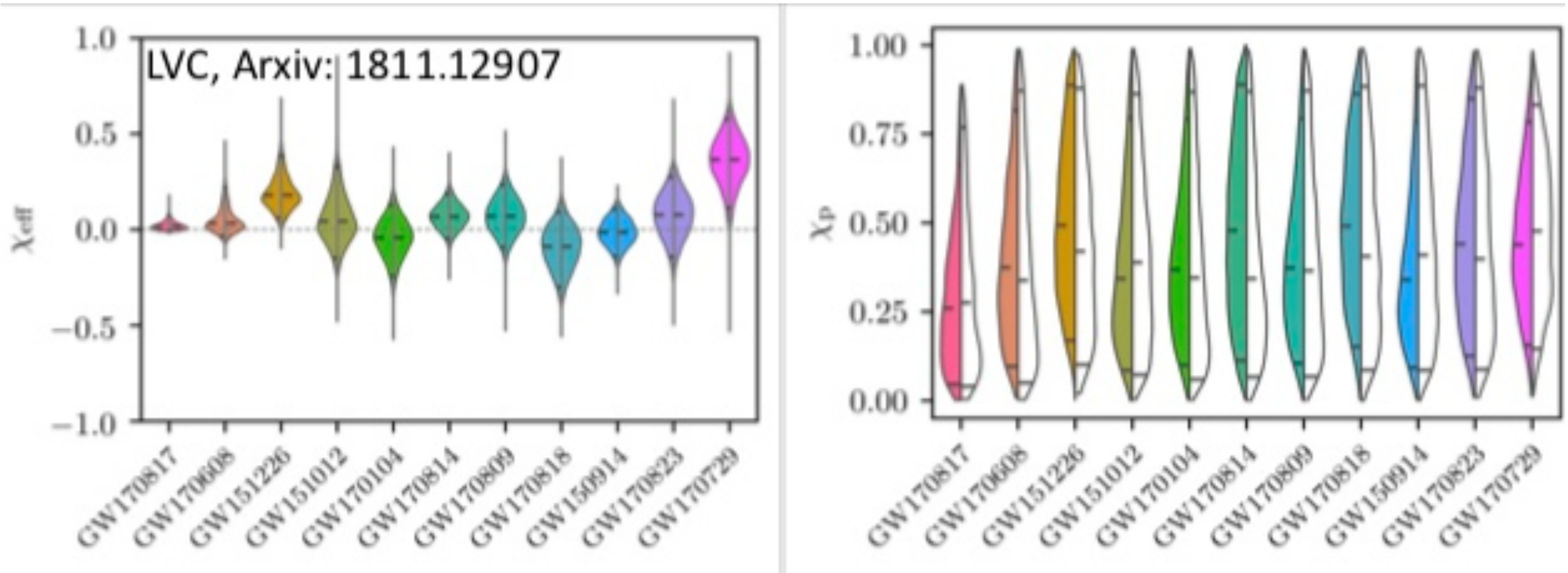

Parameter correlations – I I

In the case of low masses the signal analysis is dominated by the inspiral phase where ***mass ratio*** *$q = m_1/m_2$* and the ***component of the total spin along the orbital angular momentum***, are correlated

$q = m_1/m_2$

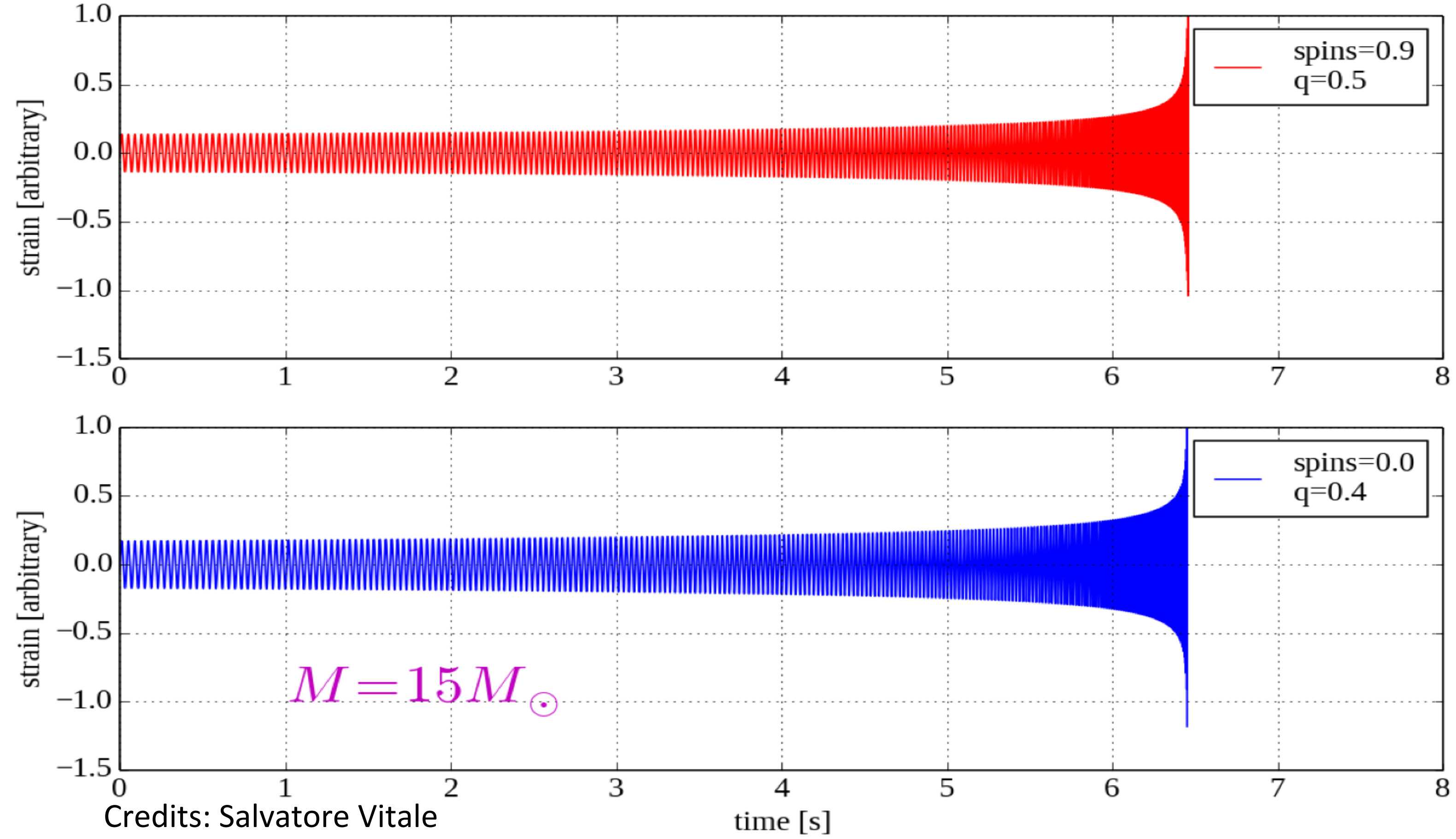

Credits: Salvatore Vitale

System Parameters derived from the O1 /O2 detected signals

Event	$m_1/\mathrm{M}_\odot$	$m_2/\mathrm{M}_\odot$	$\mathcal{M}/\mathrm{M}_\odot$	χ_{eff}	$M_{\mathrm{f}}/\mathrm{M}_\odot$	a_{f}	$E_{\mathrm{rad}}/(\mathrm{M}_\odot c^2)$	$\ell_{\mathrm{peak}}/(\mathrm{erg\,s^{-1}})$	d_L/Mpc	z	$\Delta\Omega/\mathrm{deg}^2$
GW150914	$35.6^{+4.8}_{-3.0}$	$30.6^{+3.0}_{-4.4}$	$28.6^{+1.6}_{-1.5}$	$-0.01^{+0.12}_{-0.13}$	$63.1^{+3.3}_{-3.0}$	$0.69^{+0.05}_{-0.04}$	$3.1^{+0.4}_{-0.4}$	$3.6^{+0.4}_{-0.4} \times 10^{56}$	430^{+150}_{-170}	$0.09^{+0.03}_{-0.03}$	179
GW151012	$23.3^{+14.0}_{-5.5}$	$13.6^{+4.1}_{-4.8}$	$15.2^{+2.0}_{-1.1}$	$0.04^{+0.28}_{-0.19}$	$35.7^{+9.9}_{-3.8}$	$0.67^{+0.13}_{-0.11}$	$1.5^{+0.5}_{-0.5}$	$3.2^{+0.8}_{-1.7} \times 10^{56}$	1060^{+540}_{-480}	$0.21^{+0.09}_{-0.09}$	1555
GW151226	$13.7^{+8.8}_{-3.2}$	$7.7^{+2.2}_{-2.6}$	$8.9^{+0.3}_{-0.3}$	$0.18^{+0.20}_{-0.12}$	$20.5^{+6.4}_{-1.5}$	$0.74^{+0.07}_{-0.05}$	$1.0^{+0.1}_{-0.2}$	$3.4^{+0.7}_{-1.7} \times 10^{56}$	440^{+180}_{-190}	$0.09^{+0.04}_{-0.04}$	1033
GW170104	$31.0^{+7.2}_{-5.6}$	$20.1^{+4.9}_{-4.5}$	$21.5^{+2.1}_{-1.7}$	$-0.04^{+0.17}_{-0.20}$	$49.1^{+5.2}_{-3.9}$	$0.66^{+0.08}_{-0.10}$	$2.2^{+0.5}_{-0.5}$	$3.3^{+0.6}_{-0.9} \times 10^{56}$	960^{+430}_{-410}	$0.19^{+0.07}_{-0.08}$	924
GW170608	$10.9^{+5.3}_{-1.7}$	$7.6^{+1.3}_{-2.1}$	$7.9^{+0.2}_{-0.2}$	$0.03^{+0.19}_{-0.07}$	$17.8^{+3.2}_{-0.7}$	$0.69^{+0.04}_{-0.04}$	$0.9^{+0.0}_{-0.1}$	$3.5^{+0.4}_{-1.3} \times 10^{56}$	320^{+120}_{-110}	$0.07^{+0.02}_{-0.02}$	396
GW170729	$50.6^{+16.6}_{-10.2}$	$34.3^{+9.1}_{-10.1}$	$35.7^{+6.5}_{-4.7}$	$0.36^{+0.21}_{-0.25}$	$80.3^{+14.6}_{-10.2}$	$0.81^{+0.07}_{-0.13}$	$4.8^{+1.7}_{-1.7}$	$4.2^{+0.9}_{-1.5} \times 10^{56}$	2750^{+1350}_{-1320}	$0.48^{+0.19}_{-0.20}$	1033
GW170809	$35.2^{+8.3}_{-6.0}$	$23.8^{+5.2}_{-5.1}$	$25.0^{+2.1}_{-1.6}$	$0.07^{+0.16}_{-0.16}$	$56.4^{+5.2}_{-3.7}$	$0.70^{+0.08}_{-0.09}$	$2.7^{+0.6}_{-0.6}$	$3.5^{+0.6}_{-0.9} \times 10^{56}$	990^{+320}_{-380}	$0.20^{+0.05}_{-0.07}$	340
GW170814	$30.7^{+5.7}_{-3.0}$	$25.3^{+2.9}_{-4.1}$	$24.2^{+1.4}_{-1.1}$	$0.07^{+0.12}_{-0.11}$	$53.4^{+3.2}_{-2.4}$	$0.72^{+0.07}_{-0.05}$	$2.7^{+0.4}_{-0.3}$	$3.7^{+0.4}_{-0.5} \times 10^{56}$	580^{+160}_{-210}	$0.12^{+0.03}_{-0.04}$	87
GW170817	$1.46^{+0.12}_{-0.10}$	$1.27^{+0.09}_{-0.09}$	$1.186^{+0.001}_{-0.001}$	$0.00^{+0.02}_{-0.01}$	≤ 2.8	≤ 0.89	≥ 0.04	$\geq 0.1 \times 10^{56}$	40^{+10}_{-10}	$0.01^{+0.00}_{-0.00}$	16
GW170818	$35.5^{+7.5}_{-4.7}$	$26.8^{+4.3}_{-5.2}$	$26.7^{+2.1}_{-1.7}$	$-0.09^{+0.18}_{-0.21}$	$59.8^{+4.8}_{-3.8}$	$0.67^{+0.07}_{-0.08}$	$2.7^{+0.5}_{-0.5}$	$3.4^{+0.5}_{-0.7} \times 10^{56}$	1020^{+430}_{-360}	$0.20^{+0.07}_{-0.07}$	39
GW170823	$39.6^{+10.0}_{-6.6}$	$29.4^{+6.3}_{-7.1}$	$29.3^{+4.2}_{-3.2}$	$0.08^{+0.20}_{-0.22}$	$65.6^{+9.4}_{-6.6}$	$0.71^{+0.08}_{-0.10}$	$3.3^{+0.9}_{-0.8}$	$3.6^{+0.6}_{-0.9} \times 10^{56}$	1850^{+840}_{-840}	$0.34^{+0.13}_{-0.14}$	1651

LVC, Arxiv:1811.12907

The BH Individual masses

LVC, Arxiv:1811.12907

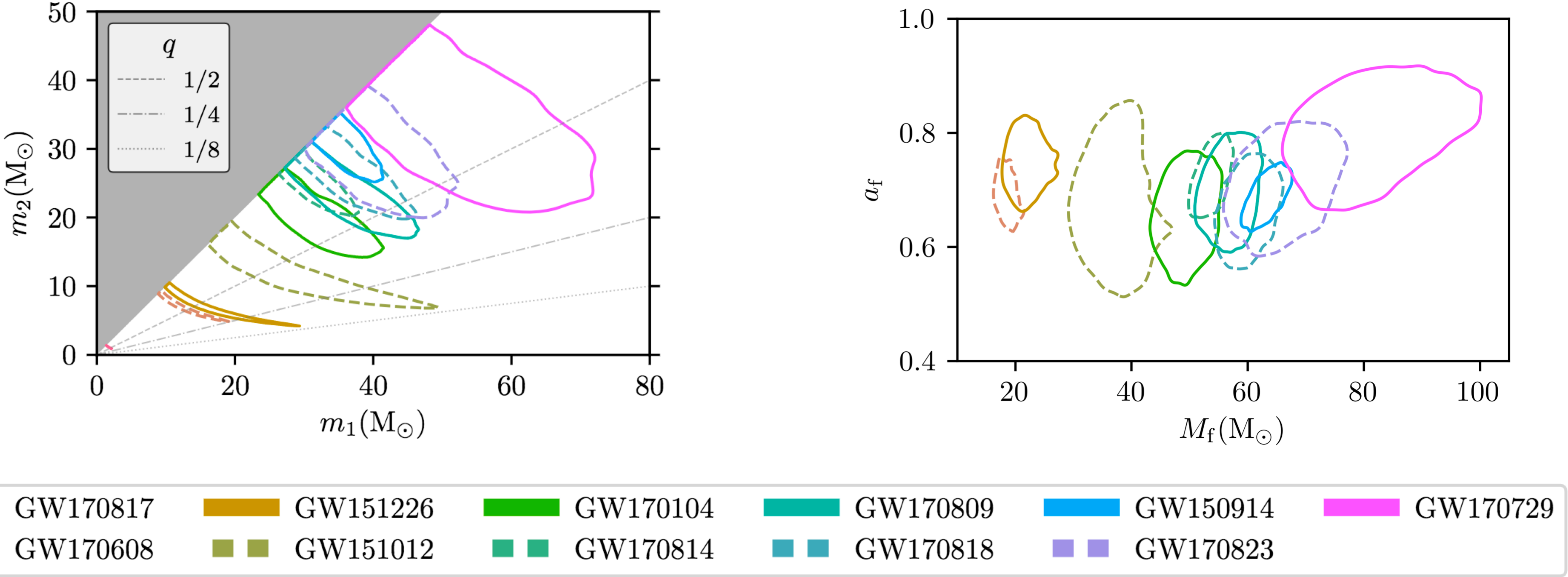

q = m₁/m₂ (assumption ➔ m₁ > m₂)

$q = m_1/m_2$ (*assumption* ➔ $m_1 > m_2$)

M_f ➔ Mass of the final BH

$a_f = c\ |\vec{S_f}|/(GM_f^2)$ ➔ normalized spin of the final BH

Mass ratio and Spin correlation

The mass ratio is not usually measured well due to correlation with the effective spin parameter (Baird et al. , Arxiv:1211.0546), which for low-mass events introduces characteristic skewness

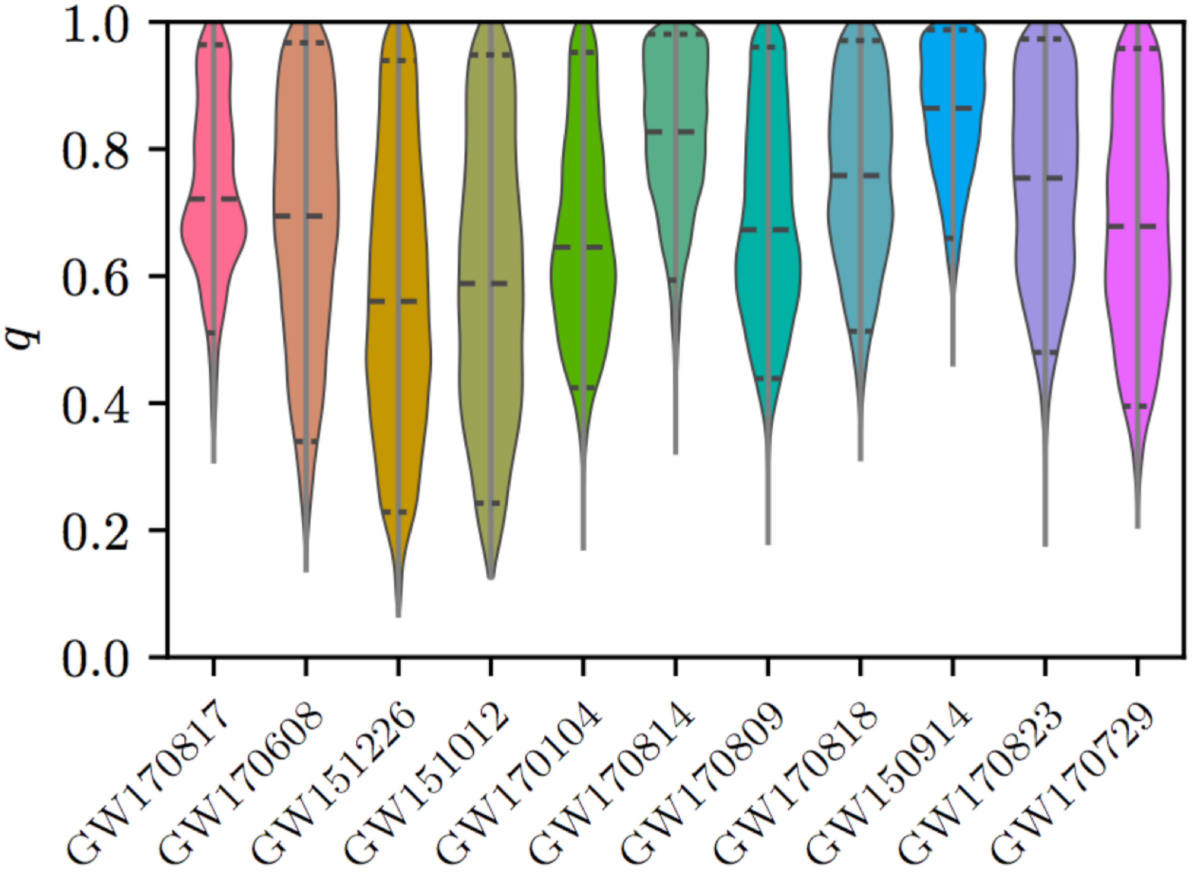

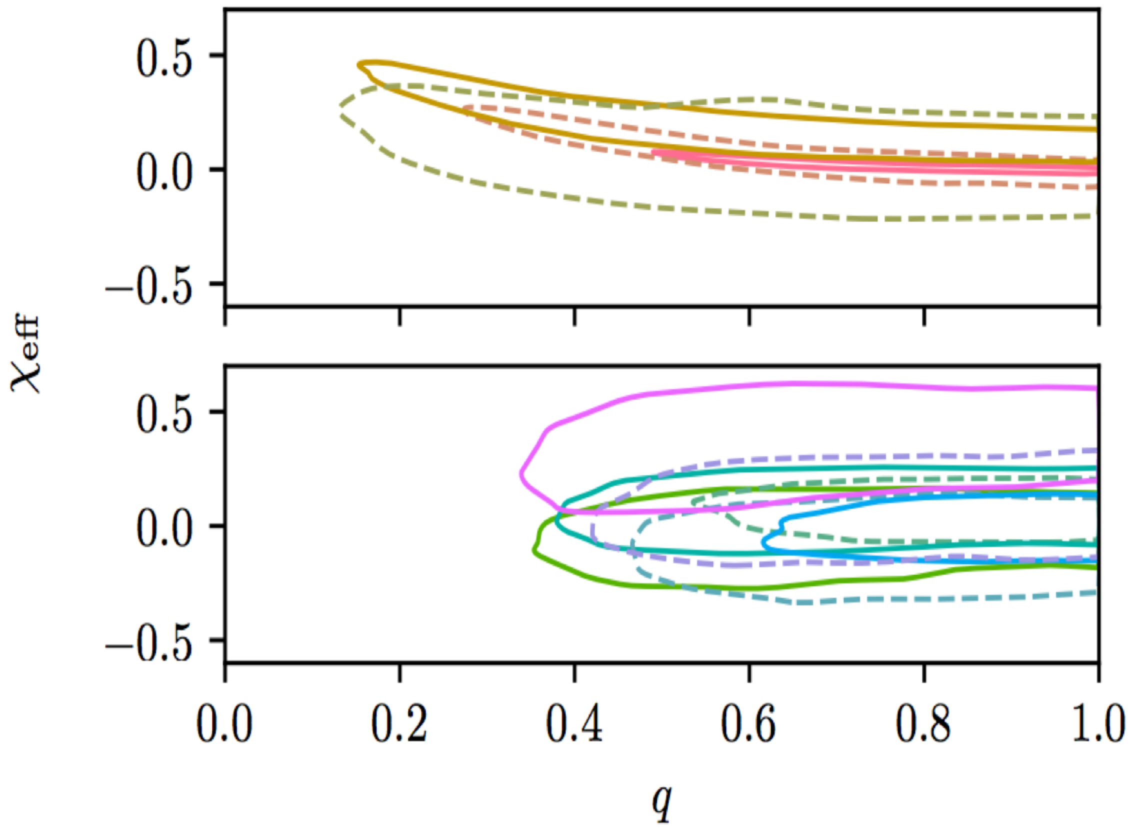

SPIN probability distribution based on all detected BH

On the base of the Spin distribution we can disentangle between the two formation channels of BBH

- ✓ Dynamical capture ➔ random spins
- ✓ Galactic fields ➔ Spins more aligned with the orbital angular momentum

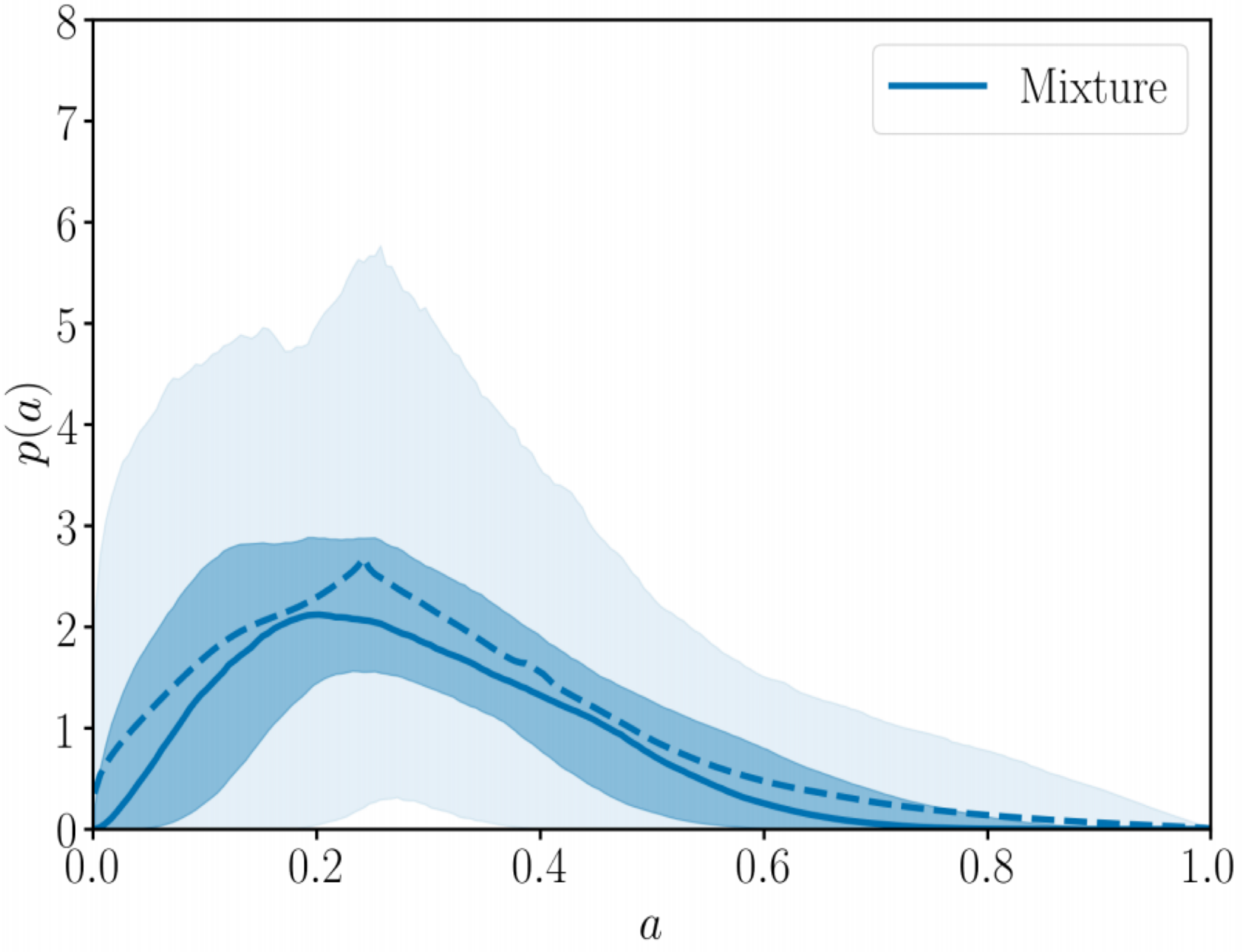

- Apparently it seems that we are detecting BHs with small spins , but…….
  - ✓ At present no significant constraints on spin populatio or their characteristics
- We will do better with more BBH detections

More results in LVC, Arxiv 1811.12940

The outcome of the NS-NS signal GW170817

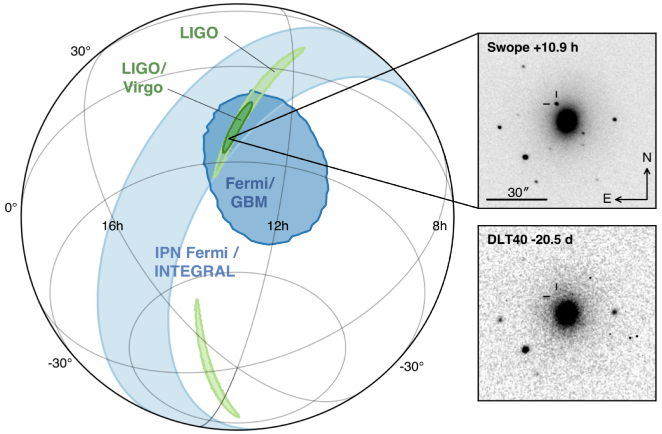

- The binary neutron star GW170817 was detected both in the GW and electromagnetic (EM) band
  - Proved BNS are progenitors of short gamma ray bursts
  - Proved BNS produce kilonovae emission, and heavy metals
  - Stringent limits on c_{GW} ➔ Graviton Mass

$m_g < 7.7 \times 10^{-23}$ eV

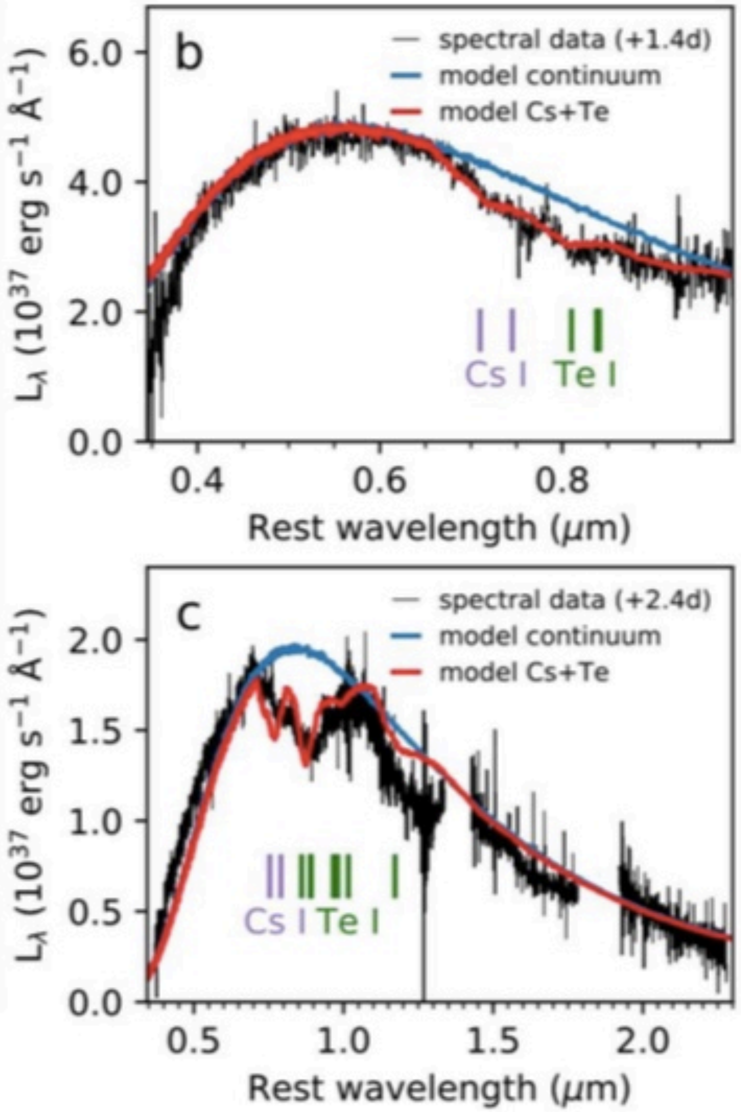

Formation of Cesium ^{55}Cs and Tellurium ^{52}Te is difficult to explain in supernova explosions

----

Evidence of spectral lines broaded by Doppler effect

Neutron Stars as Nuclear Physics Laboratories

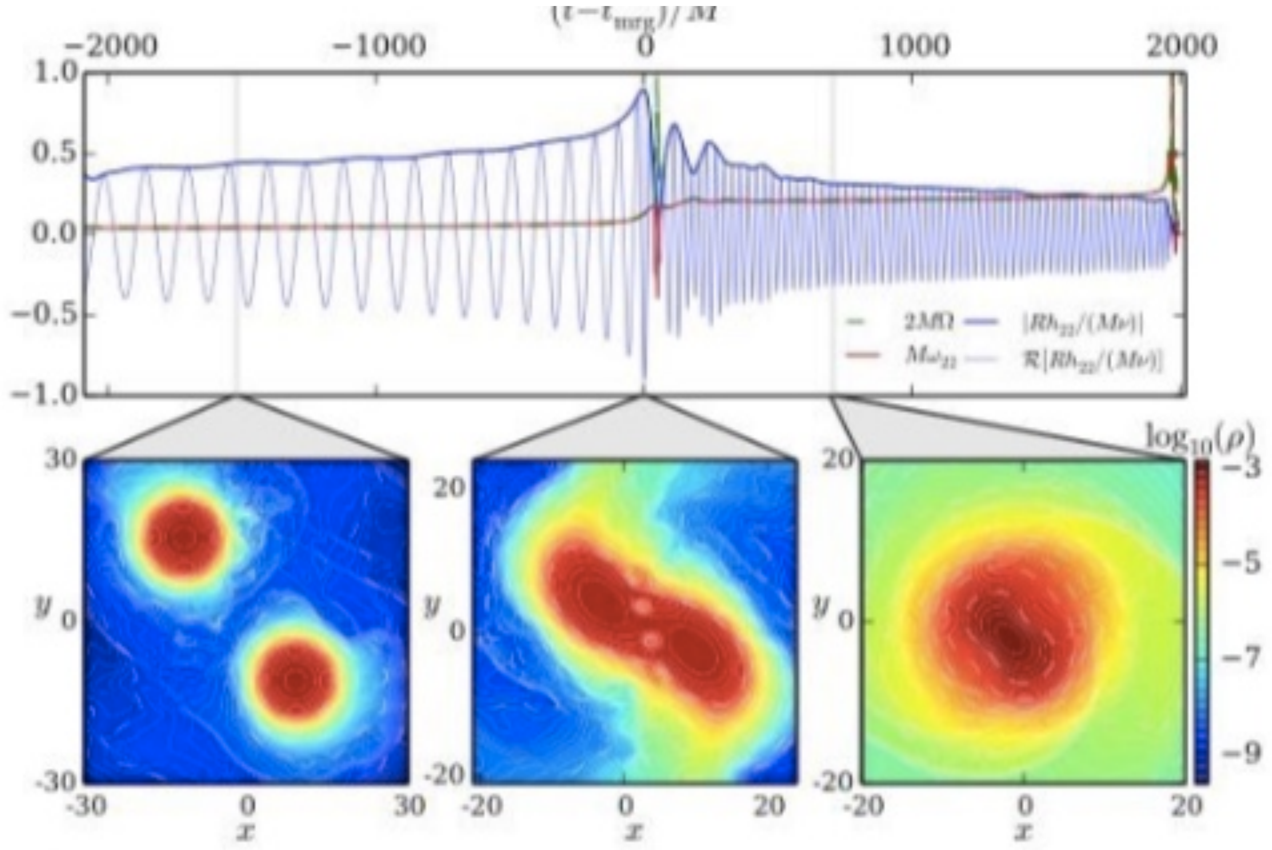

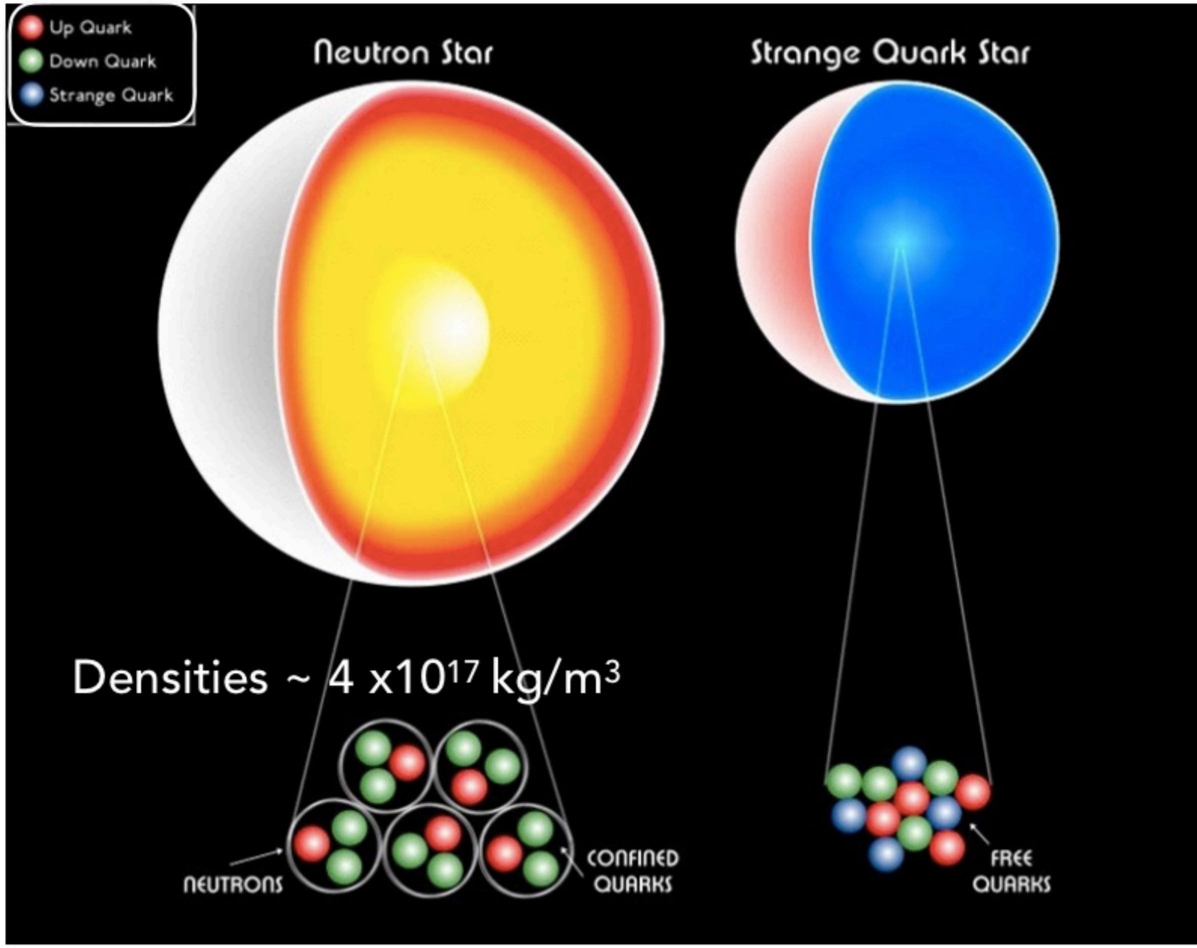

Leading tidal contribution to GW phase appears at 5 PN:

$$\tilde{\Lambda} = \frac{16}{13}\frac{(m_1+12m_2)m_1^4\Lambda_1 + (m_2+12m_1)m_2^4\Lambda_2}{(m_1+m_2)^5}$$

GW170817 and NS equation of state

LVC arxiv: 1811.12907; PRL 121, 161101; PRX 9, 011001

- The NS composition and properties determine the equation of state (EOS) and constrains how large can be a neutron star ➔ NS radius limits

- Gravitational waves carry information on the tidal deformability Λ of the coalescing bodies, which were then translated to constraints on neutron star radii

[R_1 =10.8(+2 ,-1.7) km , R_2 =10.7 (+2.1, -1.5) km](90%)

Assuming that masses can be even higher than 1.97 $M_\odot$

[R_1 =11.9 $\pm$ 1.4 km , R_2 =11.9 $\pm$ 1.4 km] (90%)

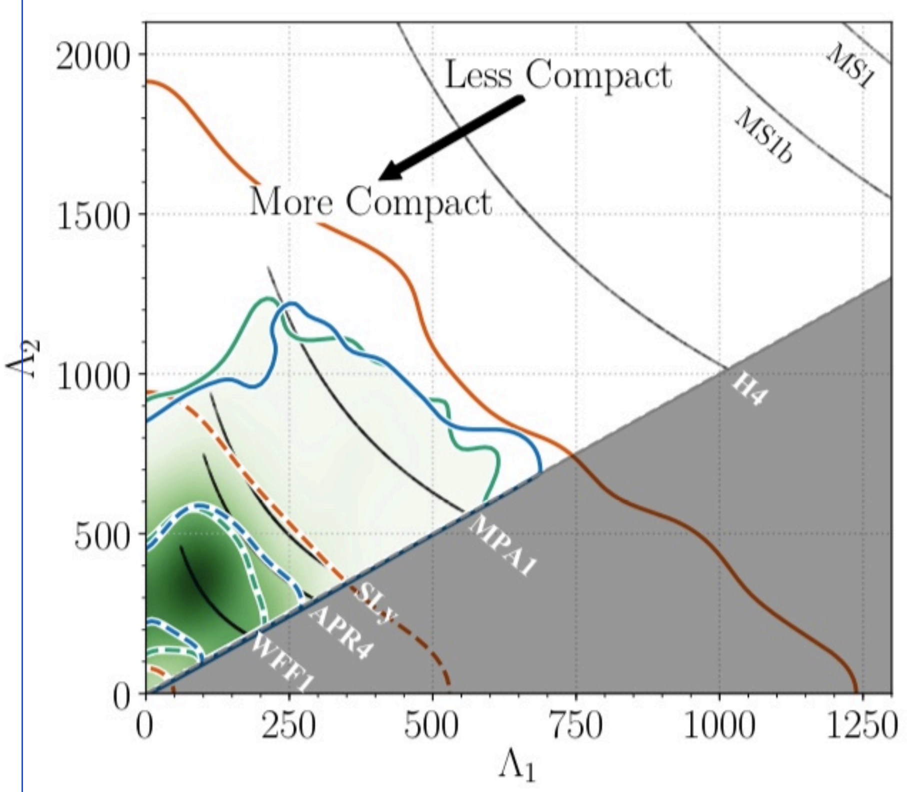

Green, blue, and orange areas ➔ equal EOS of two body, no mass limit, independent EOSs

Pressure at

P = 3.5 (+2.7 ,-1.7) x 10^{34} dyne cm^{-2}

inner density twice the nuclear saturation one

(2.8 x 10^{14} g cm^{-3})

GW170817 seems to support EOS that produce NS with smaller radius (soft EOS). ***Will do better with more sources***

GW170817: first result on cosmology

Measurement of the local Hubble parameter :

-- Distance from GW signal

-- Redshift from EM counterpart (galaxy NGC 4993)

•LVC measurement ➔ 14% (1σ) uncertainty $\begin{cases} \text{~11\% GW luminosity distance} \\ \text{~3\% peculiar velocity of the galaxy} \end{cases}$

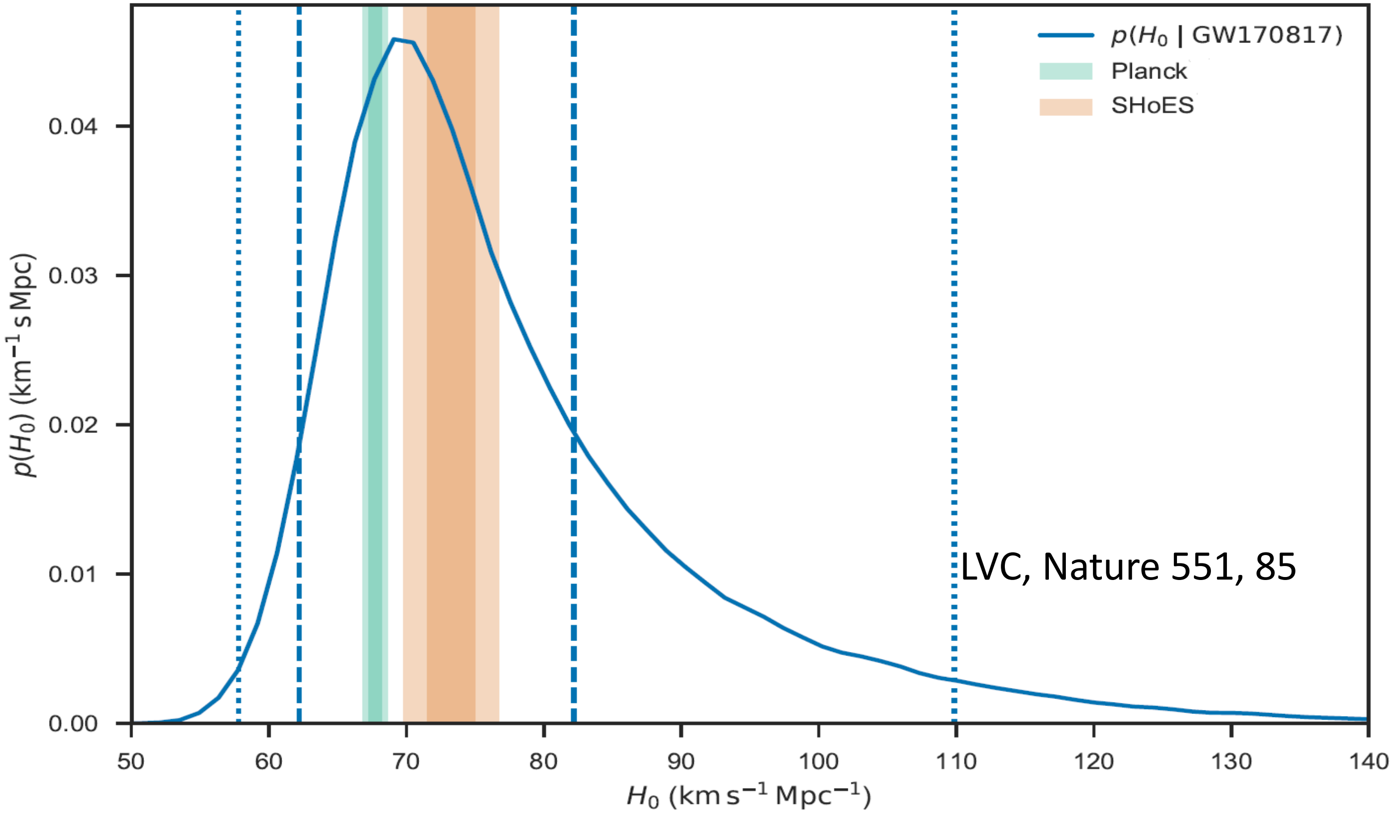

LVC, Nature 551, 85

5-σ discrepancy between CMB and SH0ES

The New Data Taking -- O3

The network in action

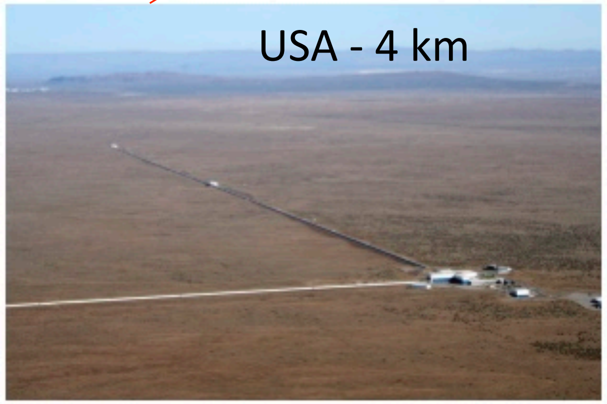

LIGO Hanford

LIGO Livingston

Virgo

GEO600

New Installation in the time window between O2 to O3

LIGO

Higher laser power

Replaced 5 of 8 test masses (better optical quality)

Added squeezed light injection systems

New baffles to mitigate scattered light

Improvements to various controls systems (seismic, alignment, etc)

Virgo

New (more powerful) laser

Replaced the suspensions of the last stage to reduce the thermal noise (monolithic fibers)

Added squeezed light injection systems

New faraday isolator and photodiodes

Improvements to various controls systems (seismic, alignment, etc)

Improved sensitivities

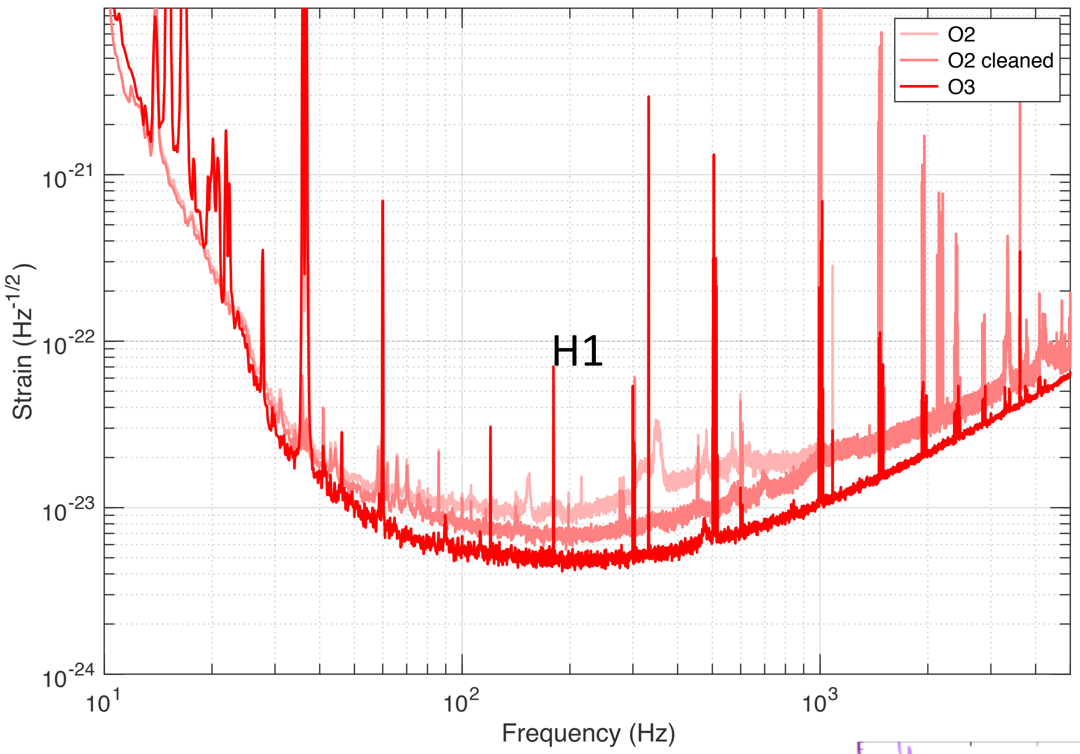

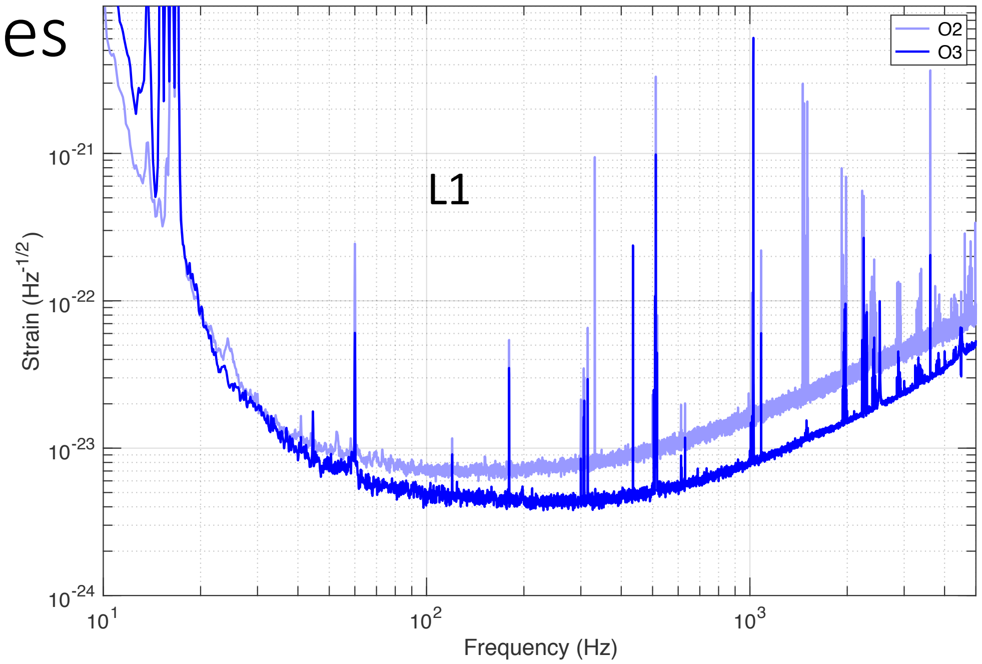

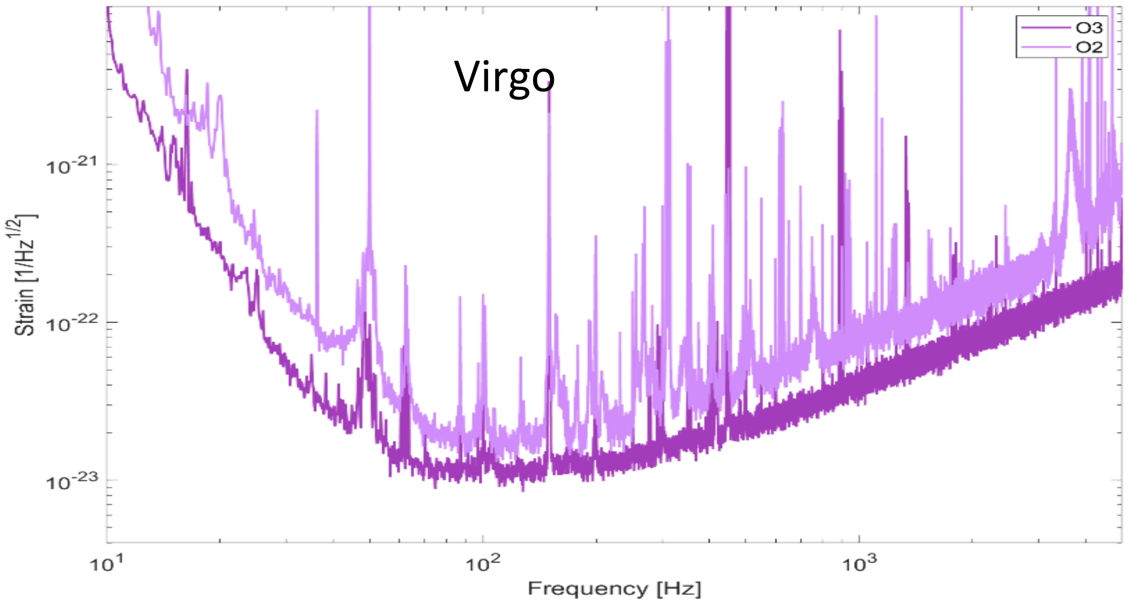

O3 RUN – Started April 1º, 2019

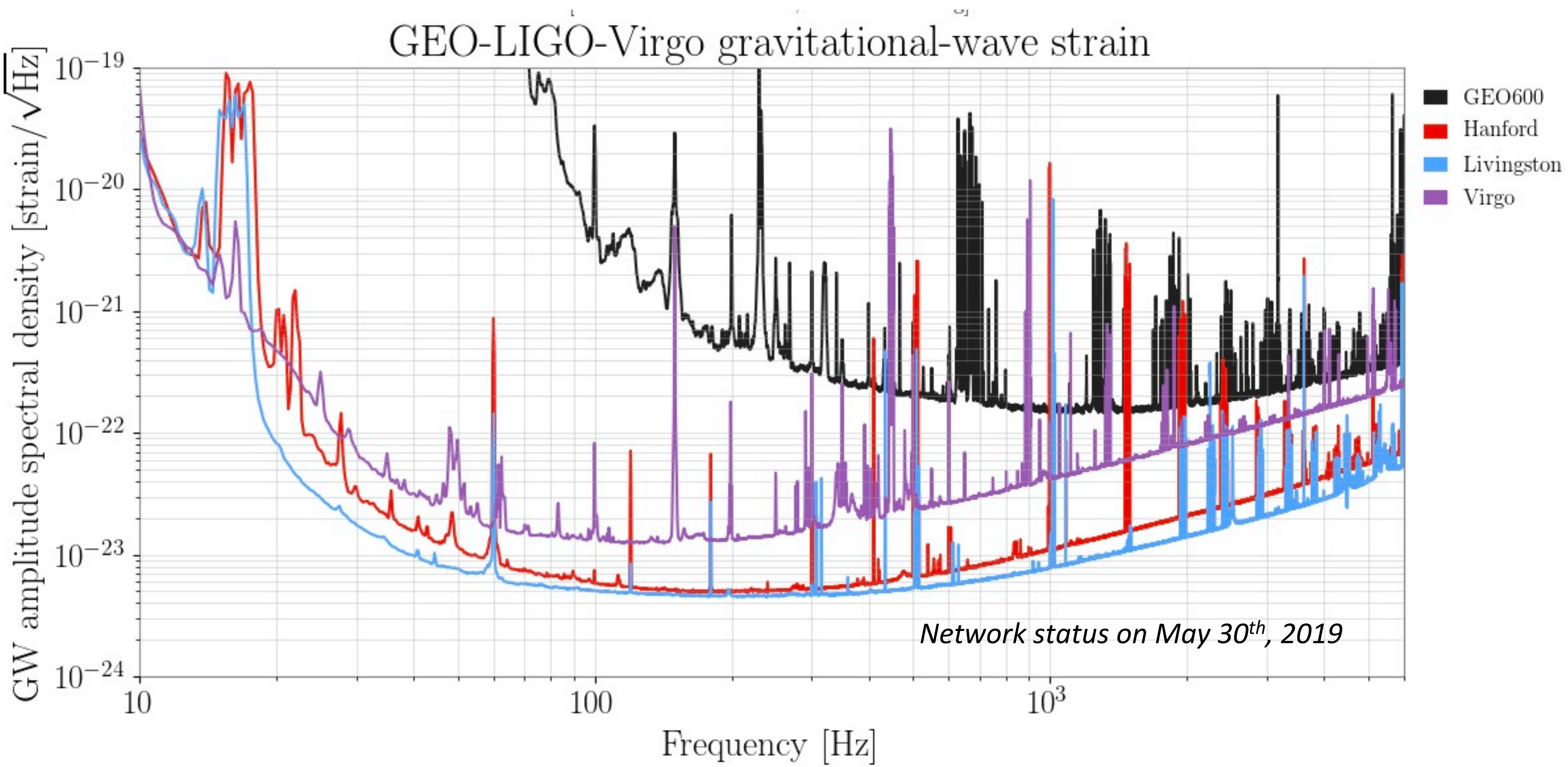

O3 and Instruments Status

O3 started in time on Mon Apr. 1st 2019 and it will last for almost 1 year

Better sensitivity than O2 for all 3 instruments.

As planned, shorter than usual commissioning time at all three sites for the first week.

Coordination between the sites to maximize 3-IFO operation.

At least one instrument tries to remain online at any given time.

Very good triple coincidence: so far more than 40%.

At least two interferometers 80% of the time.

Only 1.1% with no interferometer in observation mode.

Run status on June 4th, 2019

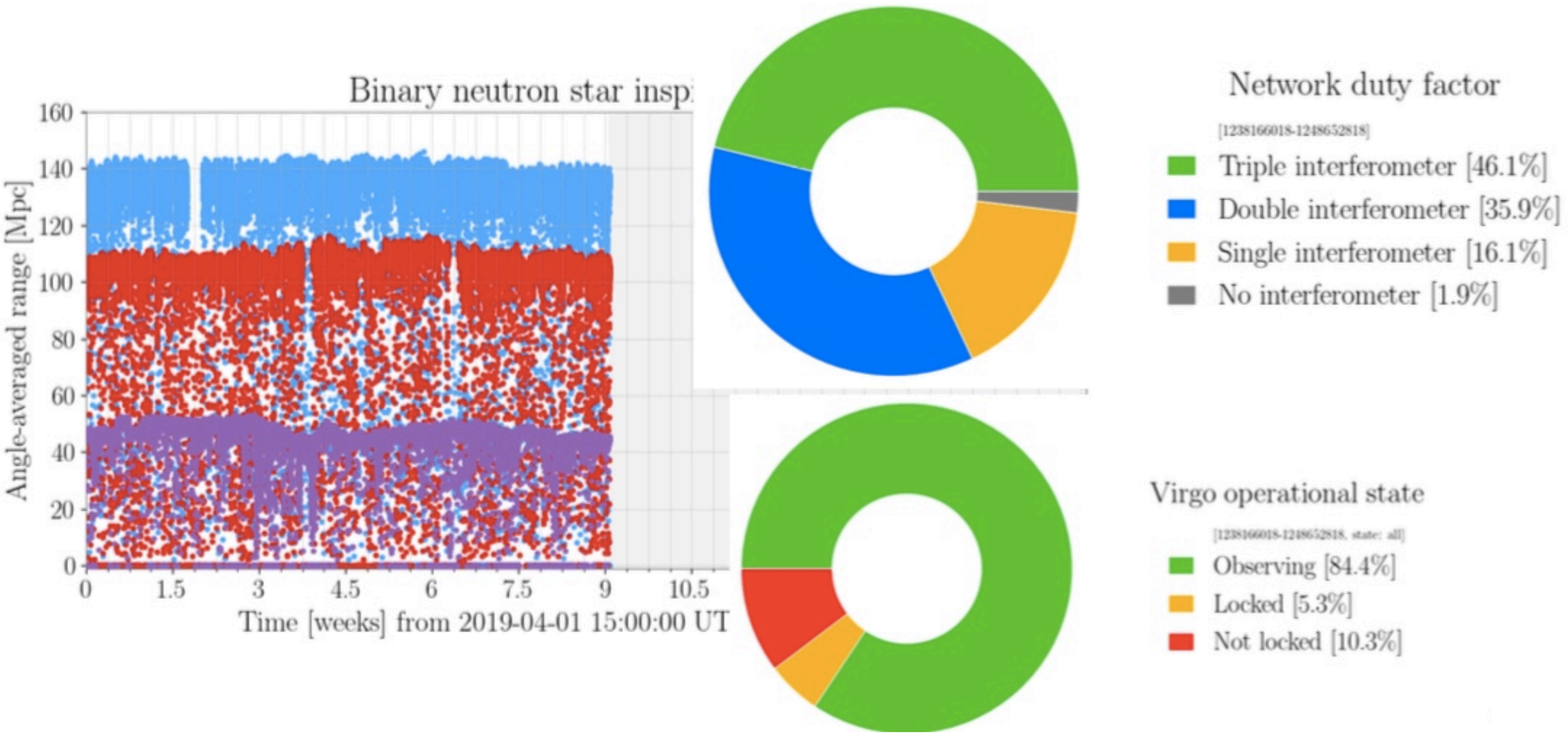

How many event do we expect?

BBH mass distribution models: Model A $m_{min} = 5\ M_\odot$, $\beta_q = 0$ and fit on α, m_{max};

Model B fit all 4 parameters $m_{min}, m_{max}, \alpha, \beta_q$

(arXiv:1811.12940)

$$p(m_1, m_2 | m_{\min}, m_{\max}, \alpha, \beta_q) \propto \begin{cases} C(m_1) m_1^{-\alpha} q^{\beta_q} & \text{if } m_{\min} \leq m_2 \leq m_1 \leq m_{\max} \\ 0 & \text{otherwise} \end{cases},$$

where $C(m_1)$ is chosen so that the marginal distribution is a power law in m: $p(m_1 | m_{min}, m_{max}, \alpha, \beta_q) = m_1^{-\alpha}$

$$R = 64.9^{+75.5}_{-33.6}\ \mathrm{Gpc}^{-3}\,\mathrm{yr}^{-1} \text{ for Model A}$$
$$R = 53.2^{+58.5}_{-28.8}\ \mathrm{Gpc}^{-3}\,\mathrm{yr}^{-1} \text{ for Models B}$$

Since we are able to observe BBH coalescence in a volume of the order of ~ 1 Gpc^3, *$R\,V$ ~ 1 week^{-1}*

NS-NS rate based on just one observed event

PDF based on the output two search algorithms GstLAL and PyCBC.

---------- uniform mass distribution --------- Gaussian mass distribution.

Vertical lines ➔ symmetric 90% confidence intervals.

Since we are able to observe NS-NS coalescence in a volume of the order of ~ 4 x 10^{-3} Gpc^3, $R\,V$ ~ few year^{-1} at the PDF peak

(arXiv:1811.12907)

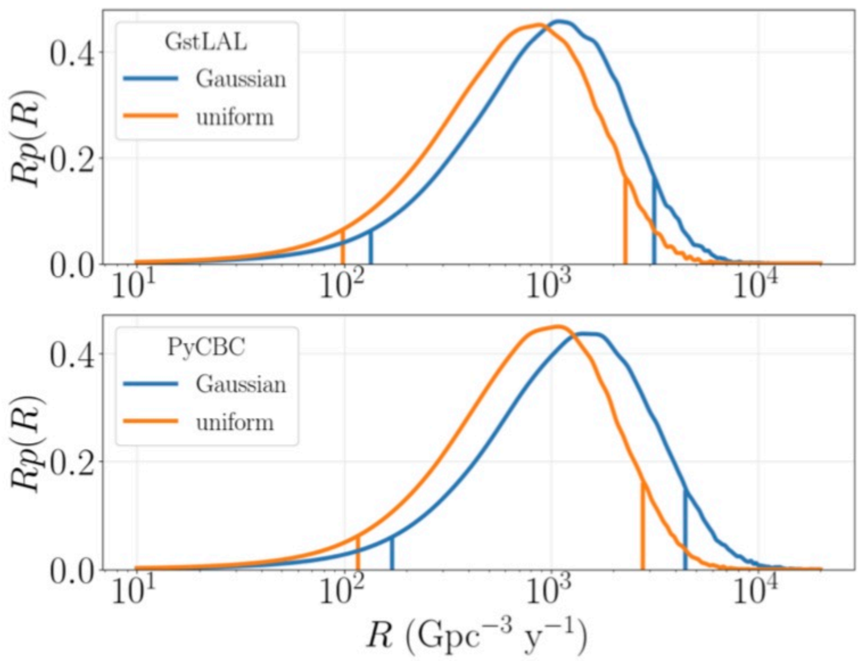

New Events – Public Alerts

https://gracedb.ligo.org/latest/

GraceDB — Gravitational Wave Candidate Event Database

HOME | SEARCH | LATEST | DOCUMENTATION | LOGIN

Latest — as of 4 June 2019 17:57:50 UTC

Test and MDC events and superevents are not included in the search results by default; see the query help for information on how to search for events and superevents in those categories.

Query:

Search for: Superevent

UID	Labels	t_start	t_0	t_end	FAR (Hz)	UTC Created
S190602aq	DQOK ADVOK SKYMAP_READY PASTRO_READY EMBRIGHT_READY GCN_PRELIM_SENT	1243533584.081266	1243533585.089355	1243533586.346191	1.901e-09	2019-06-02 17:59:51 UTC
S190524q	DQOK ADVNO SKYMAP_READY EMBRIGHT_READY PASTRO_READY GCN_PRELIM_SENT	1242708743.678669	1242708744.678669	1242708746.133301	6.971e-09	2019-05-24 04:52:30 UTC
S190521r	DQOK ADVOK SKYMAP_READY EMBRIGHT_READY PASTRO_READY GCN_PRELIM_SENT PE_READY	1242459856.453418	1242459857.460739	1242459858.642090	3.168e-10	2019-05-21 07:44:22 UTC
S190521g	DQOK ADVOK SKYMAP_READY PASTRO_READY EMBRIGHT_READY GCN_PRELIM_SENT PE_READY	1242442966.447266	1242442967.606934	1242442968.888184	3.801e-09	2019-05-21 03:02:49 UTC
S190519bj	ADVOK DQOK SKYMAP_READY EMBRIGHT_READY PASTRO_READY GCN_PRELIM_SENT PE_READY	1242315361.378873	1242315362.655762	1242315363.676270	5.702e-09	2019-05-19 15:36:04 UTC
S190518bb	DQOK ADVNO SKYMAP_READY EMBRIGHT_READY PASTRO_READY GCN_PRELIM_SENT	1242242376.474609	1242242377.474609	1242242380.922655	1.004e-08	2019-05-18 19:19:39 UTC
S190517h	DQOK ADVOK SKYMAP_READY EMBRIGHT_READY PASTRO_READY GCN_PRELIM_SENT PE_READY	1242107478.819517	1242107479.994141	1242107480.994141	2.373e-09	2019-05-17 05:51:23 UTC
S190513bm	DQOK ADVOK SKYMAP_READY EMBRIGHT_READY PASTRO_READY GCN_PRELIM_SENT	1241816085.736106	1241816086.869141	1241816087.869141	3.734e-13	2019-05-13 20:54:48 UTC
S190512at	DQOK ADVOK SKYMAP_READY EMBRIGHT_READY PASTRO_READY GCN_PRELIM_SENT PE_READY	1241719651.411441	1241719652.416286	1241719653.518066	1.901e-09	2019-05-12 18:07:42 UTC
S190510g	DQOK ADVOK SKYMAP_READY EMBRIGHT_READY PASTRO_READY GCN_PRELIM_SENT	1241492396.291636	1241492397.291636	1241492398.293185	8.834e-09	2019-05-10 03:00:03 UTC
S190503bf	DQOK PASTRO_READY EMBRIGHT_READY SKYMAP_READY ADVOK GCN_PRELIM_SENT	1240944861.288574	1240944862.412598	1240944863.422852	1.636e-09	2019-05-03 18:54:26 UTC
S190426c	DQOK EMBRIGHT_READY PASTRO_READY SKYMAP_READY ADVOK GCN_PRELIM_SENT PE_READY	1240327332.331668	1240327333.348145	1240327334.353516	1.947e-08	2019-04-26 15:22:15 UTC
S190425z	DQOK SKYMAP_READY EMBRIGHT_READY PASTRO_READY ADVOK	1240215502.011549	1240215503.011549	1240215504.018242	4.538e-13	2019-04-25 08:18:26 UTC
S190421ar	DQOK EMBRIGHT_READY PASTRO_READY SKYMAP_READY GCN_PRELIM_SENT ADVOK PE_READY	1239917953.250977	1239917954.409180	1239917955.409180	1.489e-08	2019-04-21 21:39:16 UTC
S190412m	DQOK SKYMAP_READY PASTRO_READY EMBRIGHT_READY ADVOK GCN_PRELIM_SENT PE_READY	1239082261.146717	1239082262.222168	1239082263.229492	1.683e-27	2019-04-12 05:31:03 UTC
S190408an	DQOK ADVOK SKYMAP_READY PASTRO_READY EMBRIGHT_READY GCN_PRELIM_SENT PE_READY	1238782699.268296	1238782700.287958	1238782701.359863	2.811e-18	2019-04-08 18:18:27 UTC

Example of a couple of SUPEVENTs: S190412m and S190408an

FAR= 1.683×10^{-27} Hz ➔ 1 per $1.883 \times 10^{+19}$ years

FAR= 2.81×10^{-18} Hz ➔ 1 per $1.1273 \times 10^{+10}$ years

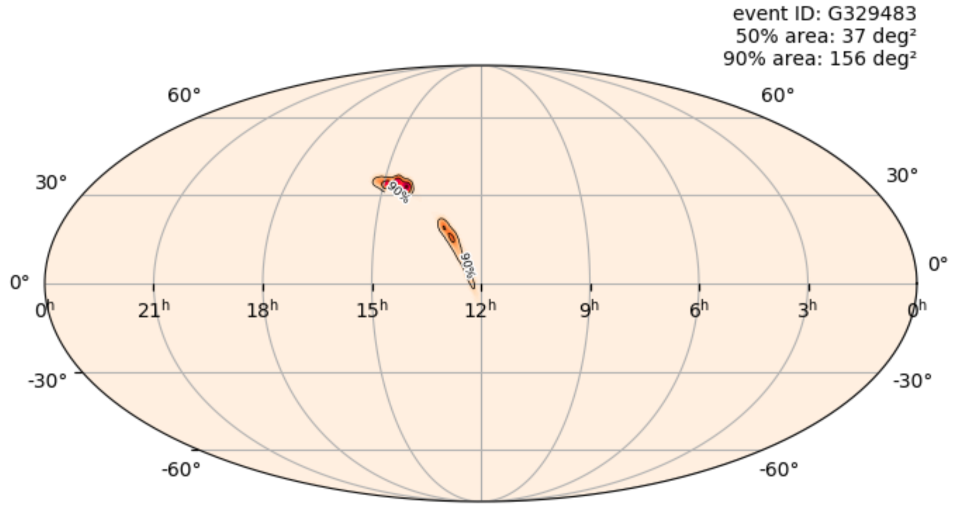

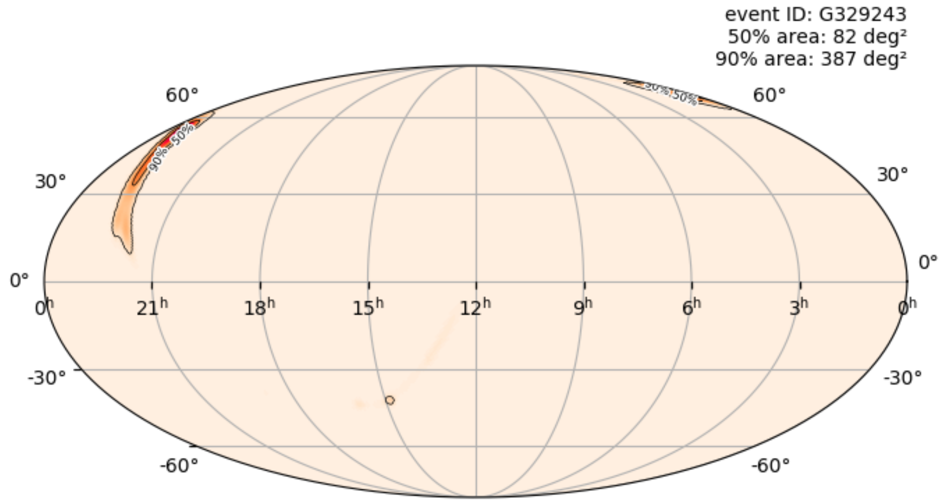

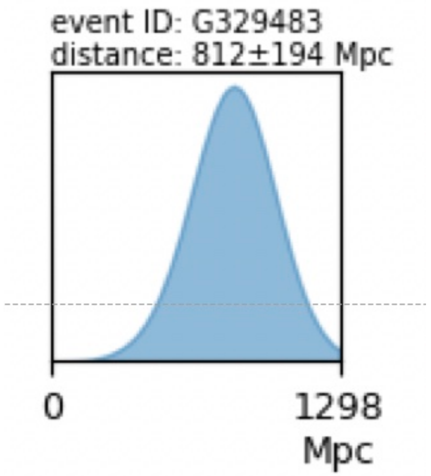

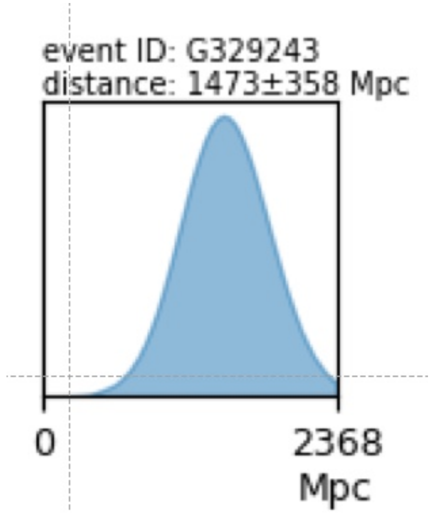

O3 and future plans

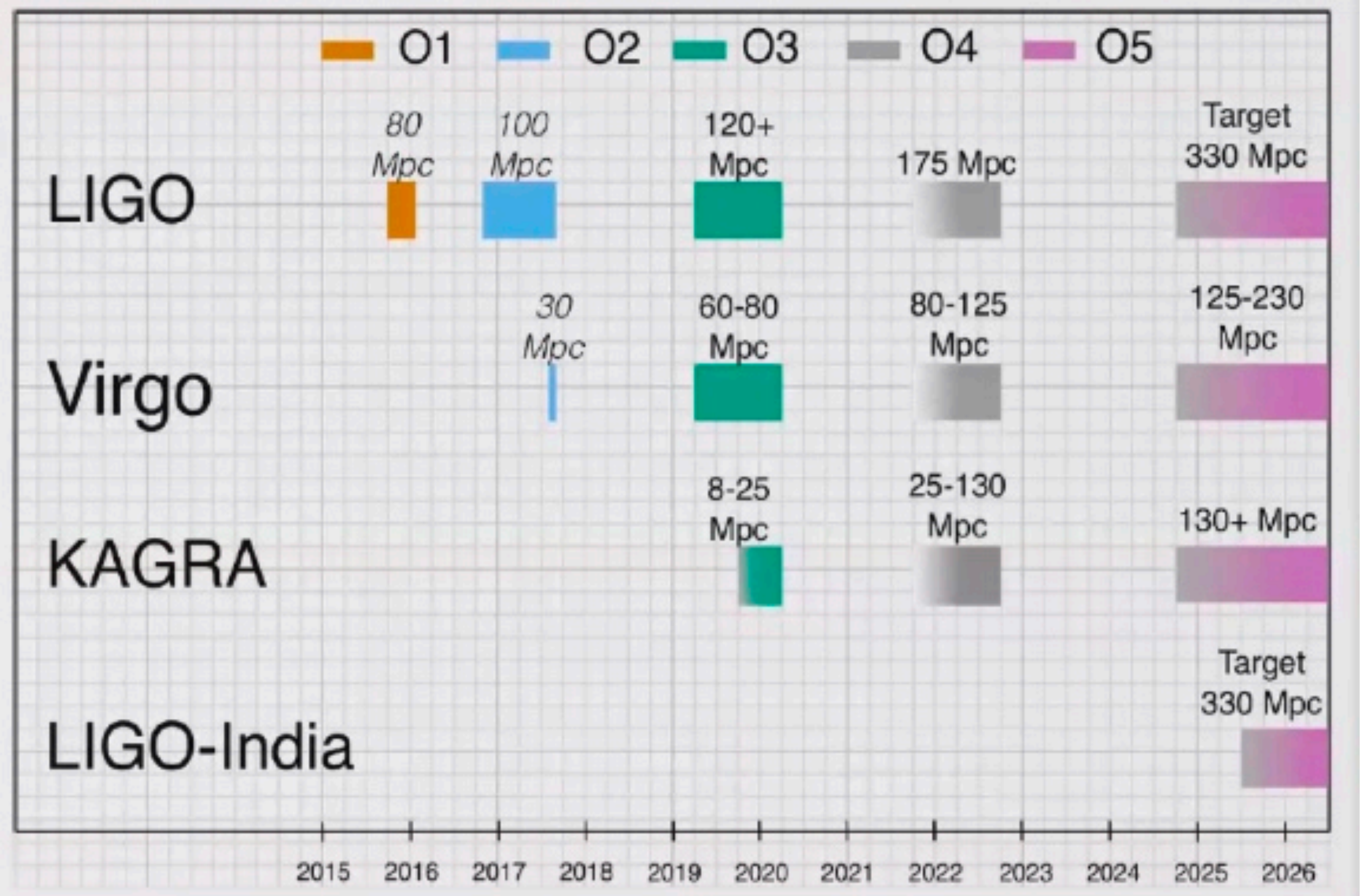

The network in the final part of O3

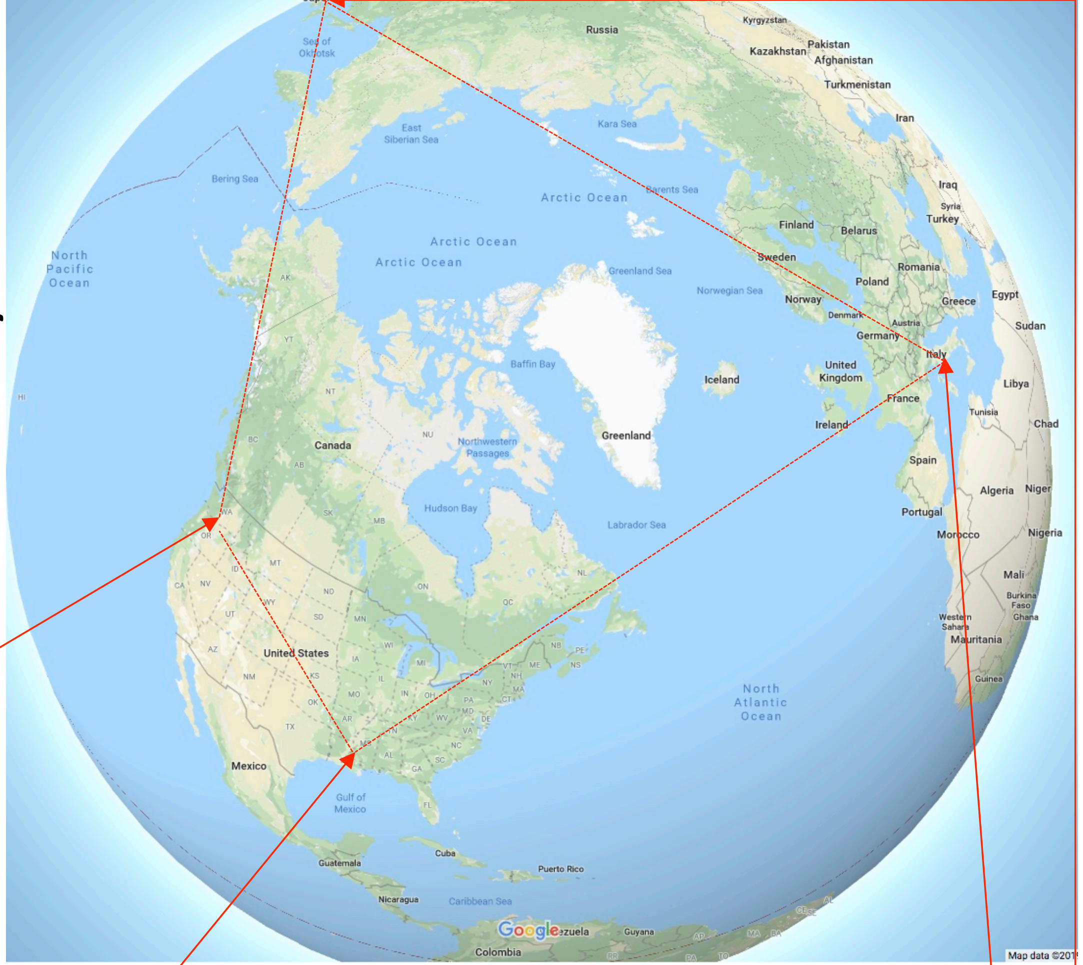

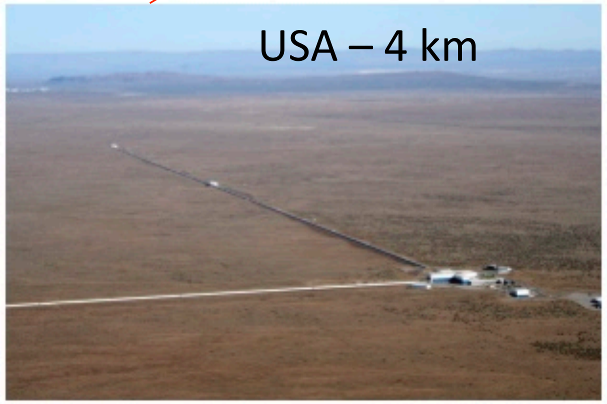

LIGO Hanford

LIGO Livingston

Virgo

KAGRA

Transient Event Localization

O2 localization: the smaller uncertainties when we have the 3 detectors : GW170814, GW170817, GW170818

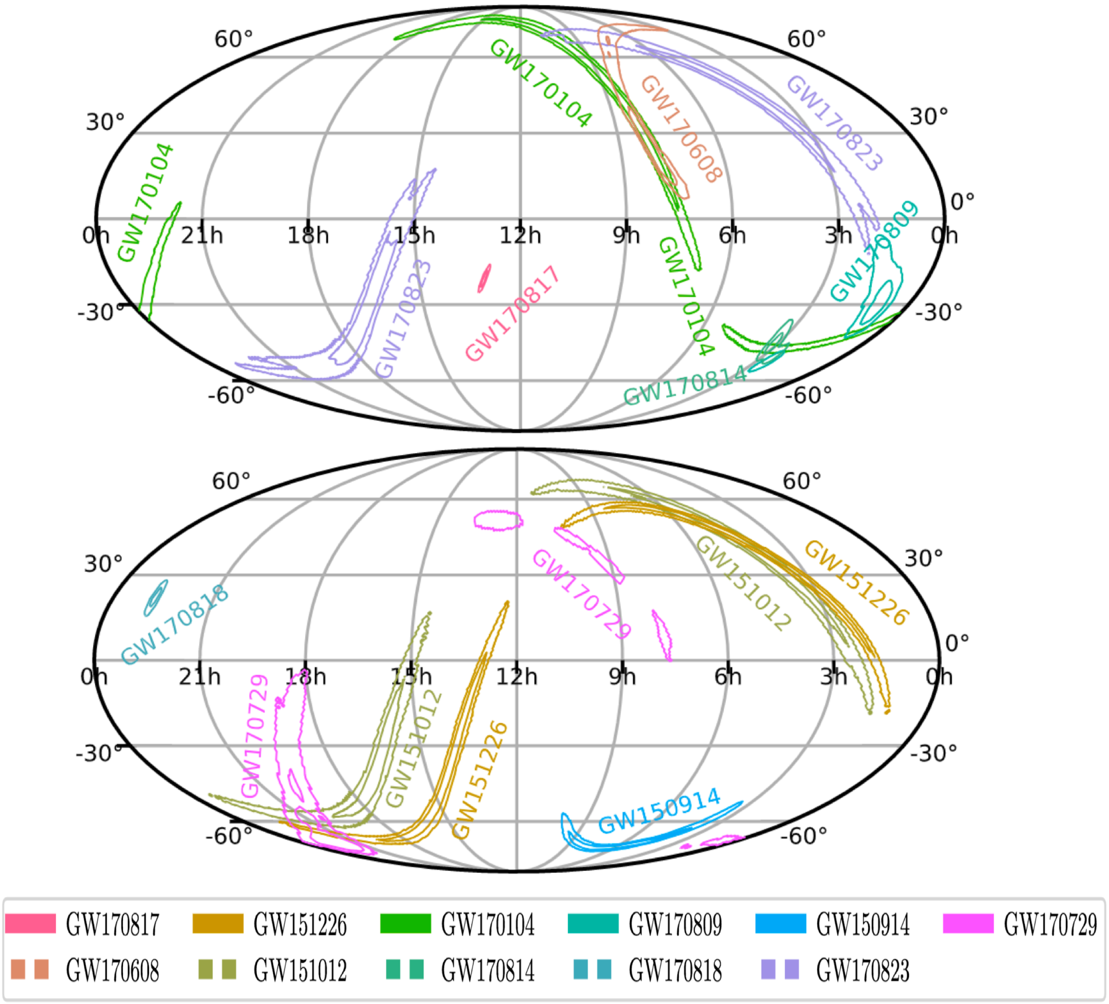

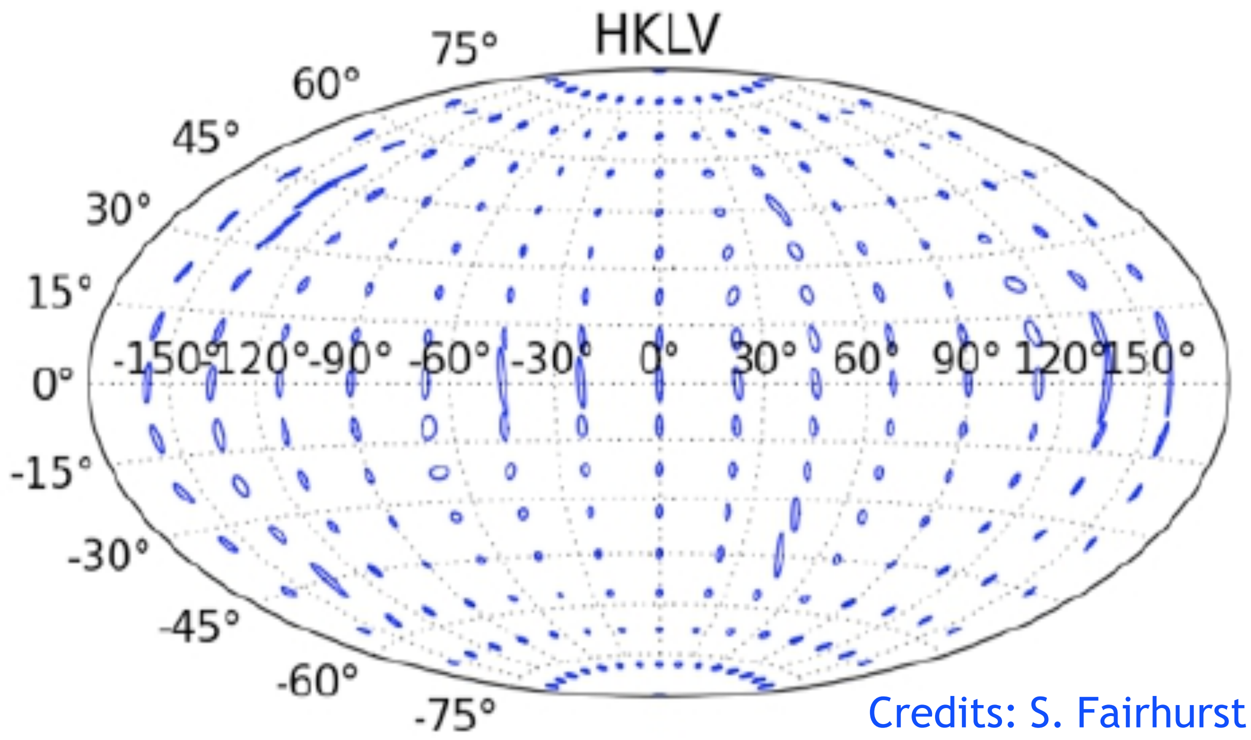

Moving forward the new 3G detectors: the Einstein Telescope case

- The GW detection and the beginning of the multimessenger astronomy stimulated a world wide acceleration toward 3G GW observatories
- In Europe we are going toward the formation of a ET collaboration, a competition between ~3 sites, candidate to host the infrastructure, the submission of an ET project proposal to the ESFRI roadmap
- In US the idea of a giant 40km detector, named Cosmic Explorer, is now born and supported, as Conceptual Design Study, by NSF
- We   set up a global coordination committee (GWIC-3G) that is attempting to harmonise the efforts and to find synergies

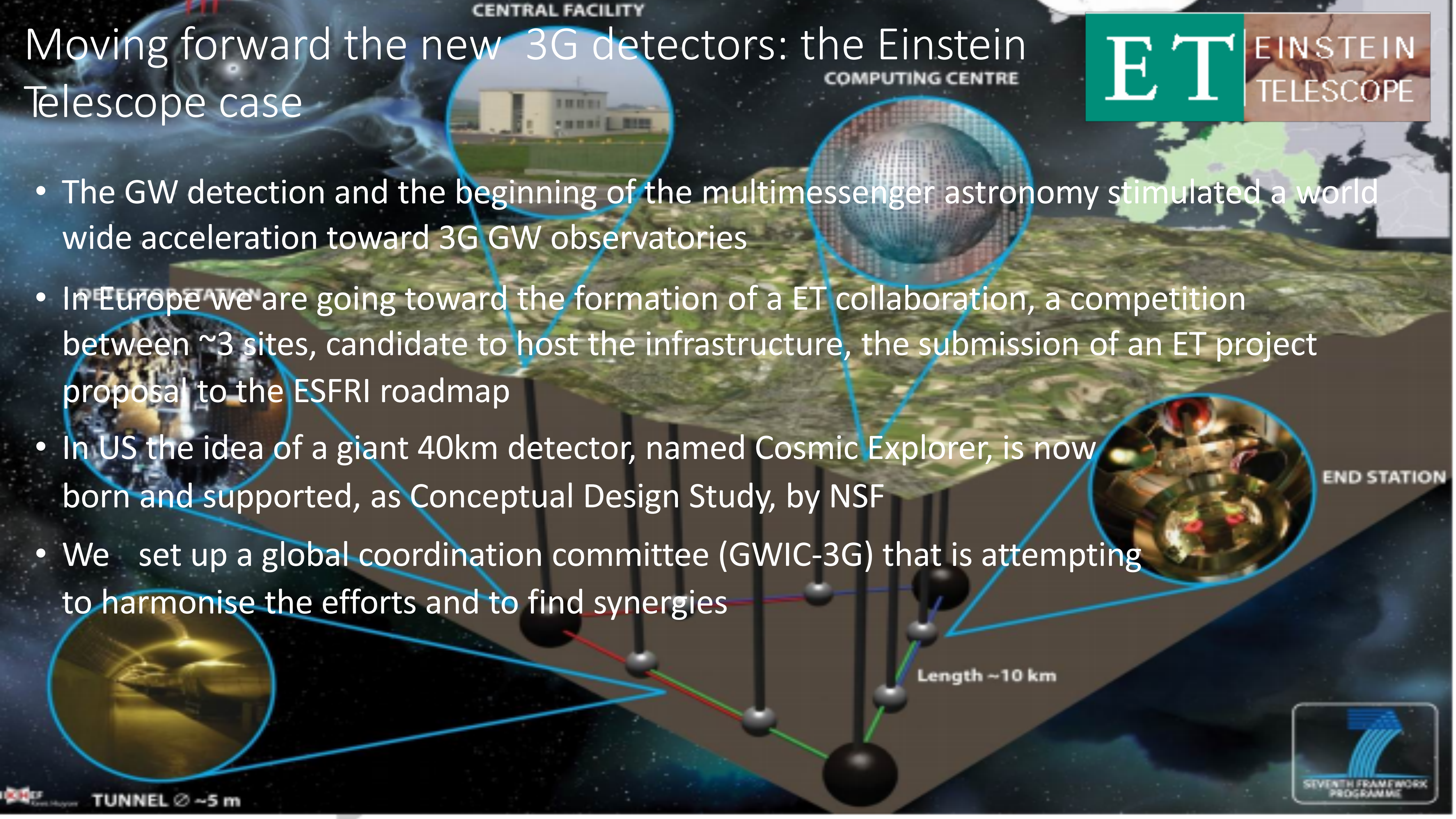

Motivations for New Detectors

- ***Expand the exploration to the entire Universe***

- Black holes through cosmic history
  - ✓ Formation, evolution and growth of black holes and their properties

- Understanding extremes of physics
  - ✓ Structure and dynamics of neutron stars
  - ✓ Physics of extreme gravity

- Probing the transient Universe
  - ✓ Gamma ray bursts, gravitational collapse and Supernovae

- Beyond GR looking for new Physics: gravstars, wormholes, new particles and fields

Why a new infrastructure

- Increase the arm length to gain in sensitivity
- Implementation of new technological plants requiring more space (cryogenics system)
- Reduce the seismic impact of the sensitivity (Underground detector)
- Permit longer data taking runs of the 2G detectors by relaxing the needs to implement new technologies on 2G
- Prepare the transition from obsolete to new infrastructures

The target should be to realize a 3G-infrastructure in the next decay choosing sites that must have specific features that can enhance the planned investments.

The 3rd GENERATION: site basic requirements

- lower seismic motion, meteorologically generated seismic noise, anthropogenic activity anthropogenic activity (local infrastructure, population density, etc.);

- lower Newtonian noise originates from fluctuations in the surround geologic and atmospheric density, causing a variation in the Newtonian gravitational field.

The Einstein Telescope (ET) case

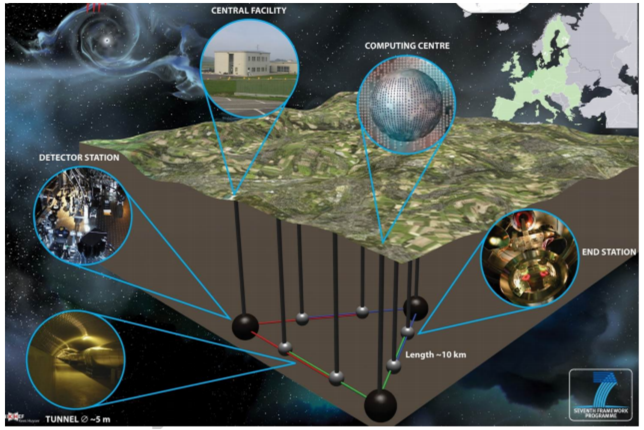

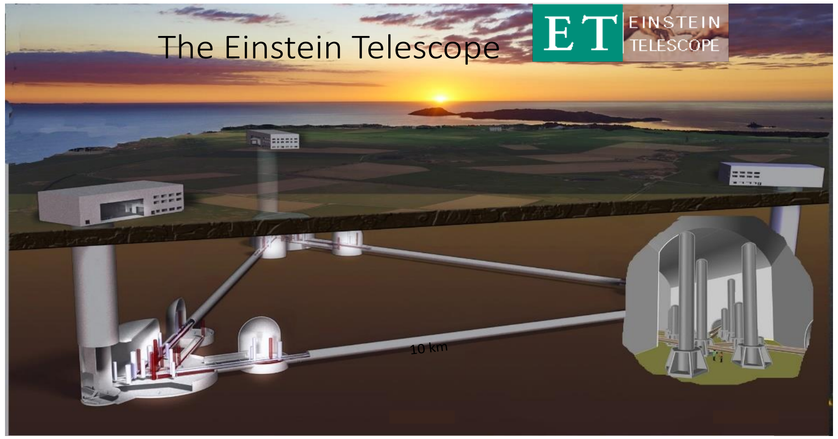

The Einstein Telescope will be located underground at a depth of about 100 m to 200 m and, in the complete configuration, will consist of three nested detectors each in turn composed of two interferometers

ET collaboration: Letter of Intent

- Addressed to all the scientists and engineers interested to the 3G GW science and technology
- The signatories (606 persons, the 24th of August) probably will become the future members of the ET collaboration

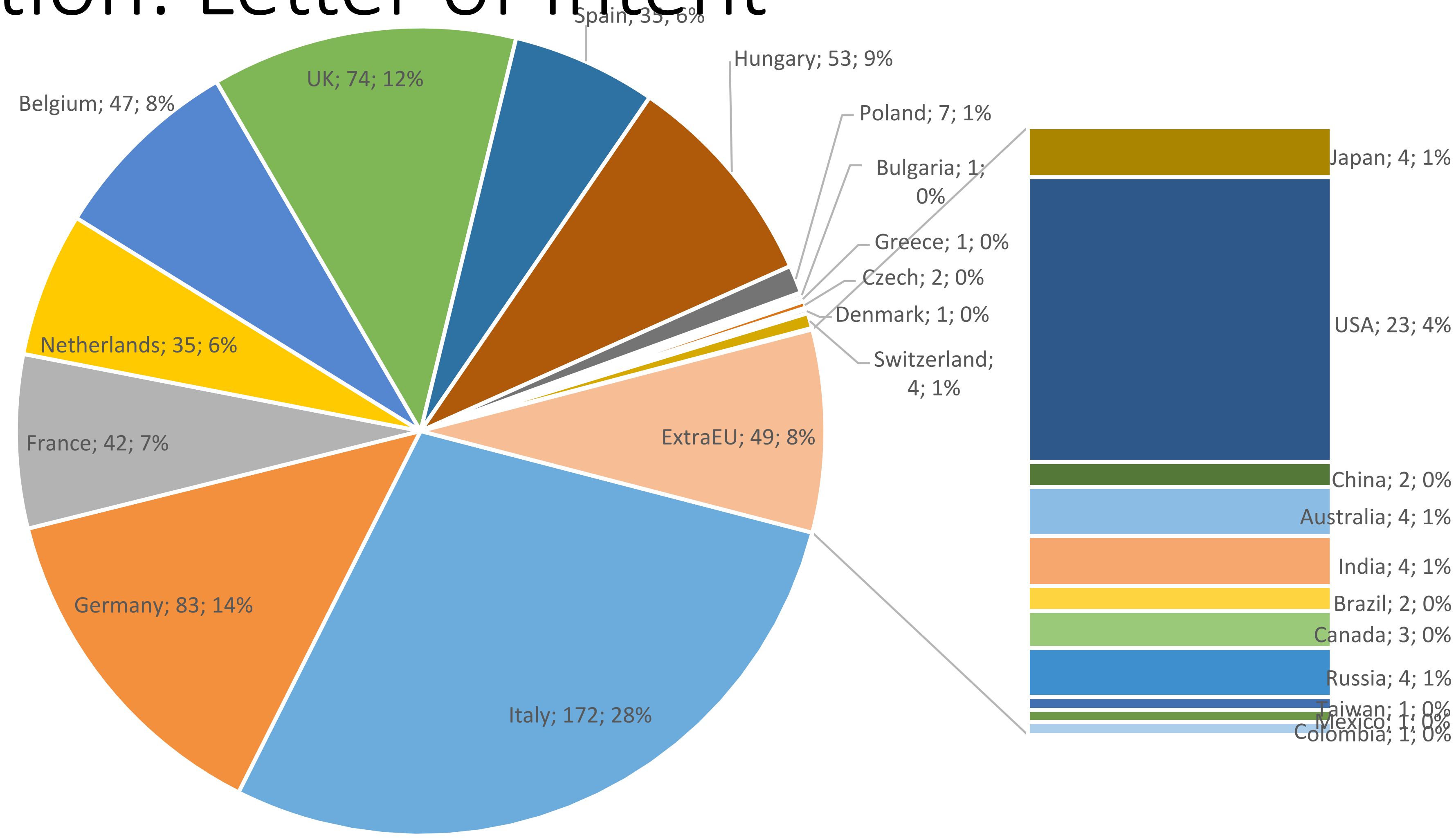

http://www.et-gw.eu/index.php/letter-of-intent

Credits: M. Punturo

ET site(s)

- In the Design Study we investigated several EU sites
  - The same instruments and methods have been used to roughly compare the sites
  - Three are survived per quality and/or interest

3 site candidates

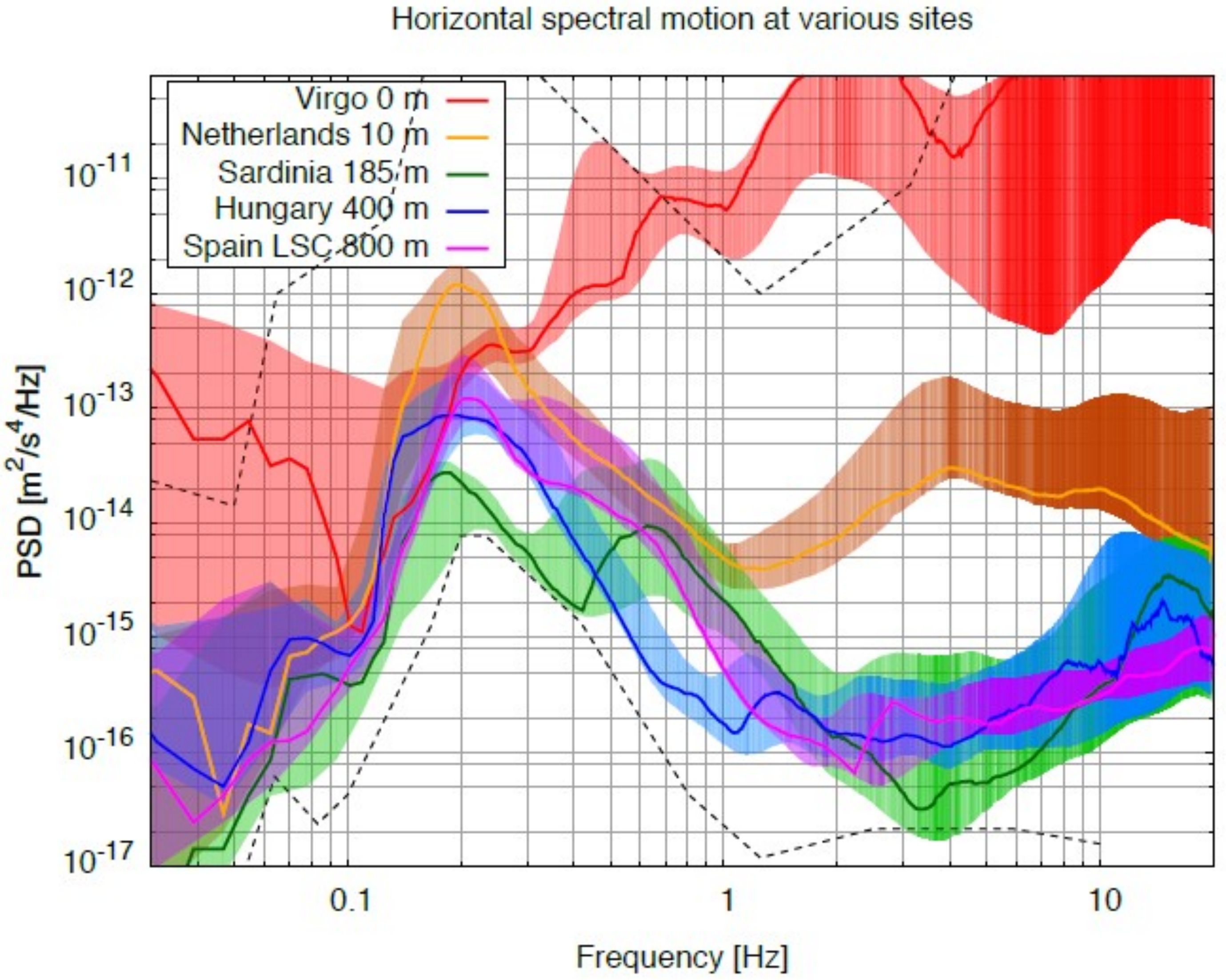

- Belgium-Germany-Netherlands
- Hungary (Matra Mountain)
- Italy (Sardinia-Sos Enattos)

Sites studies already started

- G-B-N Site, in the Meuse-Rhine region between Netherland, Belgium and Germany
- Mátra Mountain Site, in the northern of Hungary (first cancelled and now revived?)
- Lula Site, in the Sardinia - Italy.

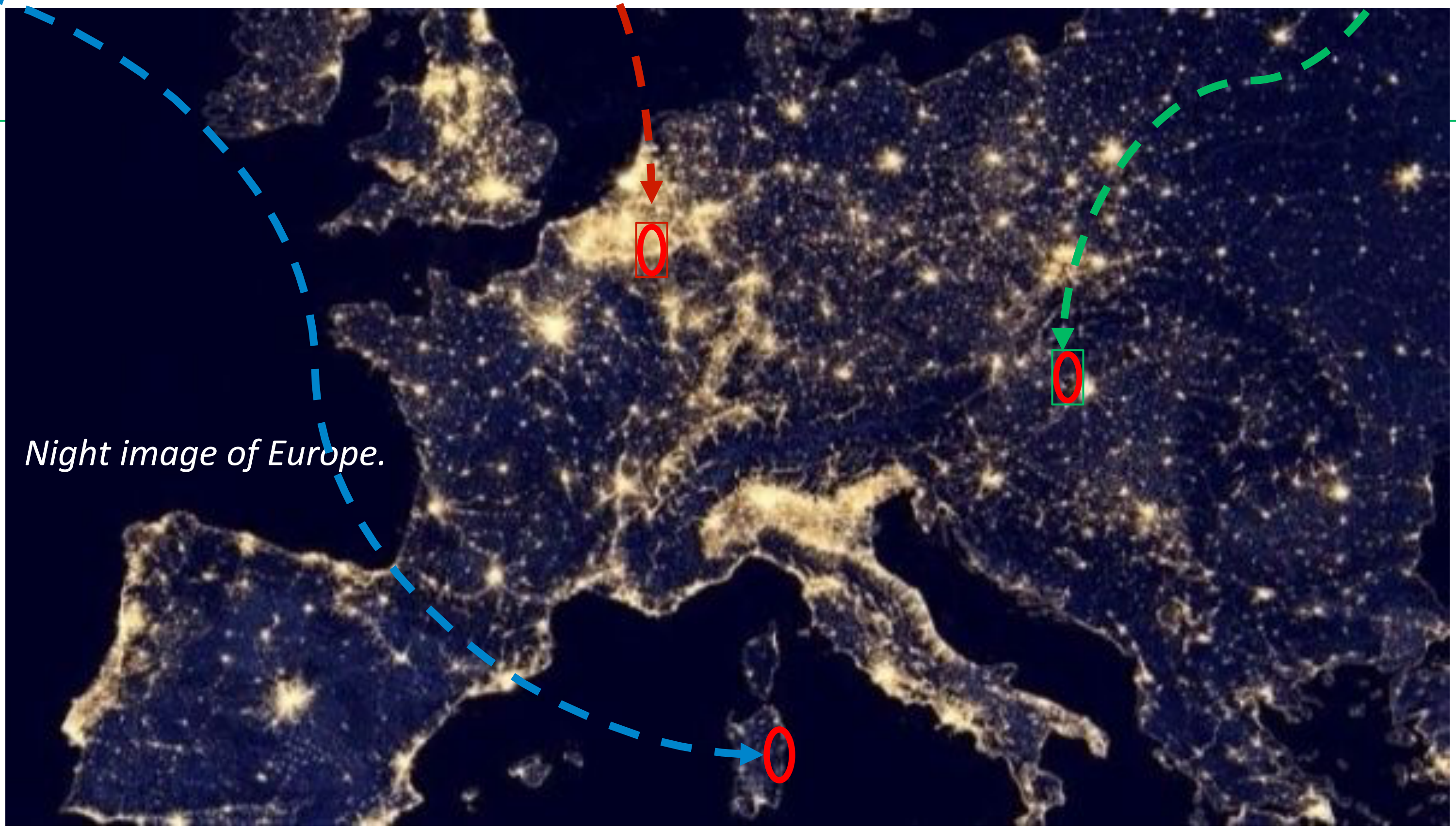

Night image of Europe.

Sardinia, Italy

- Site identified:
  - Sos Enattos, Sardina
- Site qualification: well advanced
  - Excellent seismic and geological properties
  - Small underground lab under construction funded (1M€) by local region and INFN
- Few M€ support assured by Italian government for the early phase
- International involvement to be structured

Dichiarazione di Intenti
SARDEGNA – CORSICA

Les Exécutifs corse et sarde échangent sur les thèmes majeurs de la coopération entre les deux îles

Lundi 14 Mars 2016

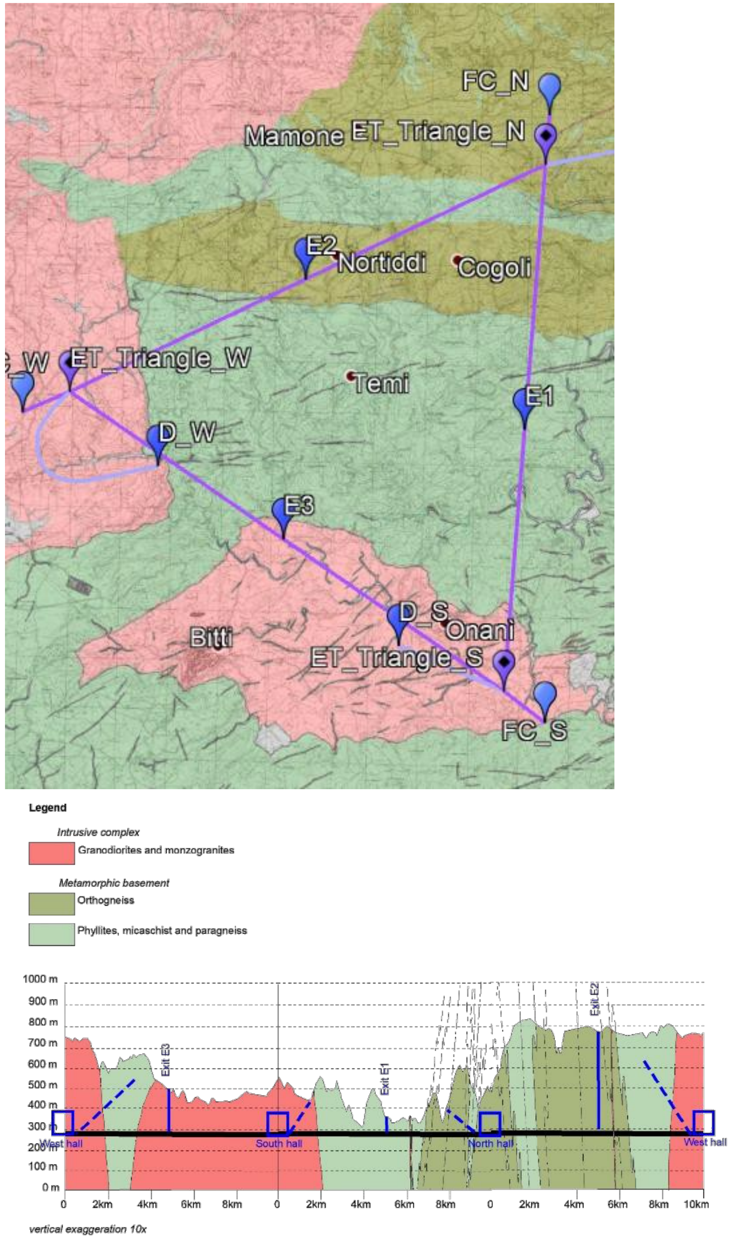

The Sos Enattos mine (Lula – SARDINIA)

We (**) have studied the placement of the ET detector in the SOS ENATTOS area.

We tried to fulfill the following requirements:

- <u>Vertexes placed in solid rock</u>
- <u>Access to caverns through tunnels</u>

(**) A. Paoli, G. Losurdo, G. Oggiano, D. D’Urso, IGEA and SWS company et al.

Ancient rocks, European continental landmass: seismically quiet. Since 16 Million Years, and after the opening of the south Thyrrenian basin, Sardinia has been excluded from the active dynamics affecting Italy along with Dinarides and Hellenides

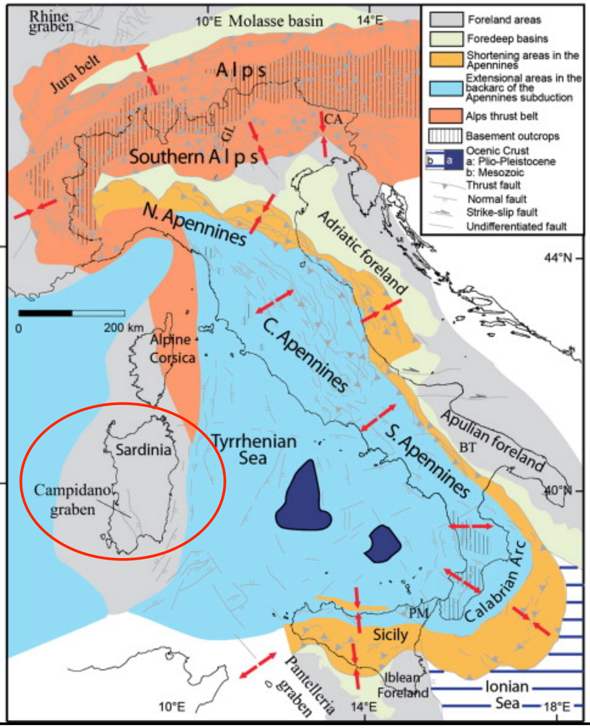

Granodiorite “Bitti type”
UCS: 72.1 MPa

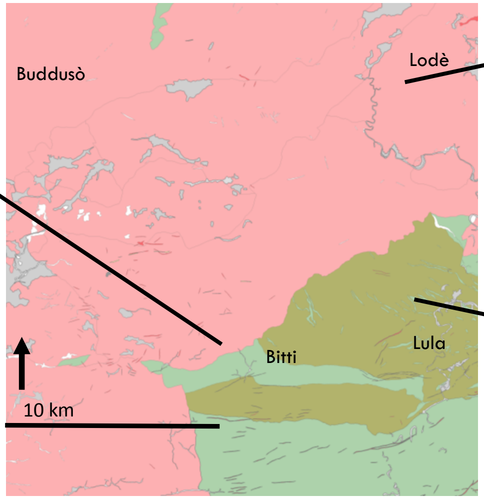

Orthogneiss “Lodè type”
UCS: 92.6/60.8 MPa

Micaschist/ Paragneiss /Quartzite
UCS:8.8/68 MPa

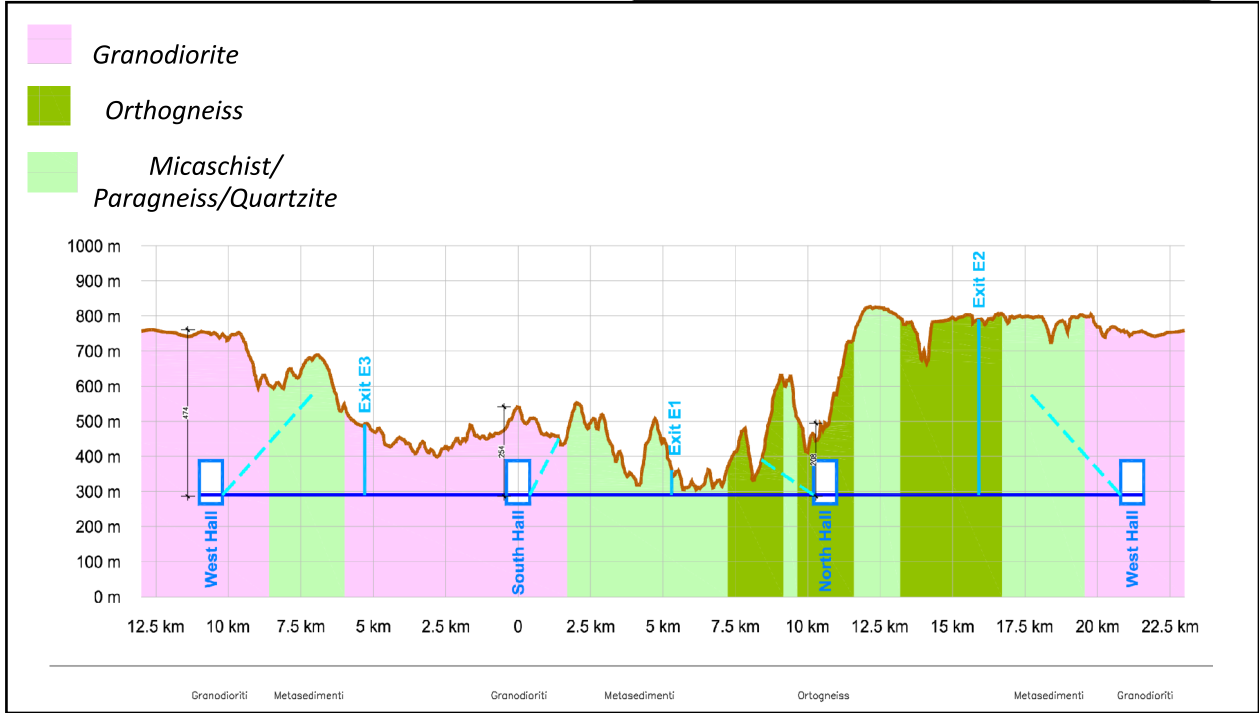

Extreme Physics with the 3G detectors

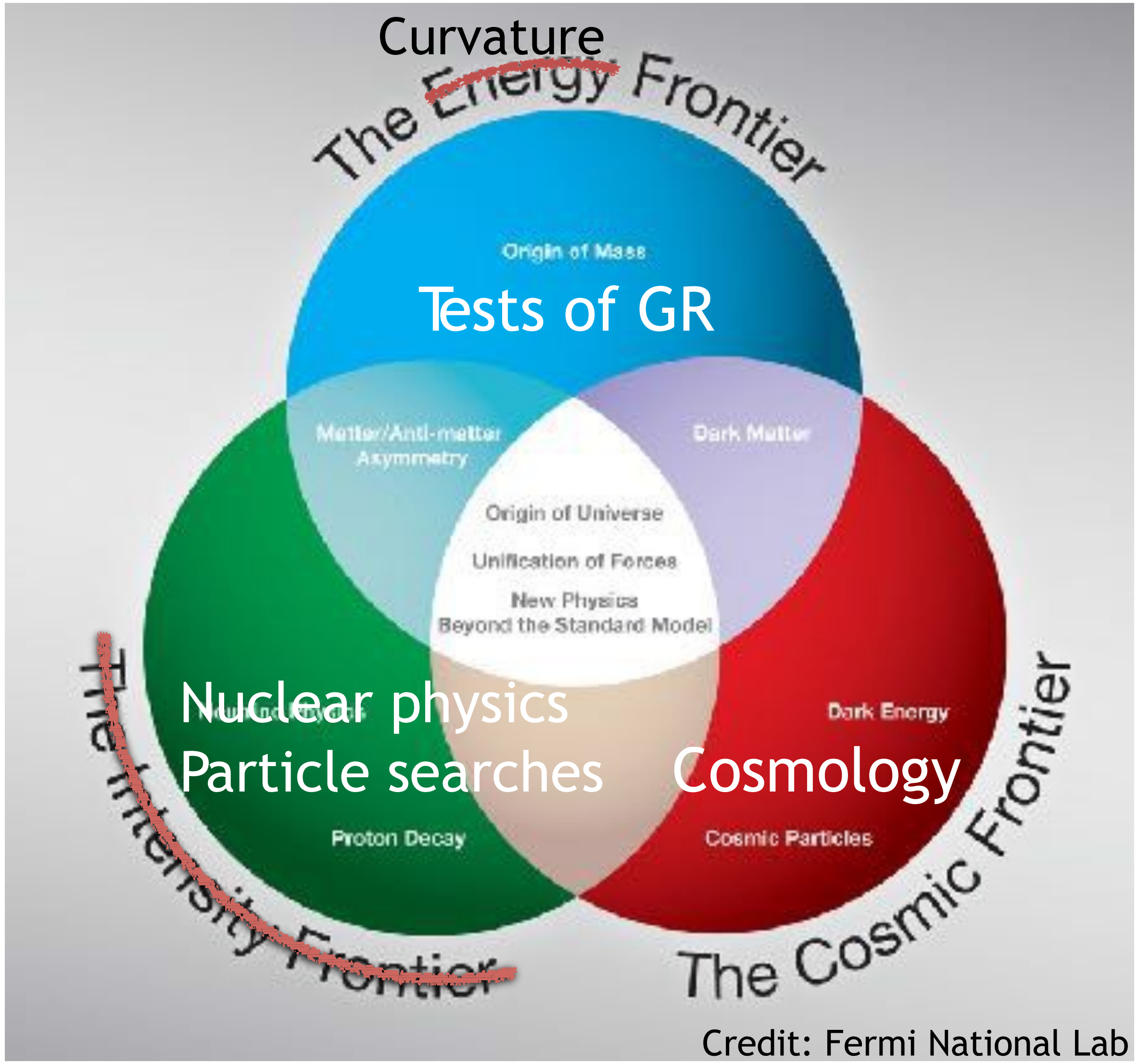

Credits Aaron Zimmerman

The supernova puzzle

Type II Supernovae unsolved problem: how the neutrino burst transfers its energy to the rest of the star producing the shock wave which causes the star to explode?

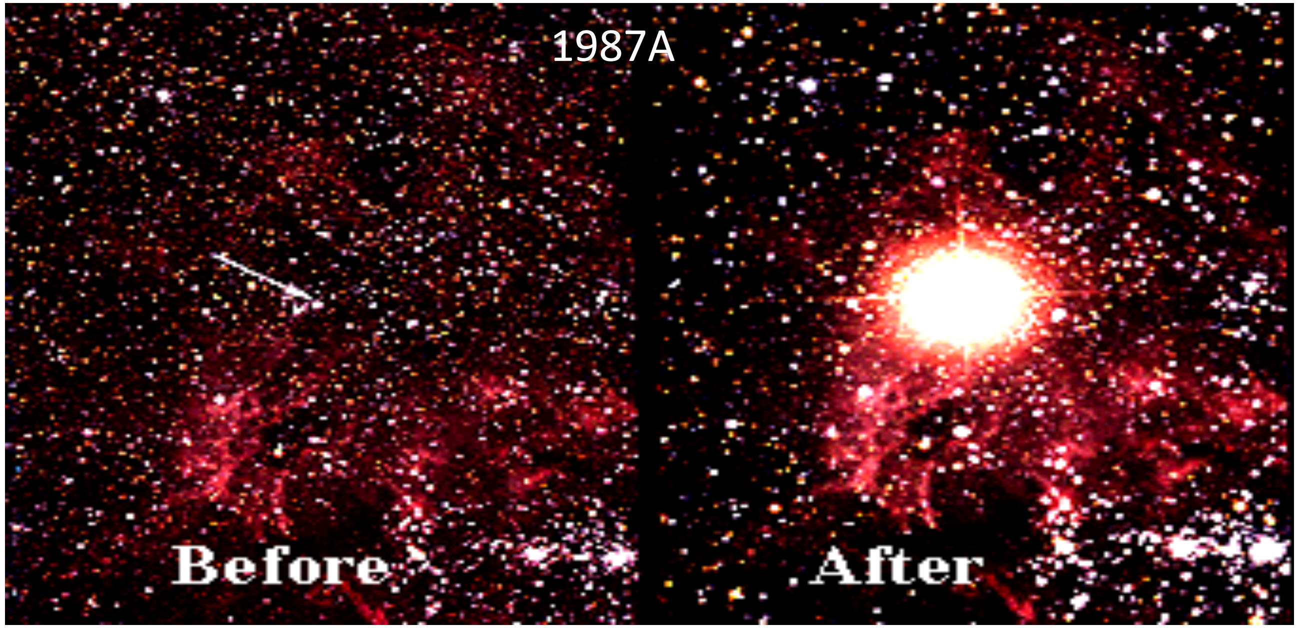

- For Type II supernovae, the collapse should be halted by short-range repulsive neutron-neutron interactions, mediated by the strong force, as well as by the degeneracy pressure of neutrons, at a density comparable to that of an atomic nucleus.

- Through a process that is not clearly understood, about 1%, of 10^{44} J of the energy released in the form of neutrinos is reabsorbed by the stalled shock, producing the supernova explosion. How does it occur this 1% energy transfer?

- Theoretical models has to include a hydrodynamical instability for re-energizing the stalled shock: ***Standing Accretion Shock Instability (SASI)*** are consequence of non-spherical oscillating perturbations, exciting the protoneutron star formed with the collapse

- *This implies that we should find characteristic features in the GW signals*

Hunting GWs: from Supernovae

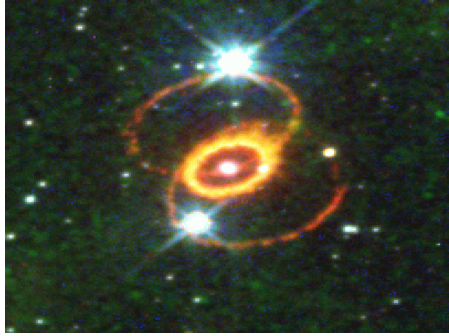

- Collapse dynamics and waveform badly predictable (giant numerical effort)
- Estimated rate: several /yr in the VIRGO cluster, but the efficiency of GW emission is strongly model dependent
- Simulations suggest E_{GW}~10^{-6} - 10^{-9} $M_{\odot}c^2$, but NS kick velocities suggest possible strong asymmetries

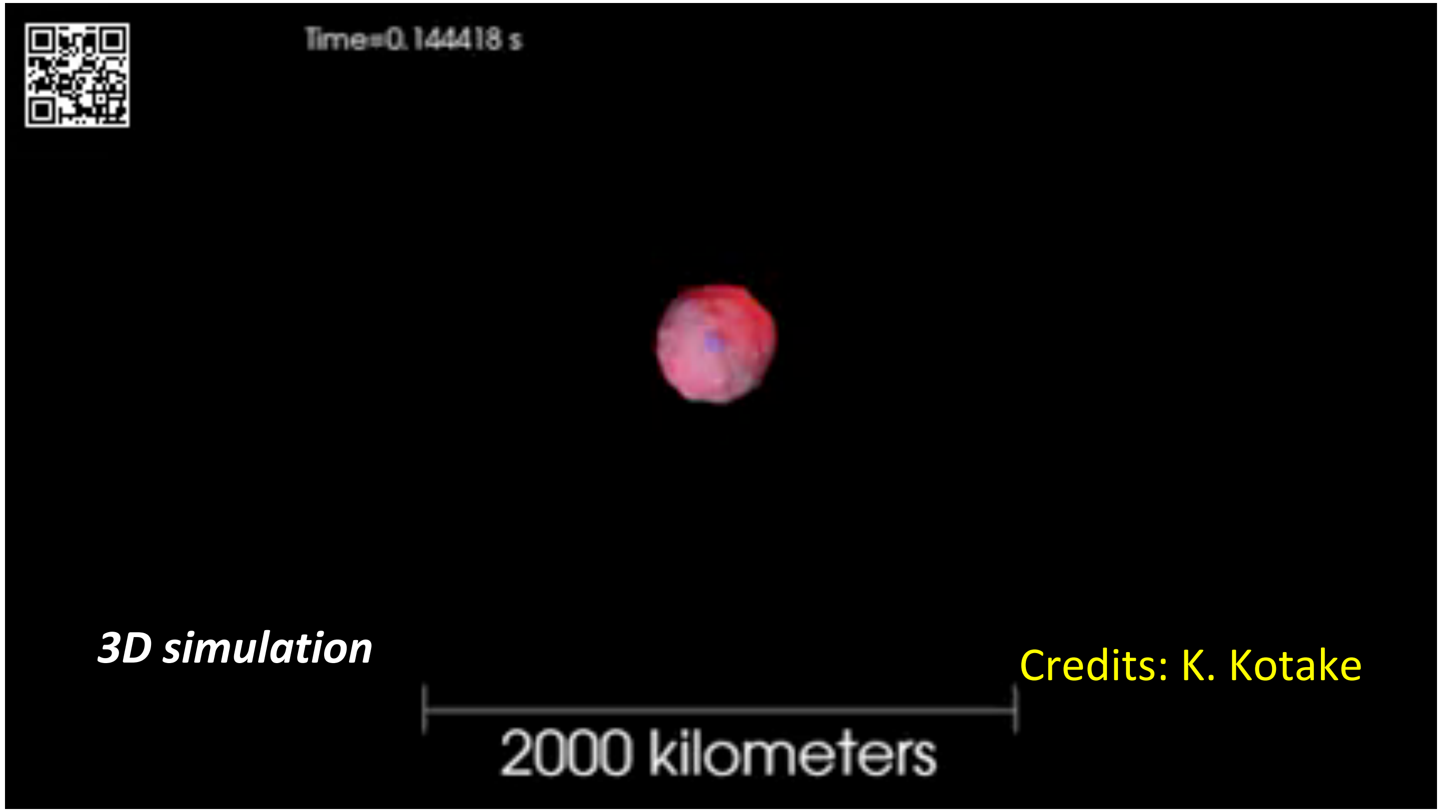

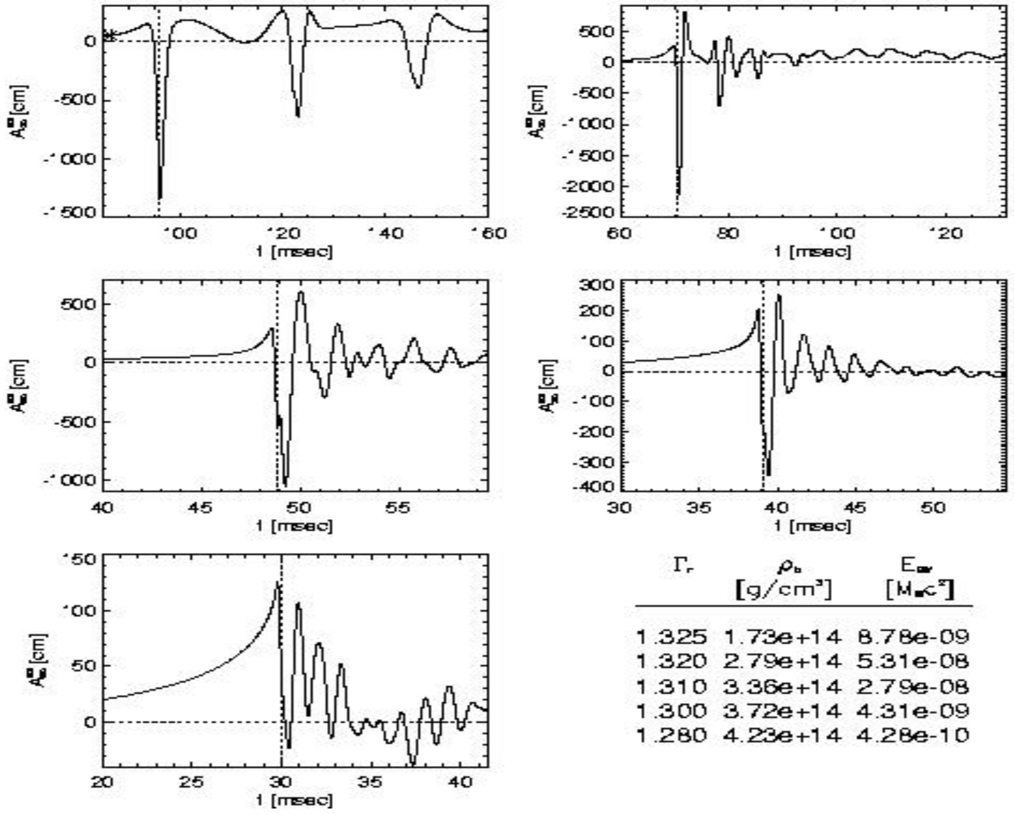

[Zwerger, Muller]

New methods to catch signal peculiarities ➔ see poster

P. Astone, Cerdá-Durán, Di Palma, M. Drago, F. Muciaccia, C. Palomba and F. Ricci , Phys. Rev. D 98, 122002 (2018)

The driving idea is to identify a set of N features in the data chunks, which are the outcomes of the CCSNe 3D simulations.

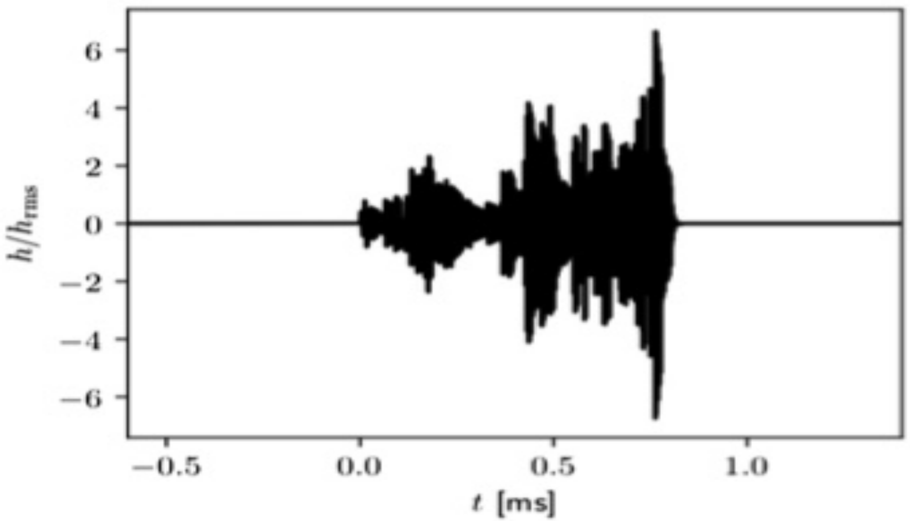

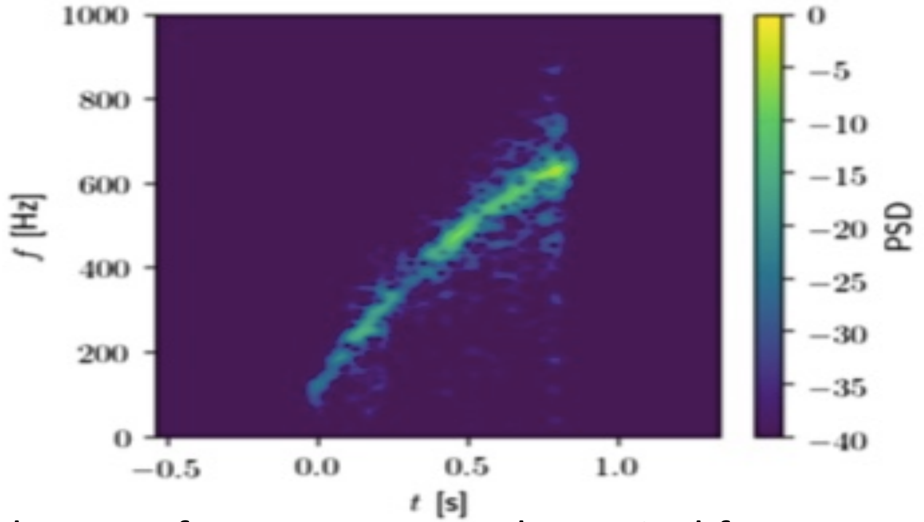

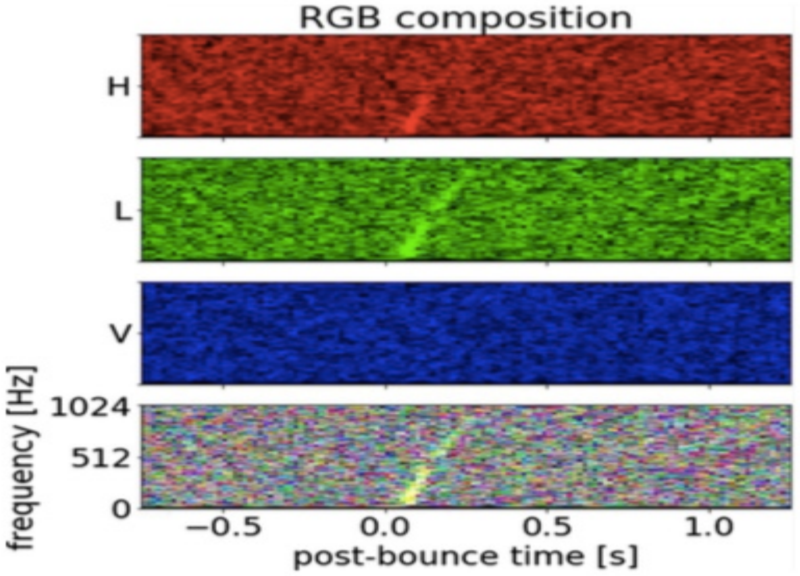

The waveforms represent the typical features observed in numerical simulations of neutrino-driven CCSNe. Their origin is well understood (g-modes in the proto-neutron star).
These features are not expected to disappear in more detailed, numerical simulations, although the parameter space of possible values for the waveform may change in the future.

BBH population study

The detected signals confirmed the existence of black holes with masses larger than 20 $M_{\odot}$

- ❖ How many black holes? Which size? How are they formed?
- ❖ How metallicity environment influence the formation ? (stellar wind depends on metallicity)

Two models for the binary black hole formation:

- ✓ Two object formed and exploded at the same time from two stars➔ similar spins with the same orientation
- ✓ Black holes in a stellar cluster sink to the center of the cluster and pair up ➔ spin randomly oriented

- ➢ Do it exist miniature black holes ?

  They may have formed immediately after the Big Bang. Rapidly expanding space may have squeezed some regions into tiny, dense black holes less massive than the sun.

BBH population study: from 2G to 3G

Under a simplified hypothesis of a uniform distribution of BBH creation on the universe history

With a 3G detector we expect

- $10^5\ y^{-1}$ BBH
- SNR ~ 10^4 for rare events

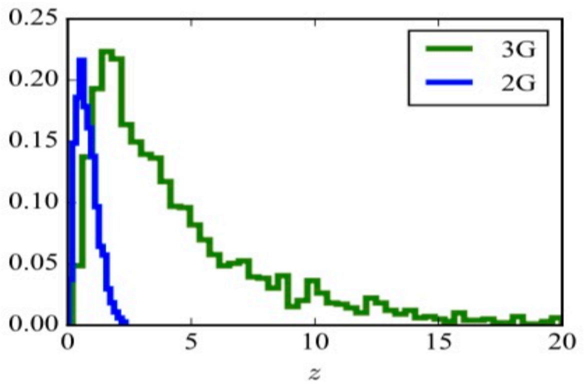

FIG. 2. The redshift distribution of detectable events with a 2-detector network of advanced detectors at design (2G) or CE-like (3G). Note that the two curves use different y scales to improve clarity.

- ➢ Population study biased in function of the achievable SNR

GW signal amplitude depends on $\mathcal{M}^{5/2}$

$\mathcal{M}$ = *chirp mass* = $(m_1 m_2)^{3/5} / (m_1 + m_2)^{1/5}$

Higher $\mathcal{M}$ ➔ easier detection

GW signal duration decreases ***with*** $M_{tot} = m_1 + m_2$

Too massive systems ➔GW signals at frequency out of the detector bandwidth

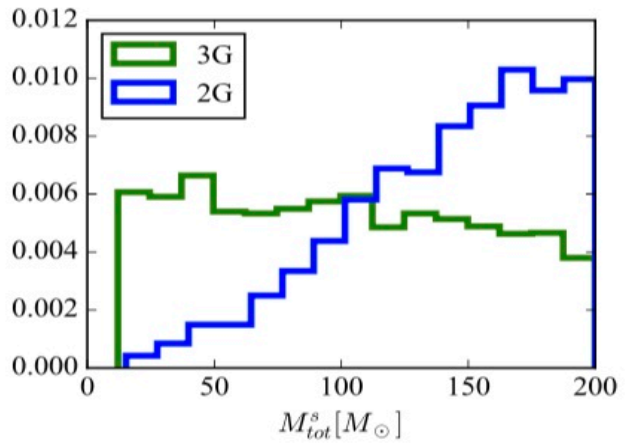

FIG. 3. The source-frame total mass distribution of detectable events with a 2 interferometers network of advanced detectors at design (2G) or CE-like (3G).

In addition the signals detected depend on the redshifted masses M (1+z)

Salvatore Vitale, Phys. Rev. D 94, 121501 (2016)

Testing GR: example via Post Parametrized Expansion

Phenom consistency test $h(f) = A(f, \vec{\theta})e^{i\Psi(f,\vec{\theta})}$

$$\Psi = f^{-5/3} \sum_{i=0}^{7} p_i(\vec{\theta}) f^{i/3} + (\log \text{terms})$$

$$p_i \to p_i(1 + \delta\hat{p}_i)$$

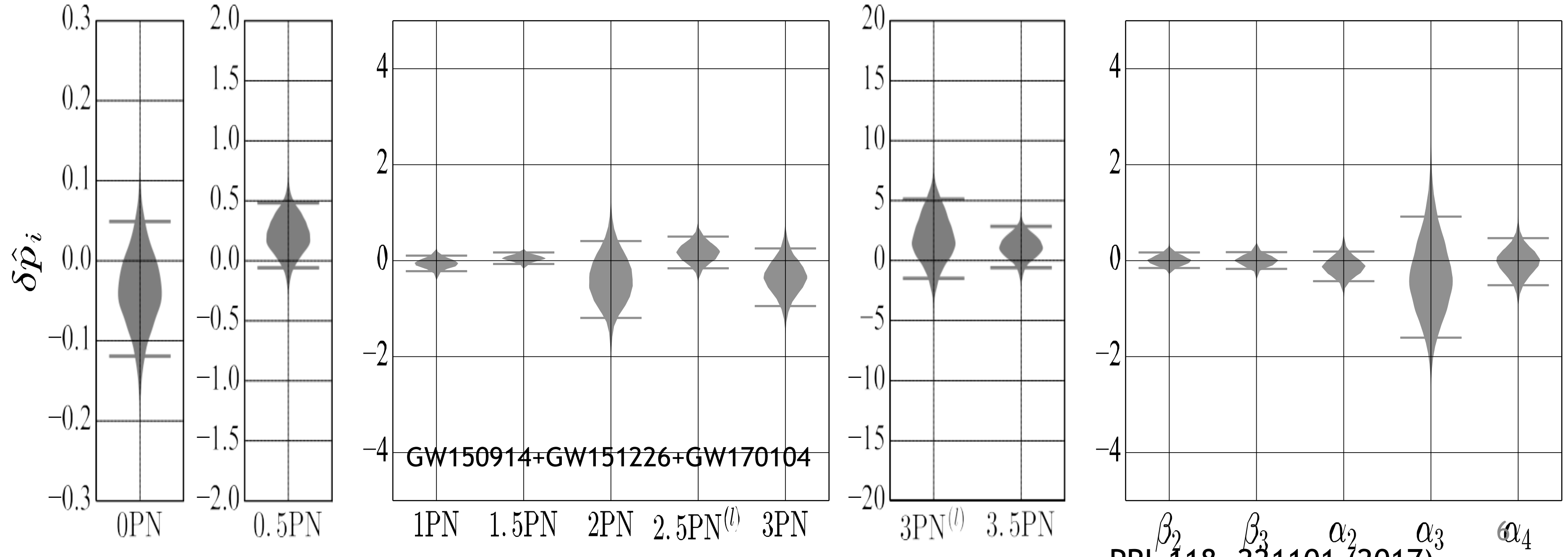

PRL 118, 221101 (2017)

Testing GR via Polarization

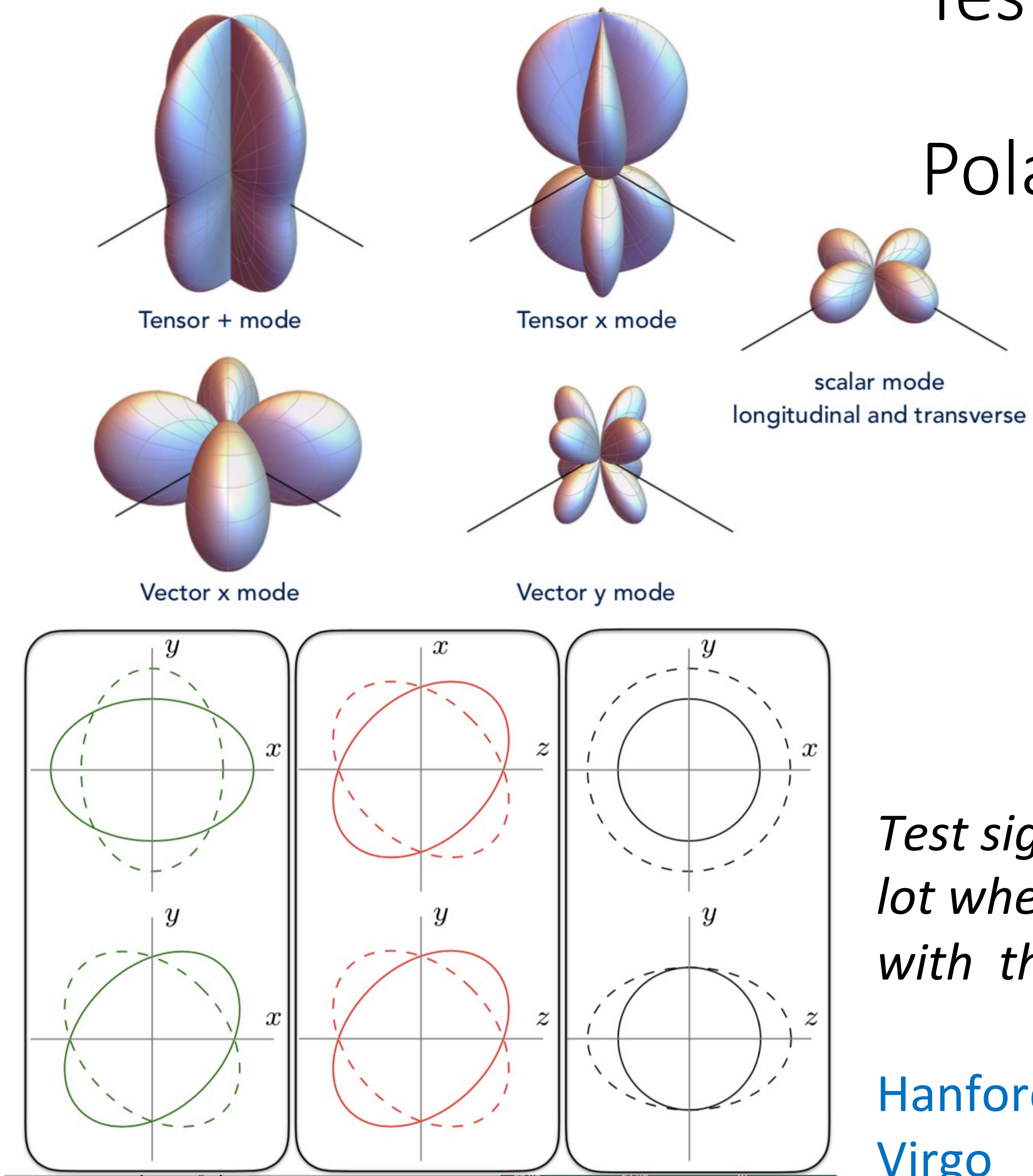

GW170814 result

Bayes factors:

- 1:200 , i.e. purely vector disfavoured vs purely tensor
- 1:1000 i.e. purely scalar disfavoured vs purely tensor mode

Test significance will improve a lot when it will be carried on with the extended network

Hanford-Livingston-KAGRA-Virgo

Looking ahead for tests of GR

- Precision era ahead: modeling challenges
  - Part in 10^{-4} -10^{-5} waveform accuracy
  - Predictions from non-GR mergers

More work on mapping constraints to theory
- Beyond leading order PPE

- New ideas/new events lead to dramatic constraints
- Target measurements to rule out classes of non- GR theories

Ringdown of a Kerr Black hole

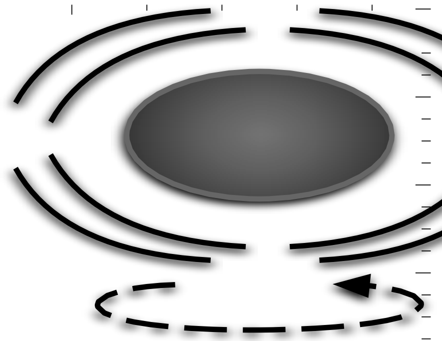

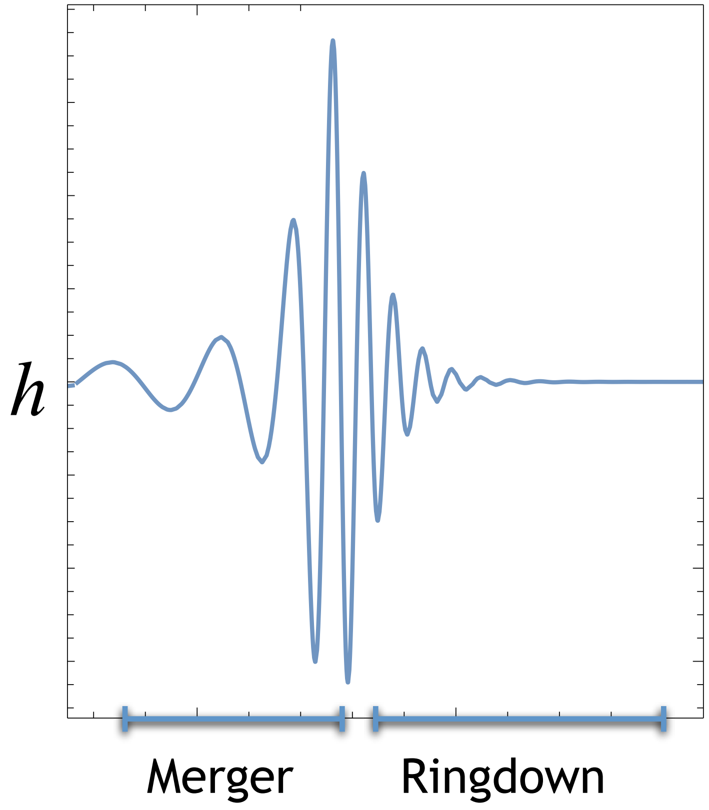

Scheel et al. PRD (2009)

The spectrum of Quasi Normal Modes (QNM) is characterized only by the BH mass and angular momentum.

The detection of a few modes from the ringdown signal can allow for precision measurements of the BH mass and spin

In addition the detection of higher multipole moments can be used to perform null- hypothesis tests of the no-hair theorems of general relativity

Black hole spectroscopy

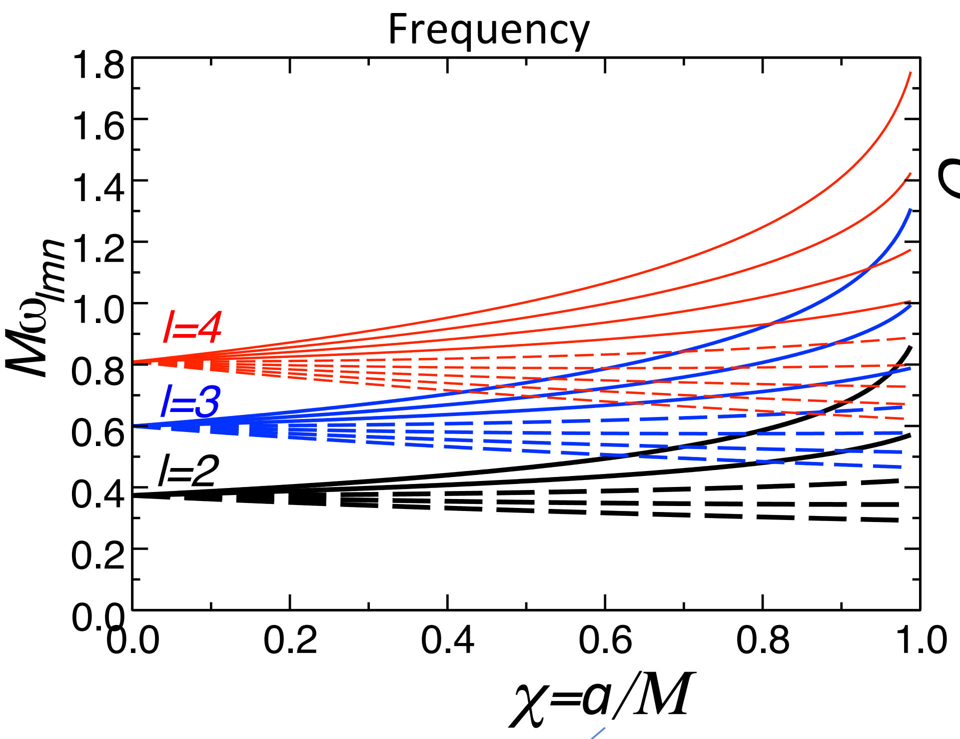

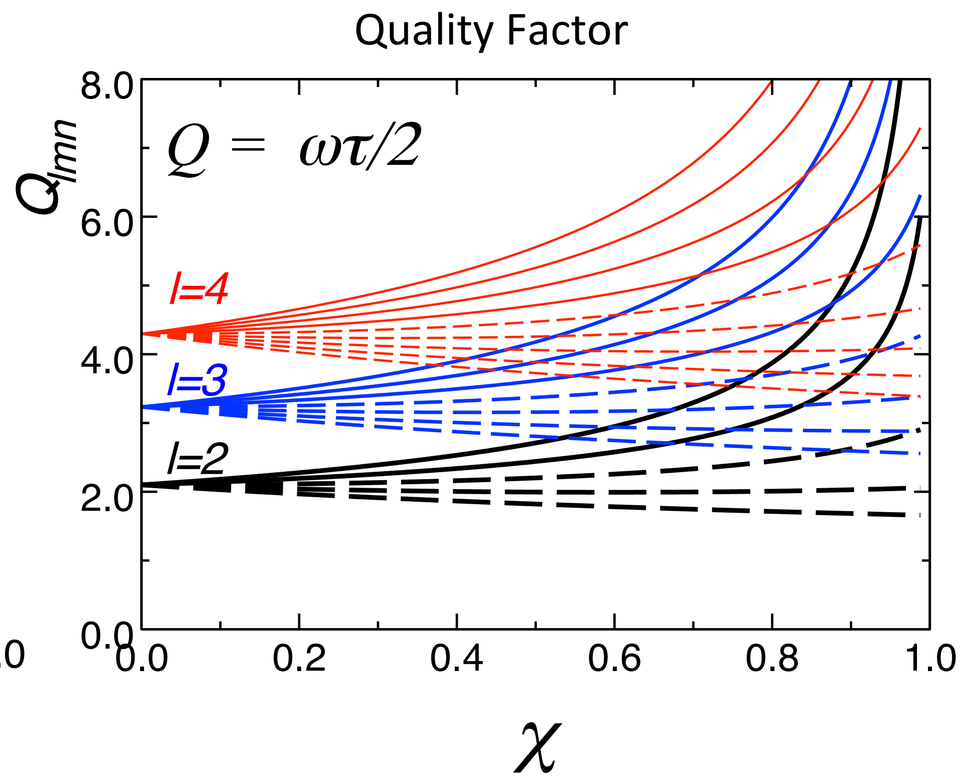

a =*J*/*M*➔Kerr rotation parameter

(ω,τ) ➔ (M, χ)

Berti,Cardoso, Starinets (2009)

BH spectroscopy with the future detectors

- ET and LISA detectors ideal for ringdown
- High-SNR events will give individual tests
- Combine many events: both 2G and 3G provide stronger constraints on GR
- Practical in active development

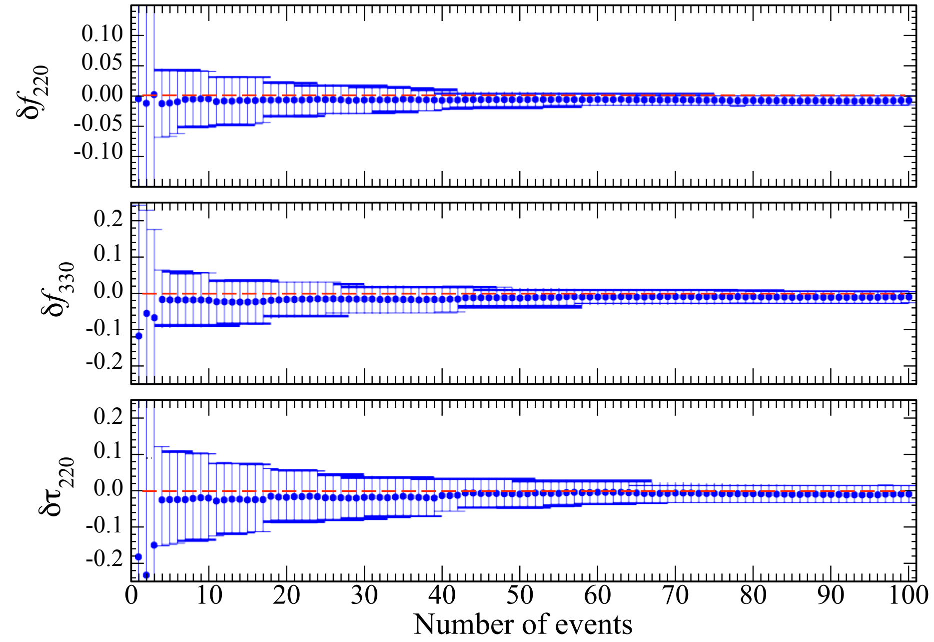

$$f_{lmn} = f_{lmn}^{GR}(1 + \delta f_{lmn})$$

Brito, Buonanno, Raymond arXiv:1805.00293

Beyond GR:
New Macro Systems,
F ields and Particles

Primordial Black Holes as Dark Matter Objects

The new detectors would settle the question if LIGO-Virgo black holes constitute dark matter and are primordial in origin

- sub-solar black holes cannot form by stellar evolution
- must be primordial in origin
- The new detectors can probe existence of light black holes

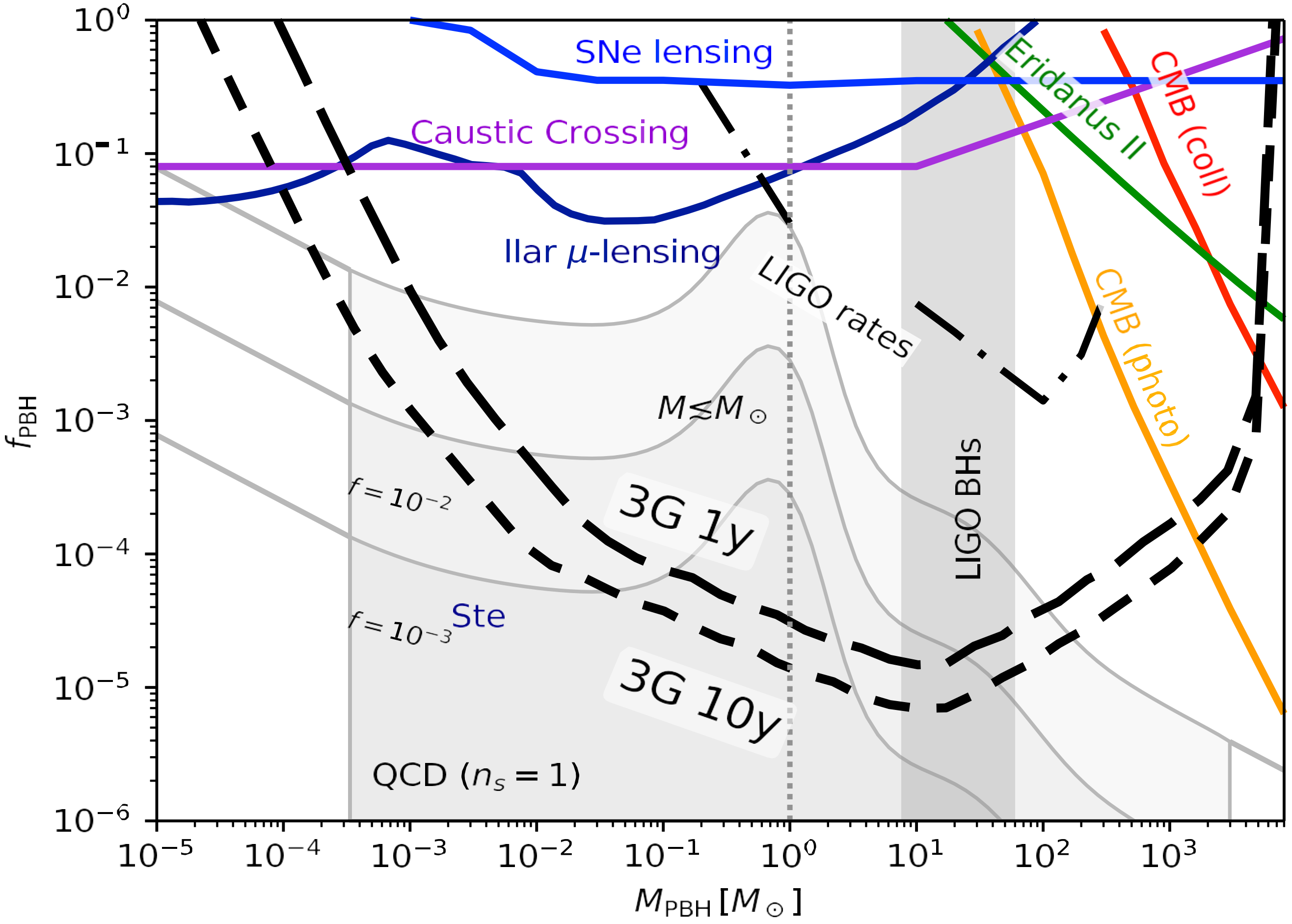

Credit:Miguel Zumalacarregui

Extremely Compact Objects

Exploring particle physics theories

The new detectors could discover extremely compact objects such as Boson stars, strange stars, gravastars, worm holes, …

- Axions, ultra-light bosons, consequence of new interactions on two-body dynamics and population characteristics
- Objects made of new matter
  - ✓ fundamental strings, boson stars, strange stars, gravastars

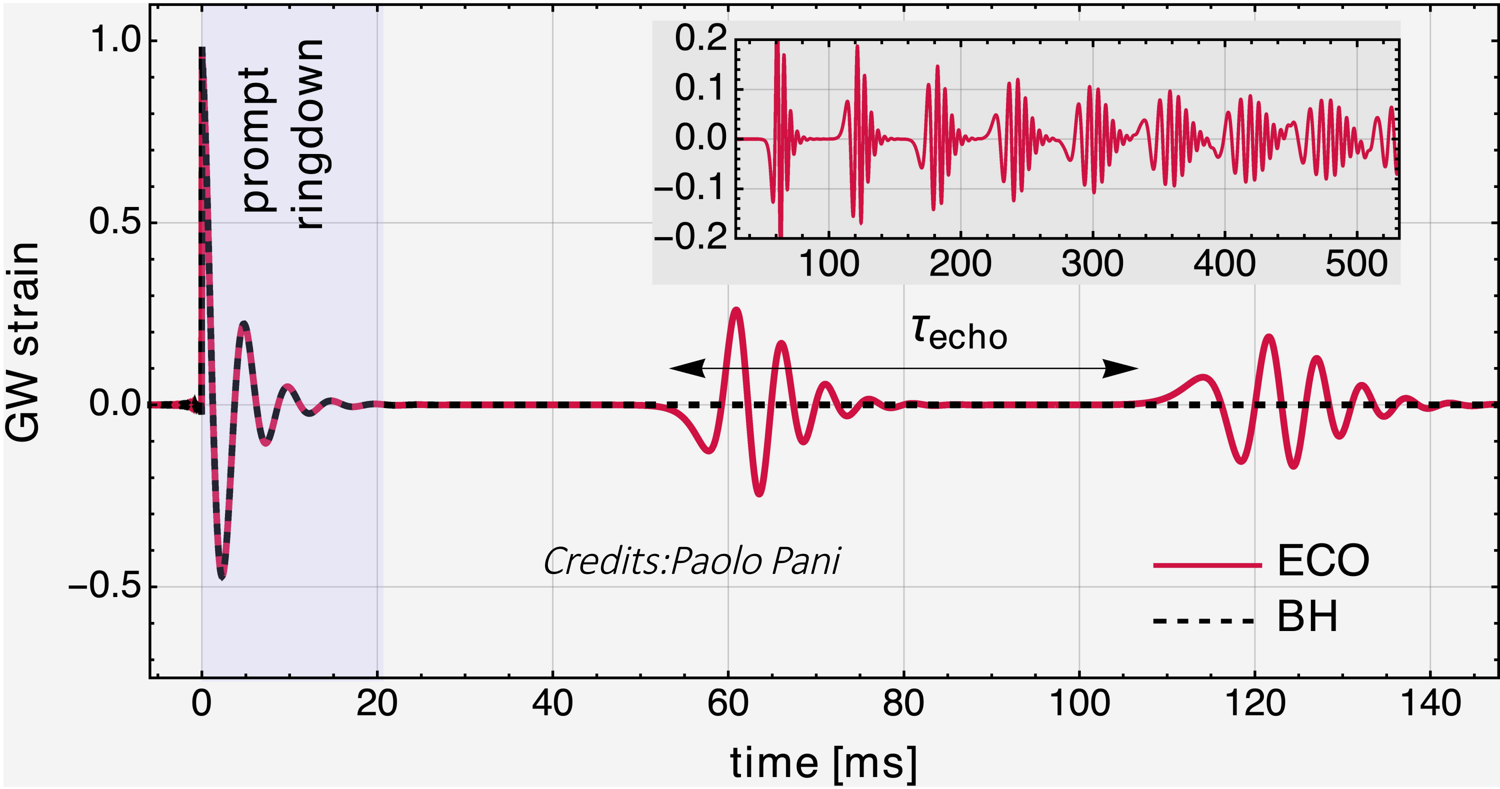

Credits:Paolo Pani

QNM to Probe Wormhole Spacetime

Cardoso, Franzin, Pani PRL 116, 171101 (2016)

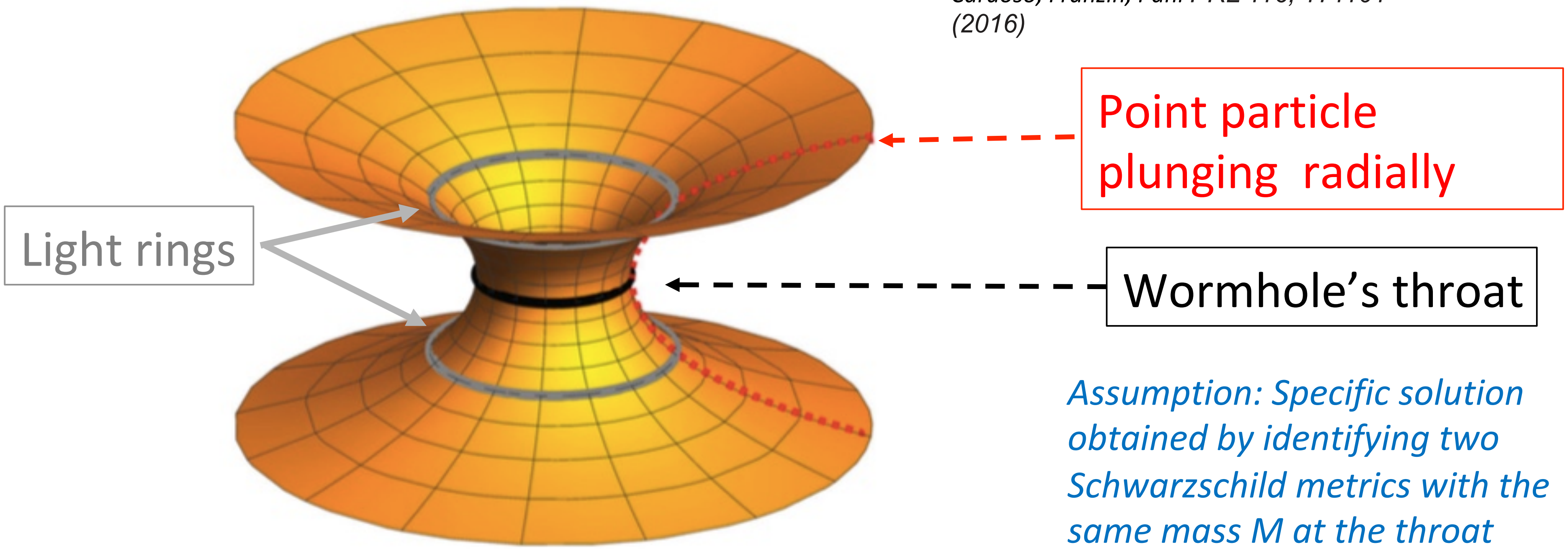

Assumption: Specific solution obtained by identifying two Schwarzschild metrics with the same mass M at the throat $r = r_0 > 2M$ ($G=c=1$)

A point particle plunges radially and emerges in another "universe". When the particle crosses each of the light rings curves<u>, it excites QNM characteristic modes </u>trapped between the light-ring potential wells

Comparison of the GW waveform between the BH and wormhole case

- Particle plunging into a Schwarzschild BH with the energy E compared to the particle crossing a traversable wormhole

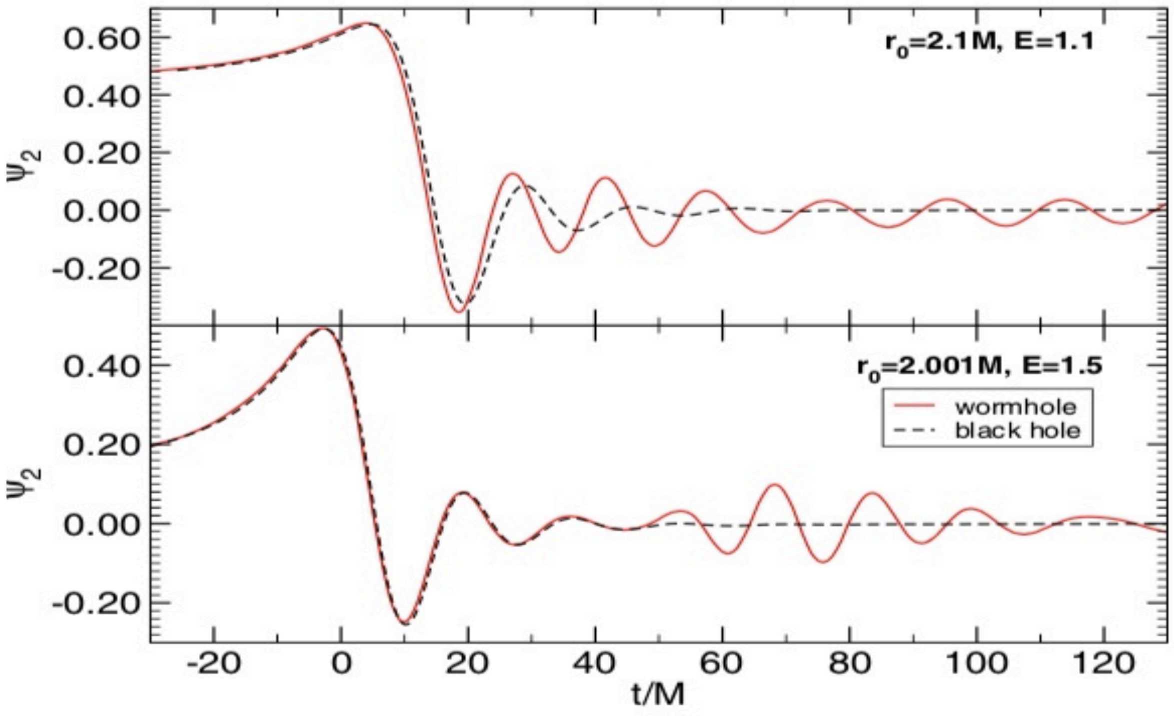

GW waveforms comparison for different values of E.

The BH waveform was shifted in time to account for the dephasing due to the light travel time from the throat to the light ring

BH and particle physics

- With a stellar mass BH we have a new precision tool that may diagnose the presence of new light (10^{-20} 10^{-10} eV) and weakly interacting bosonic particles

- When such a particle's Compton wavelength is comparable to the horizon size of a rotating BH,

$$\lambda_C \gtrsim R_s$$

the super radiance effect spins down the BH, populating bound orbits around the BH with an exponentially large number of particles

- The BH already detected by LIGO/Virgo can act as attractors of QCD axions of the upper end of a mass range, which covers the parameter space for the QCD axion

GW interferometer as detector of new elementary particles

In this proposed scenario black holes develop clouds of axions

The axion cloud will emit ~monocromatic GWs

Depending on the mechanism, these might be visible to tens of Mpc (Arvanitaki+ 1604.03958)

We can follow-up newly formed BHs and look for this signal.

Source-frame frequency depends on the mass of the axion
(Detected frequency will be redshifted)

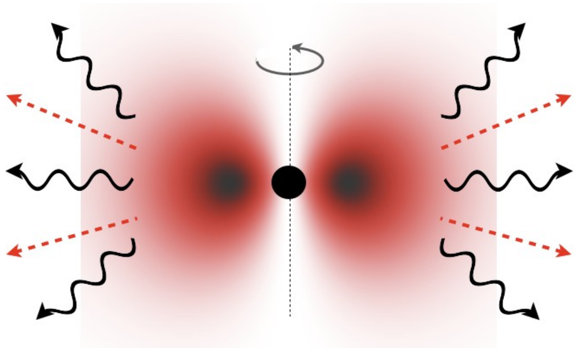

Searching for ultra-light particles

μ_a = 10^{-10} - 10^{-14} eV → λ_c = 10 - 10^5 km

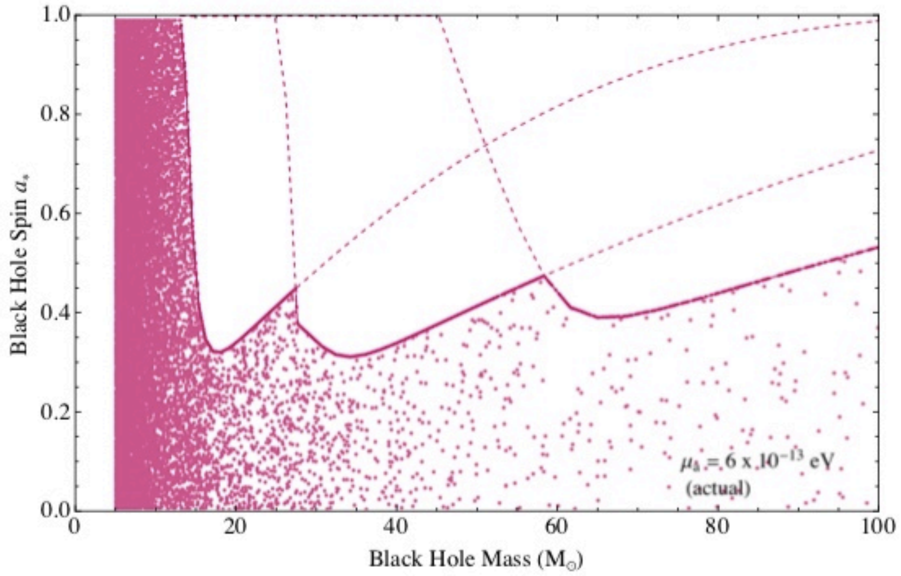

Population inferences

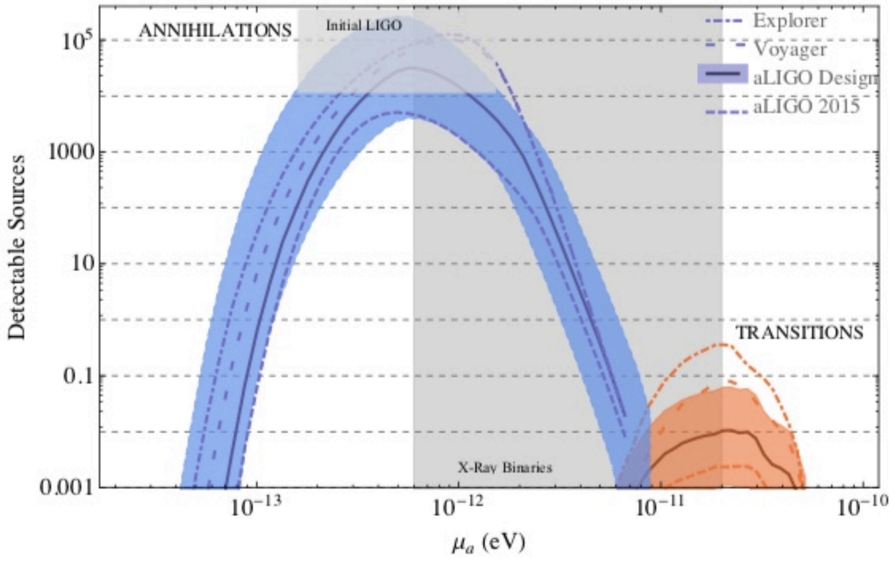

Direct searches

Arvanitaki et al.,
Phys. Rev. D 95, 043001 (2017)

PHYSICAL EFFECTS IN BINARY NEUTRON STAR COALESCENCE WAVEFORMS

Credits: Sebastiano Bernuzzi

dominated by gravitational radiation back reaction - masses and spins

tidal effects appear at high PN order, dynamical tides might be important

complex physics of the merger remnant, multi-messenger source, signature of neutron star EoS

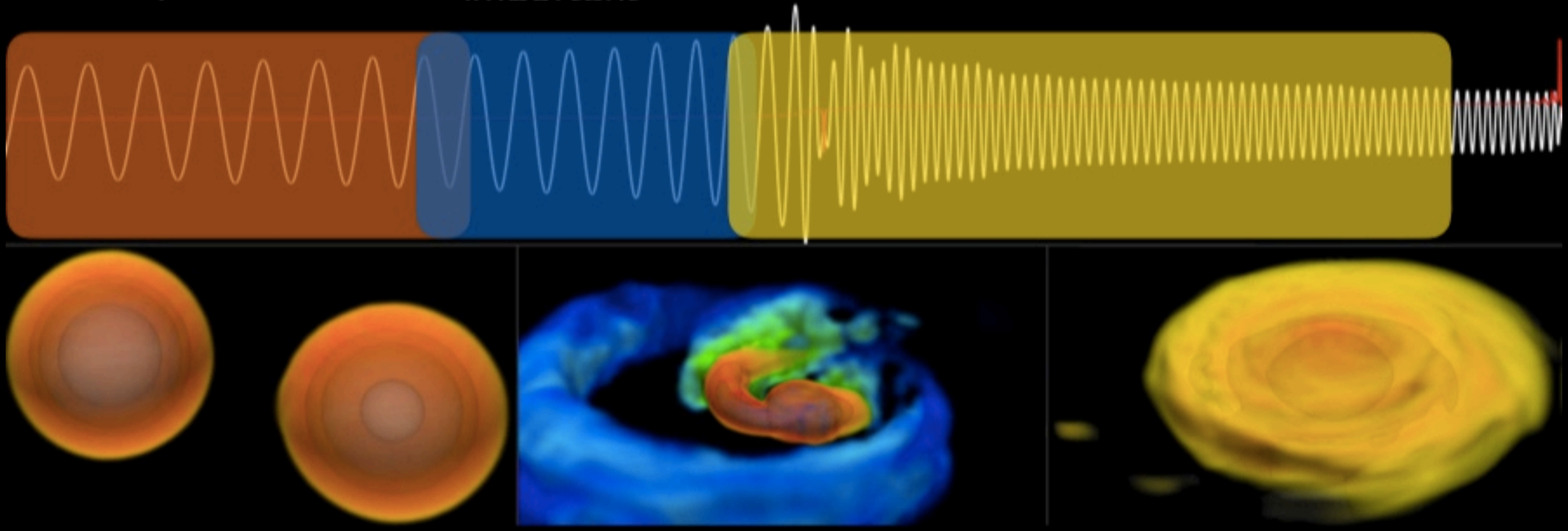

QCD Phase Diagram and Neutron Stars

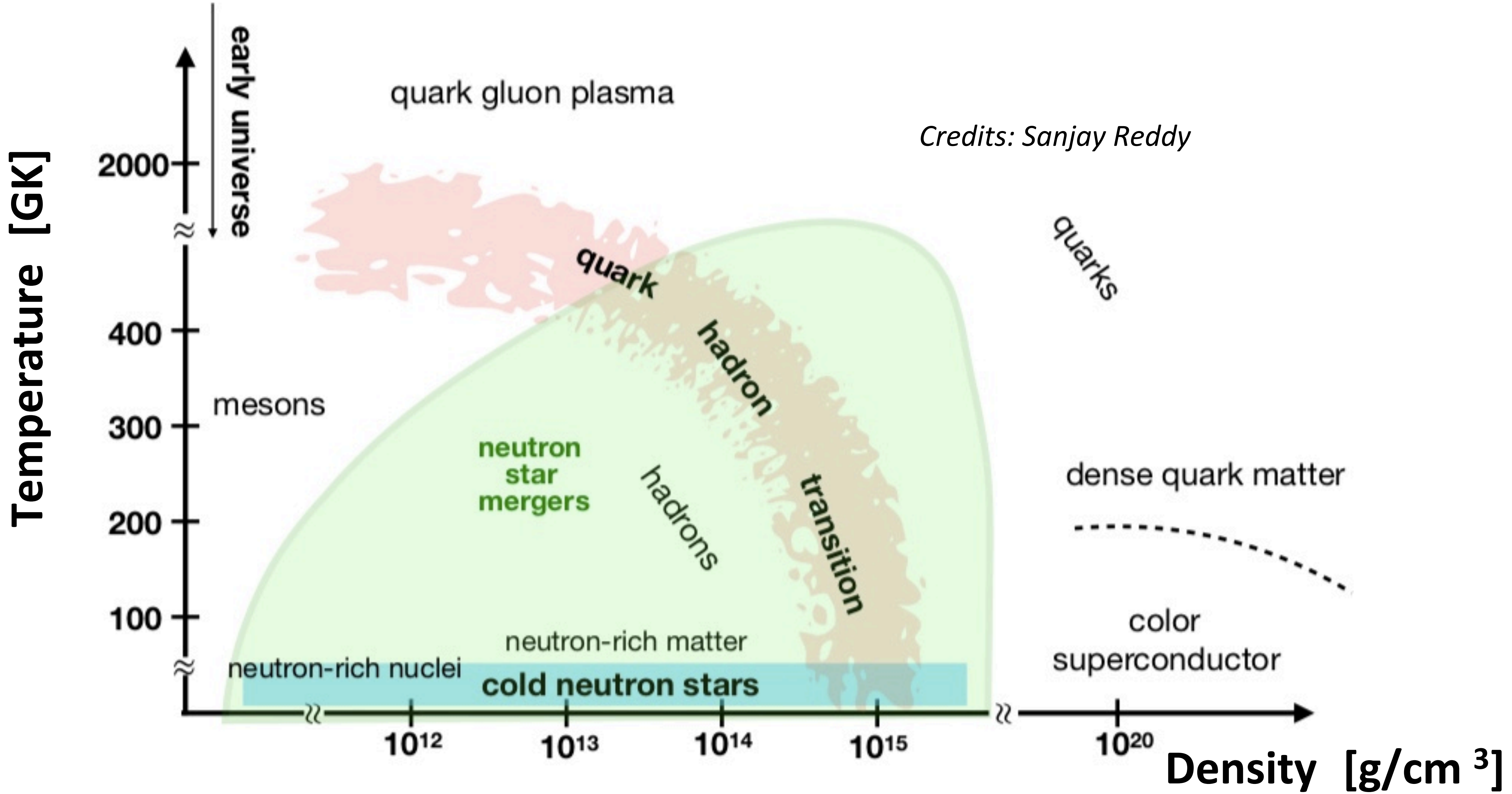

Hard NS EOS

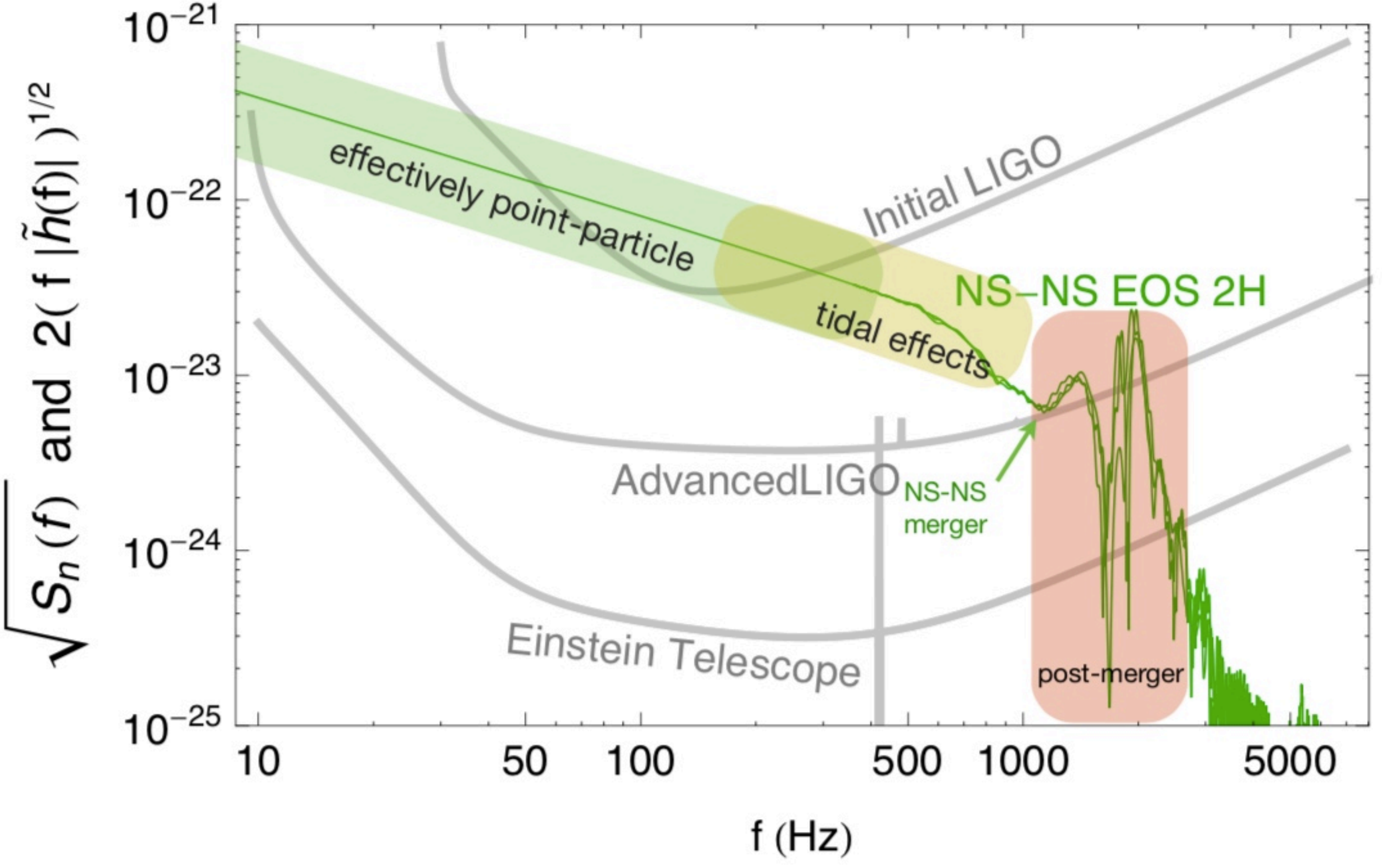

$\sqrt{S_n(f)}$ and $2(f|\tilde{h}(f)|)^{1/2}$
10^{-21}
10^{-22}
10^{-23}
10^{-24}
10^{-25}
effectively point-particle
Initial LIGO
NS–NS EOS 2H
tidal effects
AdvancedLIGO
NS-NS merger
Einstein Telescope
post-merger
10
50
100
500
1000
5000
f (Hz)

Soft NS EOS

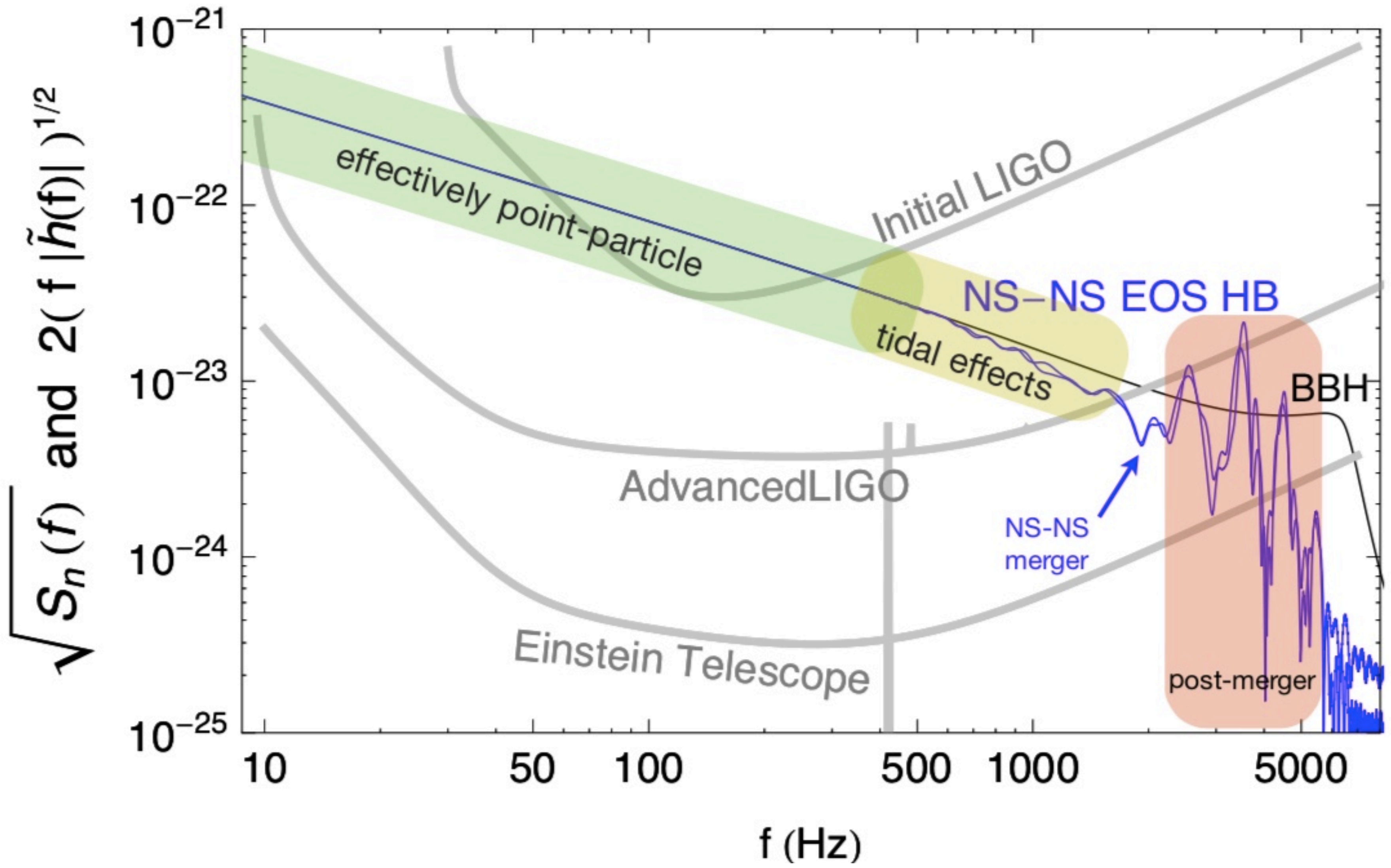

10^{-21}
10^{-22}
10^{-23}
10^{-24}
10^{-25}
$\sqrt{S_n(f)}$ and $2(\, f\,|\tilde{h}(f)|\,)^{1/2}$
effectively point-particle
Initial LIGO
NS–NS EOS HB
tidal effects
BBH
AdvancedLIGO
NS-NS
merger
Einstein Telescope
post-merger
10
50
100
500
1000
5000
f (Hz)

Cosmology

To measure the cosmology one needs luminosity distance *and* redshift of the source

$$D_L(z) = \begin{cases} \frac{(1+z)}{\sqrt{\Omega_k}} \sinh[\sqrt{\Omega_k} \int_0^z \frac{dz'}{H(z')}] & \text{for} \quad \Omega_k > 0 \\ (1+z) \int_0^z \frac{dz'}{H(z')} & \text{for} \quad \Omega_k = 0 \\ \frac{(1+z)}{\sqrt{|\Omega_k|}} \sin[\sqrt{|\Omega_k|} \int_0^z \frac{dz'}{H(z')}] & \text{for} \quad \Omega_k < 0 \end{cases}$$

$$H(z) = H_0 \sqrt{\Omega_m (1+z)^3 + \Omega_k (1+z)^2 + \Omega_\Lambda E(z, w(z))}$$

$$E(z, w(z)) = (1+z)^{3(1+w_0+w_1)} e^{-3w_1 z/(1+z)}$$

Usually, GWs provide the distance

How do we get the redshift?

Cosmological corrections to CBC Signal

- If the source is at a cosmological distance with redshift *z*, then
  - *distance* ➔ luminosity distance D_L ,
  - *Frequency* is the ***observed*** one *f red-shifted by (1+z) to the respect of the source frequency,*
  - Each mass *m* ➔*(1 +z) m*.

- <h> $\propto$ $(\mu M^{2/3} f^{2/3} / D_L)$ ➔ r.m.s. mean value of *h(t)*, averaged over the orientations of the source and the detector, referred to their joining direction.

- $\tau = f / f' \propto \mu^{-1} M^{-2/3} f^{-8/3}$

- $\langle h \rangle \tau$ is independent of the objects masses to the leading order
  - D_L ➔ $1/ (\langle h \rangle \tau^3 f^{-2})$

- D_L ➔ *z* assuming ΛCDM cosmology with H_0 = 67.9 km s^{-1} Mpc^{-1} and Ω_m =0.306

Building a new ladder up to cosmological distance

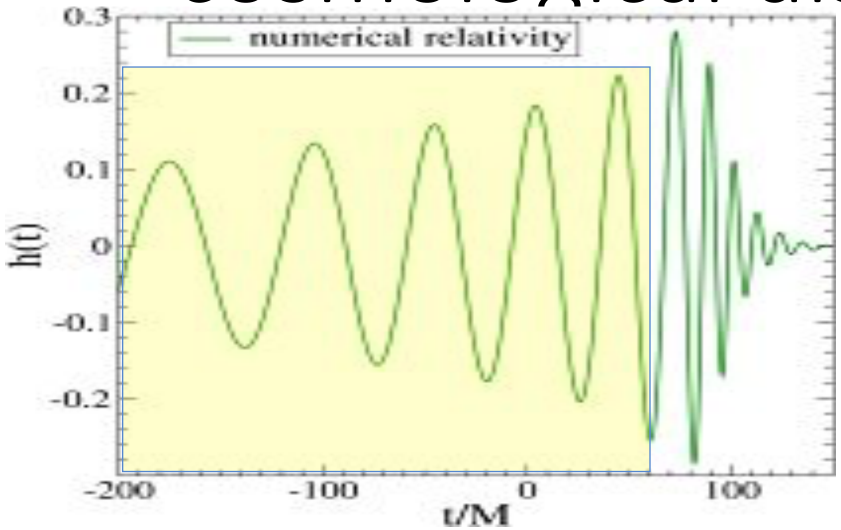

At the leading order

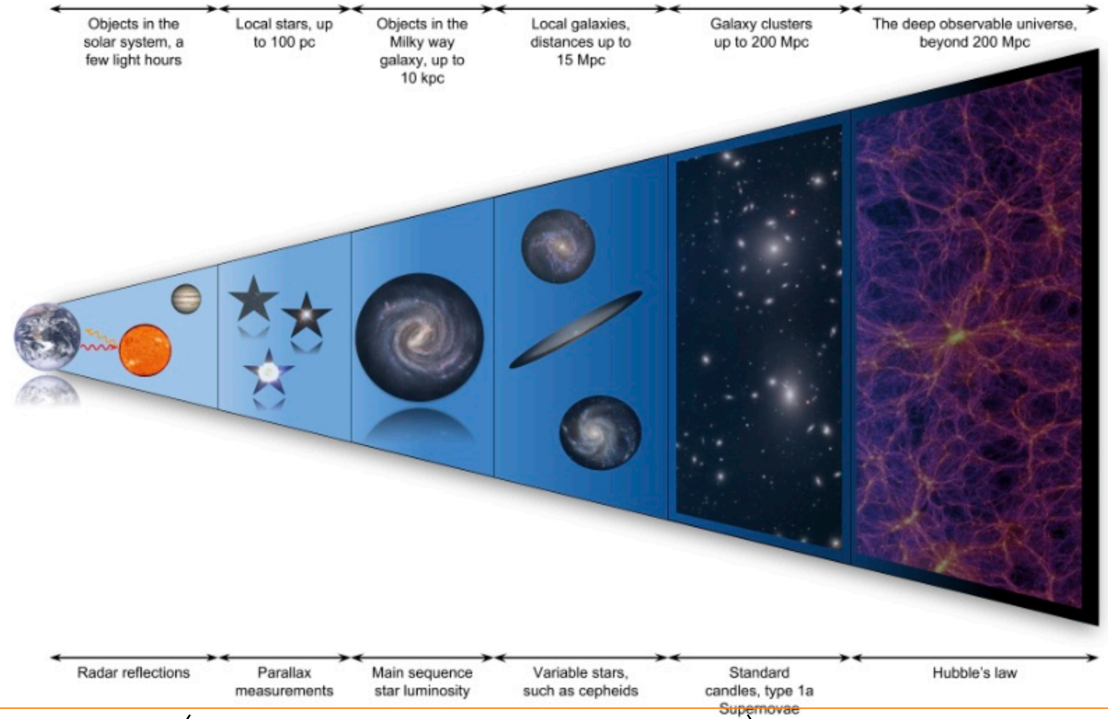

- CCB gravitational wave source is a "standard siren"
- Amplitude and phase of the GW due to **CCB** depend strongly on the chirp mass of the system, a parameter well measured. Thus, we can use the signal to infer the luminosity distance *d*
- At cosmological distances, the waves will depend on and reveal the redshifted masses *(1+z)*μ and *(1+z)*$\mathscr{M}$
- When the collision can be observed optically as well, the Doppler shift can be measured and the Hubble constant computed.

$$h_{ij}(t) = h_o(t)\begin{pmatrix} \cos\Phi(t) & \sin\Phi(t) & 0 \\ \sin\Phi(t) & -\cos\Phi(t) & 0 \\ 0 & 0 & 0 \end{pmatrix}$$

$$\Phi(t) = \int 2\omega(t)\,dt = -2\left[\frac{c^3(\tau_{coal} - t)}{5G\mathscr{M}}\right]^{5/8} + \Phi_{in}$$

$$h_o(t) = \frac{4\pi^{2/3}\mu\,\mathscr{M}^{5/3}}{d\,c^4}\,G^{5/3}\nu_{GW}^{2/3}(t) \qquad \tau_{coal} = \frac{5}{256}\frac{c^5}{G^3}\frac{r_0^4}{\mu M^2}$$

$$\mathscr{M} = \mu^{3/5}M^{2/5} = \frac{(m_1 m_2)^{3/5}}{(m_1+m_2)^{1/5}} \qquad \mathscr{M} = \frac{c^3}{G}\left(\frac{5}{96}\frac{1}{\pi^{8/3}}\nu^{-11}\frac{d\nu}{dt}\right)^{3/5}$$

How to get the redshift information

- If the CBC produces an EM counterpart (e.g. GRB) (Sathyaprakash+ CQG 27 215006, Nissanke+ 1307.2638)
- If one knows the neutron star (NS) equation of state (Read & Messenger PRL 108 091101; Del Pozzo+ 1506.06590)
  GW phase encodes the equation of state of neutron stars and it depends on the source-frame masses. If the EOS is known through other means (EM) one can measure both source-frame and redshifted masses, hence get the redshift
- If the post-merger signal is observed (Messenger+ PRX 4, 041004)
  Compare the measured redshifted frequency of the post merger phase with expected frequency gives redshift.
- If the shape of NS mass distribution is known (Taylor+ PRD 85 023535; Taylor & Gair PRD 86, 023502)
- Even if no EM is found, but there is a reliable galaxy catalog (Schutz, Nature 1986, Del Pozzo PRD 86 043011)

Conclusion

- The new run O3 with LIGO and Virgo is started on April 1st
- New GW signal have been collected already
- KAGRA in Japan will join the network before the end of the O3 run
- We are preparing plans for future upgrades a+ and AdV+ paving the way for the construction of the new 3 G detectors

Thanks for the attention

The future will be rich of new surprises and conundrums to be solved